Title
Fyn in Neonatal Hypoxic-Ischemic Brain Injury

Author
Knox, Renatta

Publication Date
2012

Peer reviewed|Thesis/dissertation

Fyn in Neonatal Hypoxic-Ischemic Brain Injury

by

Renatta Knox

DISSERTATION

Submitted in partial satisfaction of the requirements for the degree of

DOCTOR OF PHILOSOPHY

in

Biomedical Sciences

in the

GRADUATE DIVISION

of the

UNIVERSITY OF CALIFORNIA, SAN FRANCISCO

[redacted]

Acknowledgements

My deepest gratitude extend to ...

... **Donna Ferriero** for being an exceptional mentor and role model; for exposing me to the developing brain and pediatric neurology; and for teaching me to be productive, focused, and balanced;

... **Xiangning Jiang** for showing me that a scientist can be selfless and generous; and for making my training and success her highest priority;

... my thesis committee members **Raymond Swanson, Zena Vexler and David Rowitch** for providing me with thoughtful feedback and guidance at critical stages; and for being rigorous and caring;

... members of the **Neonatal Brain Disorders Research Group** for creating the most collaborative environment I've had the pleasure of working in;

... the wonderful students who volunteered on my projects (**Ashley Bach, Annika Barnett, Matthew Lam, Stefan Lowenstein, Dario Miguel Perez, Claudia Ramos, Anna Wang, and Diana Yang**);

... my undergraduate research mentors **Robin Reed, Richard Losick and Tom Maniatis** for giving me a strong foundation in research;

... the **MSTP** and **BMS** for running exceptional programs;

... **NINDS F31** for funding my research and training; **SfN Neuroscience Scholars Program** for providing me with funds to broaden my graduate experience;

... **Cynthia Fuhrmann** for creating enriching programs for the UCSF community;

... **Geoffrey Lambright, Jana Toutolmin, Kevin Shannon, Lisa Magargal and Jason Cyster** for helping me transition into an ideal research setting;

... **Tara**, **Farvardin, Salar and Arya Kamangar** for giving me the feeling of home when home seemed far away;

... **my family** for their love, encouragement and support;

... **my parents** for teaching me to be fearless in the truth.

Abstract

Fyn in Neonatal Hypoxic-Ischemic Brain Injury

Renatta Knox

Neonatal brain hypoxia-ischemia (HI) is an important cause of morbidity and mortality in infants and children. However, there are few treatments. We have recently demonstrated that Src Family Kinase (SFK) activity and NMDA receptor (NMDAR) tyrosine phosphorylation are increased following neonatal HI in mice. Inhibition of SFKs provides neuroprotection against HI. However, it is unknown which particular SFKs contribute to neonatal HI brain injury or the molecular mechanisms by which SFKs worsen brain injury. We used two transgenic mouse models to determine the role of Fyn and Fyn-mediated NR2B tyrosine phosphorylation in neonatal HI. We found that neuronal Fyn overexpression leads to increased brain injury and mortality in response to neonatal HI. These changes correlated with elevated NMDAR tyrosine phosphorylation and increased calpain activity. Mutation of tyrosine 1472 of NR2B to phenylalanine (Y1472F) resulted in decreased brain injury, NR2B tyrosine phosphorylation at specific residues, and calpain activity following HI. *In vitro* Y1472F neurons had less generation of reactive oxygen species and cell death in response to NMDA and glutamate. Taken together, these studies implicate Fyn and tyrosine phosphorylation of the NR2B subunit in neonatal hypoxic-ischemic brain injury and encourage the development of therapies targeting Fyn in neonatal HI.

Table of Contents

List of Tables

Chapter 1

Chapter 3

List of Figures

Chapter 1

Chapter 2

Chapter 3

Chapter 4

Chapter 5

Chapter 1: Fyn in Neurodevelopment and Ischemic Brain Injury

The Src Family kinases (SFKs) are nonreceptor protein tyrosine kinases that are implicated in many normal and pathogenic processes in the nervous system. The SFKs Fyn, Src, Yes, Lyn and Lck are expressed in the brain. This review will focus on Fyn, as Fyn mutant mice have striking phenotypes in the brain and Fyn is involved in ischemic brain injury in adult rodents, and with our work, in neonatal animals. An understanding of Fyn's role in neurodevelopment and disease will allow researchers to target pathogenic pathways while preserving protective ones.

Fyn Structure and Regulation

Fyn is a 59kDa protein that is expressed in neurons and glia in the nervous system (1). Alternative splicing produces three Fyn isoforms. FynB, which uses exon 7A, is enriched in the brain (2). In the rodent embryo, Fyn is present in axon tracts and growth cones, the telencephalon, hippocampal formation, cerebral cortex, and thalamic and hypothalamic nuclei (1, 3). There are elevated Fyn protein levels in white matter beginning at postnatal day 10 that coincides with myelination (3). In the mature brain, Fyn has decreased expression in axon tracts and is predominantly found in the cerebellum, telencephalon and brain stem (1, 3). Fyn expression and kinase activity increase with development (3, 4).

Fyn shares a similar structure to other SFKs, an N-terminal SH4 domain, unique region, SH3 and SH2 domains, linker regions and a C-terminal kinase domain (Figure 1A). Myristoylation at glycine 2 and palmitoylation at cysteine 3 and 6 allow Fyn to target to the plasma membrane and lipid rafts (5-7). The SH3 domain is a protein-protein interaction module that recognizes proline-rich regions (8) and the

SH2 domain recognizes phosphorylated tyrosine (pY) (9). Fyn interacts with a wide range of proteins through these domains (Figure 1B).

SFKs exist in active and inactive conformations that are partially driven by phosphorylation of two critical tyrosine residues (Figure 2). Y531 is located in the extreme C-terminus. When this residue is phosphorylated, it forms an intramolecular interaction with the SH2 domain. This conformation makes the kinase active site and SH3 domain inaccessible (10, 11). Y420 is located within the activation loop of the kinase domain. When this site is phosphorylated, it activates SFKs and makes the SH3 domain available for protein-protein interactions (12).

Phosphorylation of Y420 and Y531 provide an important level of regulation of Fyn activity and its ability to interact with other proteins. Striatal enriched phosphatase (STEP) and protein tyrosine phosphatase α (PTPα) are Fyn regulators in the mammalian brain. STEP negatively regulates Fyn kinase activity by dephosphorylating Y420 (13). PTPα activates Fyn by dephosphorylating Y531 (14-16). Once activated, Fyn can phosphorylate substrates in the brain with diverse cellular functions (Table 1). A broad range of substrates and binding partners situate Fyn upstream of many cellular processes in the brain.

Functional role of Fyn in the immature and mature nervous system

Several conclusions about Fyn function in the developing and adult nervous system can be drawn from transgenic mice where Fyn has been deleted, mutated or overexpressed. The Soriano lab generated Fyn null mice that lack expression of all

Fyn isoforms (17). Yagi *et al* produced Fyn mutant mice in which the SH2, SH3 and kinase domain is replaced with lacZ, producing a Fyn-β-galatosidase fusion protein that is catalytically inactive (18). A Fyn kinase dead mutant exists which has a point mutation in the ATP binding pocket (K296R) (19). Finally, there are two mouse models that overexpress Fyn in excitatory neurons. Wild type or constitutively active (Y531F) Fyn is driven by the calcium/calmodulin-dependent protein kinase IIα (CaMKIIα) promoter where Fyn is overexpressed postnatally in the forebrain (20, 21). Studies using these transgenic mice have implicated Fyn in migration, myelination, synaptic plasticity and the regulation of excitatory and inhibitory receptors.

Neuronal Migration

Development of the neocortex involves the coordinated migration of neurons from the ventricular zone radially toward the pial surface. Fyn is expressed in the leading processes of migratory cortical neurons during corticogenesis (22). On a molecular level, Fyn has been implicated in the Reelin pathway. Reelin is an extracellular molecule that activates signaling cascades eventually leading to "outside-in" layering of neurons in the cerebral cortex, where early-generated neurons are located superficially and later-generated neurons are present in deeper layers (23).

Reelin and the intracellular adaptor protein Dab1 lead to activation of Fyn. Then, Fyn phosphorylates Dab1 that initiates signal transduction cascades critical for neuronal migration (24, 25). Fyn null mice have abnormal stratification of layer

II-III neurons with sparing of neurons in the deeper layers (22). Fyn knockout (KO) embryos have an intermediate migration defect, however Fyn Src double KO mice have a *reeler* phenotype suggesting that both kinases function downstream of Reelin and are necessary for cortical layer formation (26)

Oligodendrocyte Maturation

One function of oligodendrocytes (OL) is myelination of axons in the central nervous system (27). Fyn null mice have significantly less myelin and OLs. Fyn kinase dead mutant mice are also hypomyelinated, suggesting that Fyn kinase activity is required for myelination (19). *In vitro*, fewer OLs develop in the absence of Fyn and fewer cells are morphologically mature. Fyn KO OLs are insensitive to IGF-1 induced maturation (28). Many of these phenotypes are recapitulated in Fyn KO mice backcrossed to the C57BL/6 background as early as postnatal day 6. These mice show severe hydrocephalus with defects in oligodendrocyte development (29).

Fyn KO mice have decreased mylein basic protein (MBP) throughout development (27). While this may be due to decreased number of OLs, Fyn also regulates MBP at the mRNA level. Activated Fyn phosphorylates RNA binding protein hnRNP A2, which stimulates translation of MBP mRNA (30). These studies suggest that Fyn does not participate in oligodendrocyte migration, but functions in oligodendrocyte maturation and may affect myelin production post-translationally (27).

Synaptic Plasticity

Synaptic plasticity refers to the ability of neuronal connections, synapses, to change over time. One experimental model of synaptic plasticity is long-term potentiation (LTP), in which repetitive stimulation of excitatory synapses leads to a long-lasting increase in synaptic strength (31). Fyn KO mice have impaired LTP in the hippocampus in response to weak intensity tetanus (32). Interestingly, LTP is normal due to Src compensation until 14 weeks of age in Fyn KO mice when compensatory Src expression is reduced and the LTP deficit begins to be observed (20). Mice overexpressing constitutively active Fyn have a lower threshold for LTP in response to a weak stimulus. These studies suggest that Fyn is not required for the initiation of LTP, but may play a modulatory role influencing the threshold of LTP induction (33).

In addition to the LTP deficit, Fyn KO mice have impaired spatial memory in the Morris water maze. Anatomically, Fyn deletion results in an abnormal localization and an increased number of granule cells in the dentate gyrus and target cells in CA3 (32). Fyn KO mice also have decreased spine density in the hippocampus at 3 months of age (34). These anatomical changes may contribute to aberrant hippocampal function in adult Fyn KO mice.

GABAergic synaptic transmission

Inhibitory neurotransmission is mediated by γ-aminobutyric acid (GABA) through activation of GABA receptors. GABA type A receptors ($GABA_AR$) are heteropentameric GABA-gated chloride channels that are derived from 19 genes

(α1-6, β1-3, γ1-3, δ, ε, θ, π, ρ1-3) (35). Several lines of evidence suggest that Fyn regulates $GABA_AR$ expression and function.

Fyn KO slices from the olfactory bulb were insensitive to the $GABA_AR$ antagonists, bicuculline and picrotoxin (36). Functional deficits in $GABA_A$ –gated chloride flux are also evident in the cerebellum of Fyn KO mice (37). $GABA_AR$ agonists have hypnotic effects, however Fyn KO mice are less sensitive to the hypnotic effects of β2/β3 agonists, but not to an α1 selective agonist (37).

The γ2 subunit of $GABA_AR$ is a Fyn substrate (Table 1). Fyn phosphorylates Y365 and Y367 that are within a consensus tyrosine-based endocytosis motif (YGYECL). Phosphorylation at Y365/7 prevents endocytosis of the $GABA_AR$, leading to increased surface expression of $GABA_ARs$ and synaptic inhibition (38). Mutation of Y365/7 to phenylalanine (Y365/7F) is embryonic lethal. Heterozygous Y365/7F mice have an increased size of inhibitory synapses and increased mini inhibitory postsynaptic currents (mIPSCs) in the CA3 region of the hippocampus. Heterozygous mice also have impaired spatial object recognition (39).

These studies suggest that Fyn deletion leads to abnormal GABAergic synaptic transmission with behavioral, functional and developmental consequences in different brain regions. Fyn may regulate $GABA_ARs$ specifically via the β2, β3 and γ2 subunits.

NMDA Receptor Surface Expression and Cleavage

The *N*-methyl-$_D$-aspartate receptor (NMDAR) is a heteromeric glutamate receptor composed of an obligatory NR1 subunit and modulatory subunits NR2A-D. NMDARs participate in fast excitatory synaptic transmission (40) and form large multi-protein complexes at synaptic membranes (41). The NR2A and NR2B subunits have multiple tyrosine residues on their C-terminal tails that are phosphorylated by SFKs Src and Fyn (40). Exogenous Fyn may upregulate NMDAR currents possibly by tyrosine phosphorylation (42).

Fyn deletion results in decreased tyrosine phosphorylation (pY) of NR2B and Fyn overexpression (Fyn OE) leads to elevated pY NR2B. Interestingly, Fyn KO mice have normal levels of pY NR2A, while Fyn OE mice have increased pY NR2A (21). These results suggest that *in vivo* Fyn may preferentially phosphorylate the NR2B subunit of the NMDAR.

In vitro, Fyn phosphorylates seven tyrosine residues on NR2B (43)(Table 1). In the developing cortex, we found that pY1070, pY1252, pY1336, pY1472 expression was highest in synaptic membranes, while pY1336 was also present in extrasynaptic membranes (44)(Knox and Jiang, unpublished observations). One study reported that pY1252 NR2B is higher in synaptic lipid rafts compared to the post-synaptic density (PSD) (45). Additionally, pY1336 promotes calpain cleavage of NR2B in response to glutamate exposure *in vitro* (46) and is associated with increased interaction of NR2B with phosphatidylinositol 3-kinase (PI-3K) (47).

Among Fyn-mediated NR2B tyrosine phosphorylation sites, Y1472 has been studied the most extensively. Phosphorylation of Y1472 maintains surface

expression of the NR2B-containing NMDARs as it is within the tyrosine endocytosis motif YEKL (48-50). Although pY1472 leads to increased surface expression and less endocytosis of NR2B, it does not affect excitatory synaptic transmission (49, 50). Interestingly, mice in which Y1472 has been replaced with phenylalanine (Y1472F) have impaired fear-related learning and decreased LTP in the amygdala, but normal LTP and spatial memory in the hippocampus. pY1472 affects NR2B tyrosine phosphorylation, as Y1472F mice have 80% less tyrosine phosphorylation in the amygdala compared to WT mice. Y1472F mice also have changes in the NR2B complex, with less α-actinin and CaMKII associated with NR2B (50). pY1472 leads to activation the CaMKII pathway in the amygdala and spinal cord (50, 51). Taken together, these results suggest that Y1472 affects NR2B tyrosine phosphorylation, surface expression, complex formation and downstream signaling cascades.

In summary, Fyn is involved in many processes critical for the development of the brain. Fyn regulates neuronal migration during corticogenesis, oligodendrocyte maturation, myelin production, long-term potentiation, and excitatory and inhibitory neuronal receptors.

Fyn in adult ischemic brain injury

Stroke is a leading cause of death and disability worldwide (52). Preclinical studies in rodents using SFK inhibitors suggest that targeting this kinase family may be protective in ischemic brain injury in humans (53). PP1 (4-amino-5-(4-methylphenyl)-7-(*t*-butyl)pyrazolo[3,4-*d*]pyrimidine) and PP2 (4-amino-5-(4-

chlorophenyl)-7-(*t*-butyl)pyrazolo[3,4-*d*]pyrimidine) are ATP-analogues which compete with ATP for the ATP binding pocket of SFKs, thereby decreasing the ability of SFKs to phosphorylate substrates. Both compounds have some selectivity for Fyn among SFKs (54). Experiments using the adult rodent middle cerebral artery occlusion (MCAO) model have shown that PP2 reduces infarct volume and blood brain barrier leakage (55). PP2 protects CA1 pyramidal neurons from transient ischemia (56). PP1 decreases infarct volume, edema, neurological deficits and increases survival when given after an ischemic insult (57).

While these inhibitors demonstrate that SFKs contribute to ischemic brain injury, few studies have examined the relative contribution of specific SFKs. Using a permanent MCAO model in adult rodents, Paul *et al* found that Src KO mice have decreased infarct volume compared to control mice. However, brain injury in Fyn KO mice (which are on C57BL/6, 129s hybrid background) did not differ from control C57BL/6 or 129s mice (57). This study would suggest that Src may be more important to the pathogenesis of stroke in adults. However it is unknown how brain injury in Fyn KO mice compares to control mice on a hybrid background. Recently, Du *et al* found in an *in vitro* model of ischemia, oxygen glucose deprivation, that Src or Fyn knockdown leads to decreased apoptotic cell death. Fyn knockdown with siRNA had a greater neuroprotective effect (58). This study would suggest that Fyn and Src both contribute to injury, and that Fyn may be more important for apoptotic cell death, which is more prevalent in the neonatal brain.

How does Fyn contribute to ischemic brain injury in adult rodents? Consistent with its role as an adaptor protein, Fyn is part of protein complexes that

assemble in response to ischemia. It may also phosphorylate proteins implicated in cell death pathways.

Fyn exists in at least three ischemia-induced complexes with the NMDAR, PSD95, L-type voltage gated calcium channel (LVGCC), and SynGAP (Figure 3A). Fyn interacts with NMDAR subunits NR2A and NR2B in response to ischemia (59). While it is unknown whether Fyn directly phosphorylates the NMDAR in this setting, its interaction with the NMDAR coincides with elevated tyrosine phosphorylation (60). Tyrosine phosphorylation of NR2A and the NR2A-Fyn association are enhanced by PSD95 after transient brain ischemia (61). Studies have shown that PSD95 and the NMDAR couple to the neurotoxic nitric oxide signaling pathway and disrupting this interaction is protective (62). It is possible that Fyn may promote this interaction, since the NMDAR and PSD95 are Fyn substrates (Table 1).

Fyn phosphorylates PSD95 at Y523, which leads to upregulation of glutamate receptor channel activity in cultured hippocampal neurons (63). The Fyn-NR2A-PSD95 complex is positively regulated by protein tyrosine kinases and negatively regulated by protein tyrosine phosphatases (61). Two neuroprotective agents, Chinese traditional medicine Sy-21 and lithium, are associated with decreased pY NR2A and decreased formation of the Fyn-PSD95-NR2A complex (64, 65). These results suggest that tyrosine phosphorylation of this complex by Fyn may contribute directly to ischemic brain injury by increasing calcium influx through the NMDAR via PSD95 while also increasing nitric oxide signaling by promoting the NMDAR-PSD95 interaction.

To add another layer of complexity, the Fyn-NR2A-PSD95 complex is enhanced by NMDAR and L-type voltage gated calcium channel (L-VGCC) activity. Fyn interacts directly with the α1c subunit of L-VGCC during the peak of its tyrosine phosphorylation (66). Fyn also interacts with PSD95 associated GTPase SynGAP during ischemia. Pei *et al* found that SynGAP tyrosine phosphorylation increases after ischemia, as does its association with Fyn. It is unknown whether Fyn regulates SynGAP phosphorylation or how SynGAP participates in ischemia (67).

Taken together, these studies suggest that Fyn forms complexes in response to ischemia in the adult brain. Fyn may phosphorylate several proteins such as PSD95, SynGAP and membrane channels leading to increased calcium flux and cell death signaling pathways (Figure 3A). While these studies implicate Fyn in the pathogenesis of ischemic brain injury in adults, much less is known about the contribution of Fyn to ischemic brain injury in neonates.

Fyn in neonatal hypoxic-ischemic brain injury

Neonatal encephalopathy affects 1-6/1000 live births (68). Encephalopathy is derived from the Greek words *enkephalos* (brain) and *pathos* (disease) and refers to a disorder of the brain resulting in global dysfunction. Neonatal hypoxic-ischemic encephalopathy (HIE) is caused by hypoxia-ischemia during the prenatal, perinatal or postnatal periods (68). Neonatal HIE is modeled in postnatal day 7 rodents by exposing them to unilateral common carotid artery ligation followed by systemic hypoxia. This leads to injury in the cortex, hippocampus and striatum ipsilateral to the ligation (69-71).

To date there is only one paper from our lab examining the role for Fyn in hypoxic-ischemic brain injury in neonates. We found that SFKs are activated in response to hypoxia-ischemia (HI) in neonatal mice. SFK activity correlates with elevated NR2A and NR2B tyrosine phosphorylation. Fyn has increased association with NR2A and NR2B in response to injury. Significantly, SFK inhibitor PP2 was protective (72). While this study is consistent with the adult ischemia literature, namely that Fyn forms a complex with the NMDAR during HI and PP2 is protective, much remains to be determined about the mechanism by which Fyn contributes to HI brain injury (Figure 3B).

This dissertation focuses on the function of Fyn in neonatal HI brain injury. Chapter 2 examines the subcellular distribution of Fyn and related signaling molecules in the immature and mature brain. Chapter 3 determines whether neuronal Fyn overexpression affects brain injury and NMDAR tyrosine phosphorylation. Chapter 4 explores whether Fyn-mediated NR2B phosphorylation at Y1472 is functionally important. This work sheds light on the role of Fyn in neonatal HI brain injury and provides insight into the molecular mechanisms by which Fyn contributes to cell death.

Figure Legends

Figure 1. Structure of FynB. A) Domain structure of FynB including N-terminal myristoylation and palmitoylation sites as well as regulatory tyrosine residues. B) Fyn binding partners in the **unique region** (**black**), **SH3 domain** (**red**) and **SH2 domain** (**orange**).

Figure 2. Inactive and active conformations of Fyn. Phosphorylation of Y531 in the C-terminus leads to intramolecular interactions which prevent kinase activity and protein-protein interactions while phosphorylation of Y420 leads to an open structure which is catalytically active and accessible to binding partners.

Figure 3. Fyn complexes during ischemia in adult and neonatal rodents. A) In response to ischemia in adult rodents, Fyn interacts with two receptors that flux calcium, the NMDA receptor and α1c subunit of L-type voltage gated calcium channel. PSD95 facilitates the interaction between Fyn and NR2A. Fyn also associates with SynGAP. B) Fyn forms a complex with NMDA receptor subunits NR2A and NR2B during neonatal hypoxic-ischemic brain injury. These proteins are tyrosine phosphorylated, potentially by Fyn, which strengthens complex formation and may contribute to pathogenic calcium signaling in the setting of ischemia.

Fig. 1

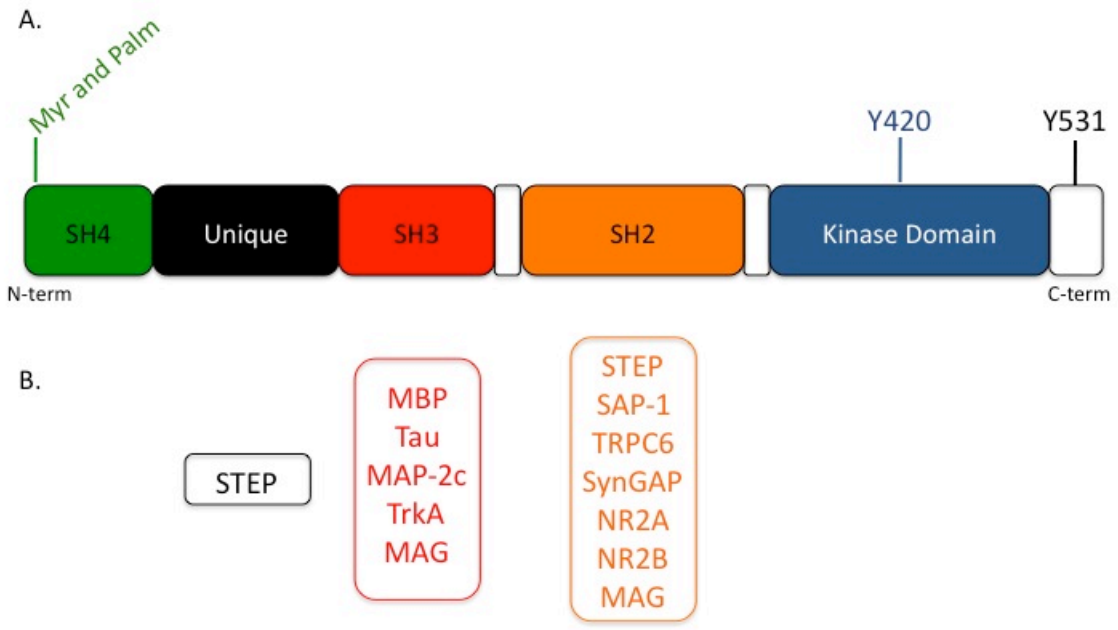

Figure 1. Structure of FynB. A) Domain structure of FynB including N-terminal myristoylation and palmitoylation sites as well as regulatory tyrosine residues. B) Fyn binding partners in the **unique region** (**black**), **SH3 domain** (**red**) and **SH2 domain** (**orange**).

Fig. 2

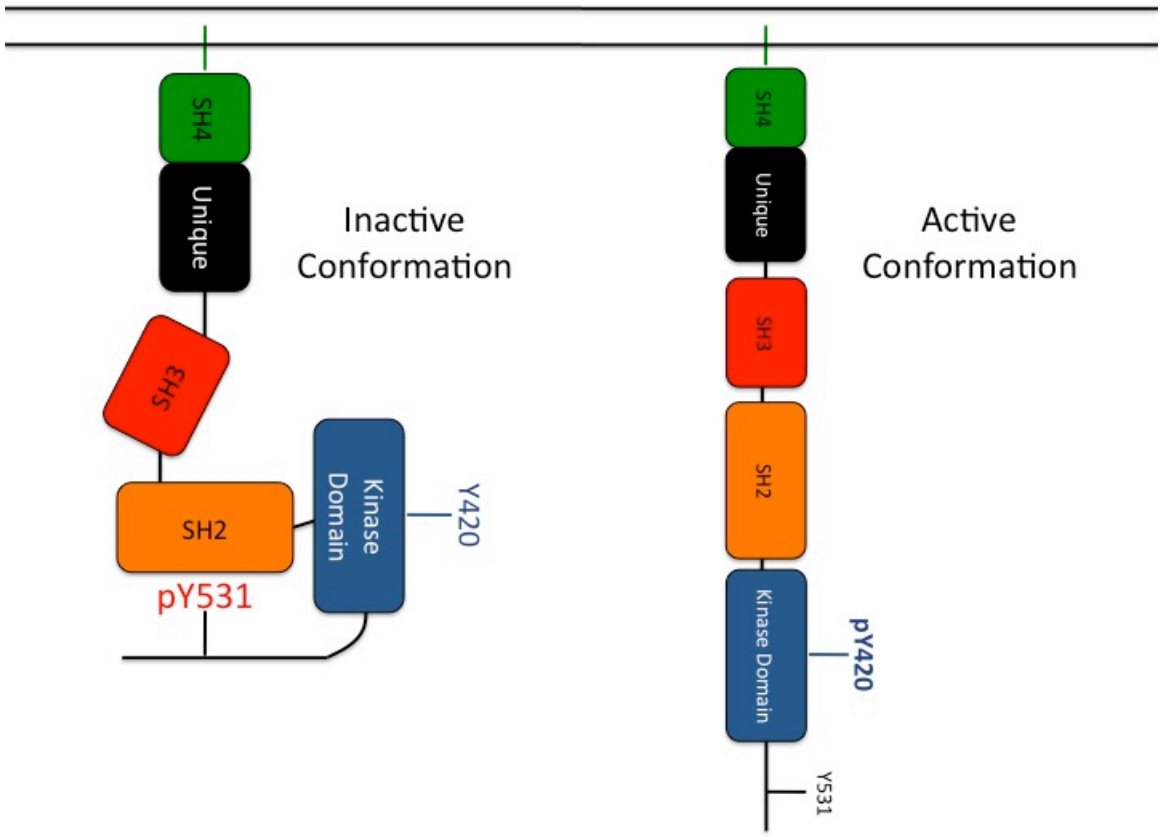

Figure 2. Inactive and active conformations of Fyn. Phosphorylation of Y531 in the C-terminus leads to intramolecular interactions which prevent kinase activity and protein-protein interactions while phosphorylation of Y420 leads to an open structure which is catalytically active and accessible to binding partners.

Table 1. Direct Fyn substrates in the Brain.

Substrate	Site(s)	Outcome of phosphorylation	Refs
PTPRT (Protein Tyrosine Phosphatase Receptor T)	Y912	Decreases phosphatase activity Promotes homophilic interactions Inhibits synapse formation	(73)
TrkA receptor	ND	Promotes transactivation of TrkA by G-Coupled Protein Receptors (GPCRs)	(74)
$Na_v1.2$	ND	Decreases sodium currents	(75)
γ2 subunit $GABA_A$ receptor	Y365, Y367	Prevents clathrin-mediated endocytosis Enhances synaptic inhibition	(39) (38)
NR2A subunit NMDA receptor	ND	ND	(76)
NR2B subunit NMDA receptor	Y932, Y1039, Y1070,Y1109, Y1252,Y1336, Y1472	Y1472: prevents clathrin-mediated endocytosis Y1336: promotes calpain cleavage of NR2B; increased interaction with PI3-K	(76) (43) (48) (46) (47)
TCGAP	Y406	Negatively regulates activity	(77)
p250GAP	ND	Increases association with Fyn	(78)
p190RhoGAP	ND	ND	(79)
Cdk5	Y15	Increases kinase activity Promotes sema3a induced growth cone collapse	(80)
Tau	Y18	Prevents inhibition of anterograde fast axonal transport	(81) (82)
MAP-2c	Y67	Increased interaction with Grb2	(83) (84)
PSD93	Y348	ND	(85)
PSD95	Y523	Increases NMDA receptor currents	(86)
rSLM-1	ND	Prevents splice site selection	(87)
α-synuclein	Y125	ND	(88)
c-Cbl	ND	ND	(89)
N-WASP	Y253	Arp2/3 complex mediated actin polymerization Neurite extension	(90)
Dab1	Y185,Y198	Permits phosphorylation of other Y sites of Dab1 Increases interaction with Fyn Akt activation Degradation of Dab1	(25) (24) (91)

* ND, Not Determined

Fig. 3

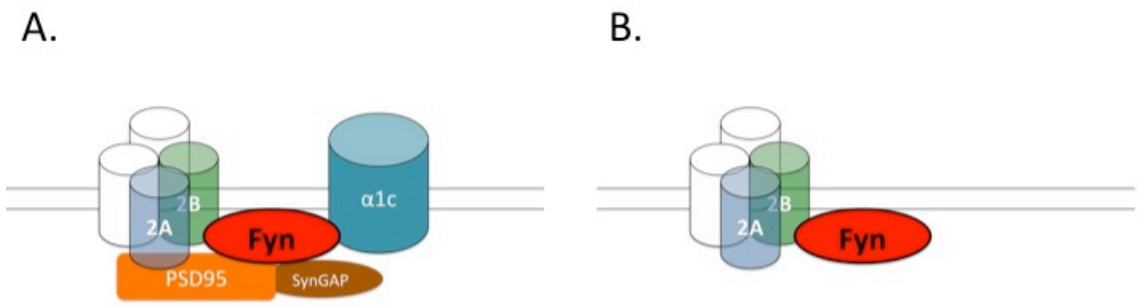

Figure 3. Fyn complexes during ischemia in adult and neonatal rodents. A) In response to ischemia in adult rodents, Fyn interacts with two receptors that flux calcium, the NMDA receptor and α1c subunit of L-type voltage gated calcium channel. PSD95 facilitates the interaction between Fyn and NR2A. Fyn also associates with SynGAP. B) Fyn forms a complex with NMDA receptor subunits NR2A and NR2B during neonatal hypoxic-ischemic brain injury. These proteins are tyrosine phosphorylated, potentially by Fyn, which strengthens complex formation and may contribute to pathogenic calcium signaling in the setting of ischemia.

References

1. Bare, D. J., Lauder, J. M., Wilkie, M. B., and Maness, P. F. (1993) p59fyn in rat brain is localized in developing axonal tracts and subpopulations of adult neurons and glia. In *Oncogene* Vol. 8 pp. 1429-1436
2. Schenone, S., Brullo, C., Musumeci, F., Biava, M., Falchi, F., and Botta, M. (2011) Fyn kinase in brain diseases and cancer: the search for inhibitors. In *Curr Med Chem* Vol. 18 pp. 2921-2942
3. Umemori, H., Wanaka, A., Kato, H., Takeuchi, M., Tohyama, M., and Yamamoto, T. (1992) Specific expressions of Fyn and Lyn, lymphocyte antigen receptor-associated tyrosine kinases, in the central nervous system. In *Brain Res Mol Brain Res* Vol. 16 pp. 303-310
4. Inomata, M., Takayama, Y., Kiyama, H., Nada, S., Okada, M., and Nakagawa, H. (1994) Regulation of Src family kinases in the developing rat brain: correlation with their regulator kinase, Csk. In *J. Biochem.* Vol. 116 pp. 386-392
5. Alland, L., Peseckis, S. M., Atherton, R. E., Berthiaume, L., and Resh, M. D. (1994) Dual myristylation and palmitylation of Src family member p59fyn affects subcellular localization. In *J Biol Chem* Vol. 269 pp. 16701-16705
6. Shenoy-Scaria, A. M., Dietzen, D. J., Kwong, J., Link, D. C., and Lublin, D. M. (1994) Cysteine3 of Src family protein tyrosine kinase determines palmitoylation and localization in caveolae. In *J Cell Biol* Vol. 126 pp. 353-363

7. Hof, W., and Resh, M. D. (1997) Rapid plasma membrane anchoring of newly synthesized p59fyn: selective requirement for NH2-terminal myristoylation and palmitoylation at cysteine-3. In *J Cell Biol* Vol. 136 pp. 1023-1035

8. Ren, R., Mayer, B. J., Cicchetti, P., and Baltimore, D. (1993) Identification of a ten-amino acid proline-rich SH3 binding site. In *Science* Vol. 259 pp. 1157-1161

9. Moran, M. F., Koch, C. A., Anderson, D., Ellis, C., England, L., Martin, G. S., and Pawson, T. (1990) Src homology region 2 domains direct protein-protein interactions in signal transduction. In *Proc Natl Acad Sci USA* Vol. 87 pp. 8622-8626

10. Cooper, J. A., Gould, K. L., Cartwright, C. A., and Hunter, T. (1986) Tyr527 is phosphorylated in pp60c-src: implications for regulation. In *Science* Vol. 231 pp. 1431-1434

11. Xu, W., Harrison, S. C., and Eck, M. J. (1997) Three-dimensional structure of the tyrosine kinase c-Src. In *Nature* Vol. 385 pp. 595-602

12. Gonfloni, S., Weijland, A., Kretzschmar, J., and Superti-Furga, G. (2000) Crosstalk between the catalytic and regulatory domains allows bidirectional regulation of Src. In *Nat Struct Mol Biol* Vol. 7 pp. 281-286

13. Nguyen, T.-H., Liu, J., and Lombroso, P. J. (2002) Striatal enriched phosphatase 61 dephosphorylates Fyn at phosphotyrosine 420. *J Biol Chem* 277, 24274-24279

14. Bhandari, V., Lim, K. L., and Pallen, C. J. (1998) Physical and functional interactions between receptor-like protein-tyrosine phosphatase alpha and p59fyn. In *J Biol Chem* Vol. 273 pp. 8691-8698

15. Ponniah, S., Wang, D. Z., Lim, K. L., and Pallen, C. J. (1999) Targeted disruption of the tyrosine phosphatase PTPalpha leads to constitutive downregulation of the kinases Src and Fyn. In *Curr Biol* Vol. 9 pp. 535-538

16. Wang, P.-S., Wang, J., Xiao, Z.-C., and Pallen, C. J. (2009) Protein-tyrosine phosphatase alpha acts as an upstream regulator of Fyn signaling to promote oligodendrocyte differentiation and myelination. In *J Biol Chem* Vol. 284 pp. 33692-33702

17. Stein, P. L., Lee, H. M., Rich, S., and Soriano, P. (1992) pp59fyn mutant mice display differential signaling in thymocytes and peripheral T cells. In *Cell* Vol. 70 pp. 741-750

18. Yagi, T., Aizawa, S., Tokunaga, T., Shigetani, Y., Takeda, N., and Ikawa, Y. (1993) A role for Fyn tyrosine kinase in the suckling behaviour of neonatal mice. In *Nature* Vol. 366 pp. 742-745

19. Sperber, B. R., Boyle-Walsh, E. A., Engleka, M. J., Gadue, P., Peterson, A. C., Stein, P. L., Scherer, S. S., and McMorris, F. A. (2001) A unique role for Fyn in CNS myelination. In *J Neurosci* Vol. 21 pp. 2039-2047

20. Kojima, N., Wang, J., Mansuy, I. M., Grant, S. G., Mayford, M., and Kandel, E. R. (1997) Rescuing impairment of long-term potentiation in fyn-deficient mice by introducing Fyn transgene. In *Proc Natl Acad Sci USA* Vol. 94 pp. 4761-4765

21. Kojima, N., Ishibashi, H., Obata, K., and Kandel, E. R. (1998) Higher seizure susceptibility and enhanced tyrosine phosphorylation of N-methyl-D-aspartate receptor subunit 2B in fyn transgenic mice. *Learn Mem* 5, 429-445

22. Yuasa, S., Hattori, K., and Yagi, T. (2004) Defective neocortical development in Fyn-tyrosine-kinase-deficient mice. In *Neuroreport* Vol. 15 pp. 819-822

23. Honda, T., Kobayashi, K., Mikoshiba, K., and Nakajima, K. (2011) Regulation of cortical neuron migration by the Reelin signaling pathway. In *Neurochem Res* Vol. 36 pp. 1270-1279

24. Bock, H. H., and Herz, J. (2003) Reelin activates SRC family tyrosine kinases in neurons. In *Curr Biol* Vol. 13 pp. 18-26

25. Arnaud, L., Ballif, B. A., Förster, E., and Cooper, J. A. (2003) Fyn tyrosine kinase is a critical regulator of disabled-1 during brain development. In *Curr Biol* Vol. 13 pp. 9-17

26. Kuo, G., Arnaud, L., Kronstad-O'Brien, P., and Cooper, J. A. (2005) Absence of Fyn and Src causes a reeler-like phenotype. In *J Neurosci* Vol. 25 pp. 8578-8586

27. Krämer-Albers, E.-M., and White, R. (2011) From axon-glial signalling to myelination: the integrating role of oligodendroglial Fyn kinase. In *Cell Mol Life Sci* Vol. 68 pp. 2003-2012

28. Sperber, B. R., and McMorris, F. A. (2001) Fyn tyrosine kinase regulates oligodendroglial cell development but is not required for morphological differentiation of oligodendrocytes. In *J Neurosci Res* Vol. 63 pp. 303-312

29. Goto, J., Tezuka, T., Nakazawa, T., Sagara, H., and Yamamoto, T. (2008) Loss of Fyn tyrosine kinase on the C57BL/6 genetic background causes hydrocephalus with defects in oligodendrocyte development. In *Molecular and Cellular Neuroscience* Vol. 38 pp. 203-212

30. White, R., Gonsior, C., Krämer-Albers, E.-M., Stöhr, N., Hüttelmaier, S., and Trotter, J. (2008) Activation of oligodendroglial Fyn kinase enhances translation of mRNAs transported in hnRNP A2-dependent RNA granules. In *The Journal of Cell Biology* Vol. 181 pp. 579-586

31. Malenka, R. C., and Nicoll, R. A. (1999) Long-term potentiation--a decade of progress? In *Science* Vol. 285 pp. 1870-1874

32. Grant, S. G., O'Dell, T. J., Karl, K. A., Stein, P. L., Soriano, P., and Kandel, E. R. (1992) Impaired long-term potentiation, spatial learning, and hippocampal development in fyn mutant mice. In *Science* Vol. 258 pp. 1903-1910

33. Lu, Y. F., Kojima, N., Tomizawa, K., Moriwaki, A., Matsushita, M., Obata, K., and Matsui, H. (1999) Enhanced synaptic transmission and reduced threshold for LTP induction in fyn-transgenic mice. In *Eur J Neurosci* Vol. 11 pp. 75-82

34. Babus, L. W., Little, E. M., Keenoy, K. E., Minami, S. S., Chen, E., Song, J. M., Caviness, J., Koo, S.-Y., Pak, D. T. S., Rebeck, G. W., Turner, R. S., and Hoe, H.-S. (2011) Decreased dendritic spine density and abnormal spine morphology in Fyn knockout mice. In *Brain Res* Vol. 1415 pp. 96-102

35. Luscher, B., Fuchs, T., and Kilpatrick, C. L. (2011) GABAA receptor trafficking-mediated plasticity of inhibitory synapses. In *Neuron* Vol. 70 pp. 385-409

36. Kitazawa, H., Yagi, T., Miyakawa, T., Niki, H., and Kawai, N. (1998) Abnormal synaptic transmission in the olfactory bulb of Fyn-kinase-deficient mice. In *J Neurophysiol* Vol. 79 pp. 137-142

37. Boehm, S. L., Peden, L., Harris, R. A., and Blednov, Y. A. (2004) Deletion of the fyn-kinase gene alters sensitivity to GABAergic drugs: dependence on beta2/beta3 GABAA receptor subunits. In *J Pharmacol Exp Ther* Vol. 309 pp. 1154-1159

38. Jurd, R., Tretter, V., Walker, J., Brandon, N. J., and Moss, S. J. (2010) Fyn kinase contributes to tyrosine phosphorylation of the GABA(A) receptor gamma2 subunit. In *Mol Cell Neurosci* Vol. 44 pp. 129-134

39. Tretter, V., Revilla-Sanchez, R., Houston, C., Terunuma, M., Havekes, R., Florian, C., Jurd, R., Vithlani, M., Michels, G., Couve, A., Sieghart, W., Brandon, N., Abel, T., Smart, T. G., and Moss, S. J. (2009) Deficits in spatial memory correlate with modified {gamma}-aminobutyric acid type A receptor tyrosine phosphorylation in the hippocampus. In *Proceedings of the National Academy of Sciences* Vol. 106 pp. 20039-20044

40. Salter, M., and Kalia, L. (2004) Src kinases: a hub for NMDA receptor regulation. In *Nat Rev Neurosci* Vol. 5 pp. 317-328

41. Husi, H., Ward, M. A., Choudhary, J. S., Blackstock, W. P., and Grant, S. G. (2000) Proteomic analysis of NMDA receptor-adhesion protein signaling complexes. *Nat Neurosci* 3, 661-669

42. Köhr, G., and Seeburg, P. H. (1996) Subtype-specific regulation of recombinant NMDA receptor-channels by protein tyrosine kinases of the src family. *J Physiol (Lond)* 492, 445-452

43. Nakazawa, T., Komai, S., Tezuka, T., Hisatsune, C., Umemori, H., Semba, K., Mishina, M., Manabe, T., and Yamamoto, T. (2001) Characterization of Fyn-mediated tyrosine phosphorylation sites on GluR epsilon 2 (NR2B) subunit of the N-methyl-D-aspartate receptor. *J Biol Chem* 276, 693-699

44. Jiang, X., Knox, R., Pathipati, P., and Ferriero, D. (2011) Developmental localization of NMDA receptors, Src and MAP kinases in mouse brain. In *Neurosci Lett* Vol. 503 pp. 215-219

45. Delint-Ramirez, I., Fernández, E., Bayés, A., Kicsi, E., Komiyama, N. H., and Grant, S. G. N. (2010) In Vivo Composition of NMDA Receptor Signaling Complexes Differs between Membrane Subdomains and Is Modulated by PSD-95 And PSD-93. In *J Neurosci* Vol. 30 pp. 8162-8170

46. Wu, H., Hsu, F., Gleichman, A., Baconguis, I., Coulter, D., and Lynch, D. (2007) Fyn-mediated Phosphorylation of NR2B Tyr-1336 Controls Calpain-mediated NR2B Cleavage in Neurons and Heterologous Systems. *Journal of Biological Chemistry* 282, 20075-20087

47. Hisatsune, C., Umemori, H., Mishina, M., and Yamamoto, T. (1999) Phosphorylation-dependent interaction of the N-methyl-D-aspartate receptor epsilon 2 subunit with phosphatidylinositol 3-kinase. In *Genes Cells* Vol. 4 pp. 657-666

48. Lavezzari, G., McCallum, J., Lee, R., and Roche, K. W. (2003) Differential binding of the AP-2 adaptor complex and PSD-95 to the C-terminus of the NMDA receptor subunit NR2B regulates surface expression. In *Neuropharmacology* Vol. 45 pp. 729-737

49. Prybylowski, K., Chang, K., Sans, N., Kan, L., Vicini, S., and Wenthold, R. J. (2005) The synaptic localization of NR2B-containing NMDA receptors is controlled by interactions with PDZ proteins and AP-2. *Neuron* 47, 845-857

50. Nakazawa, T., Komai, S., Watabe, A. M., Kiyama, Y., Fukaya, M., Arima-Yoshida, F., Horai, R., Sudo, K., Ebine, K., Delawary, M., Goto, J., Umemori, H., Tezuka, T., Iwakura, Y., Watanabe, M., Yamamoto, T., and Manabe, T. (2006) NR2B tyrosine phosphorylation modulates fear learning as well as amygdaloid synaptic plasticity. *EMBO J* 25, 2867-2877

51. Matsumura, S., Kunori, S., Mabuchi, T., Katano, T., Nakazawa, T., Abe, T., Watanabe, M., Yamamoto, T., Okuda-Ashitaka, E., and Ito, S. (2010) Impairment of CaMKII activation and attenuation of neuropathic pain in mice lacking NR2B phosphorylated at Tyr1472. In *European Journal of Neuroscience* Vol. 32 pp. 798-810

52. Davis, S. M., and Donnan, G. A. (2012) Clinical practice. Secondary prevention after ischemic stroke or transient ischemic attack. In *N Engl J Med* Vol. 366 pp. 1914-1922

53. Chico, L. K., Van Eldik, L. J., and Watterson, D. M. (2009) Targeting protein kinases in central nervous system disorders. In *Nat Rev Drug Discov* Vol. 8 pp. 892-909

54. Hanke, J. H., Gardner, J. P., Dow, R. L., Changelian, P. S., Brissette, W. H., Weringer, E. J., Pollok, B. A., and Connelly, P. A. (1996) Discovery of a novel, potent, and Src family-selective tyrosine kinase inhibitor. Study of Lck- and FynT-dependent T cell activation. In *J Biol Chem* Vol. 271 pp. 695-701

55. Takenaga, Y., Takagi, N., Murotomi, K., Tanonaka, K., and Takeo, S. (2009) Inhibition of Src activity decreases tyrosine phosphorylation of occludin in brain capillaries and attenuates increase in permeability of the blood-brain barrier after transient focal cerebral ischemia. In *J Cereb Blood Flow Metab* Vol. 29 pp. 1099-1108

56. Hou, X.-Y., Liu, Y., and Zhang, G.-Y. (2007) PP2, a potent inhibitor of Src family kinases, protects against hippocampal CA1 pyramidal cell death after transient global brain ischemia. In *Neuroscience Letters* Vol. 420 pp. 235-239

57. Paul, R., Zhang, Z. G., Eliceiri, B. P., Jiang, Q., Boccia, A. D., Zhang, R. L., Chopp, M., and Cheresh, D. A. (2001) Src deficiency or blockade of Src activity in mice provides cerebral protection following stroke. In *Nat Med* Vol. 7 pp. 222-227

58. Du, C.-P., Tan, R., and Hou, X.-Y. (2012) Fyn Kinases Play a Critical Role in Neuronal Apoptosis Induced by Oxygen and Glucose Deprivation or Amyloid-β Peptide Treatment. In *CNS Neurosci Ther* pp. n/a-n/a

59. Takagi, N., Cheung, H. H., Bissoon, N., Teves, L., Wallace, M. C., and Gurd, J. W. (1999) The effect of transient global ischemia on the interaction of Src and Fyn with the N-methyl-D-aspartate receptor and postsynaptic densities: possible involvement of Src homology 2 domains. *J Cereb Blood Flow Metab* 19, 880-888

60. Cheung, H. H., Takagi, N., Teves, L., Logan, R., Wallace, M. C., and Gurd, J. W. (2000) Altered association of protein tyrosine kinases with postsynaptic densities after transient cerebral ischemia in the rat brain. In *J Cereb Blood Flow Metab* Vol. 20 pp. 505-512

61. Chen, M., Hou, X., and Zhang, G. (2003) Tyrosine kinase and tyrosine phosphatase participate in regulation of interactions of NMDA receptor subunit 2A with Src and Fyn mediated by PSD-95 after transient brain ischemia. In *Neuroscience Letters* Vol. 339 pp. 29-32

62. Aarts, M. (2002) Treatment of Ischemic Brain Damage by Perturbing NMDA Receptor- PSD-95 Protein Interactions. In *Science* Vol. 298 pp. 846-850

63. Du, C.-P., Gao, J., Tai, J.-M., Liu, Y., Qi, J., Wang, W., and Hou, X.-Y. (2009) Increased tyrosine phosphorylation of PSD-95 by Src family kinases after brain ischaemia. In *Biochem J* Vol. 417 pp. 277-285

64. Chen, M., Wang, Y., Liu, Y., Hou, X.-Y., Zhang, Q.-G., Meng, F.-j., and Zhang, G.-Y. (2003) Possible mechanisms underlying the protective effects of SY-21, an extract of a traditional Chinese herb, on transient brain ischemia/reperfusion-induced neuronal death in rat hippocampus. In *Brain Res* Vol. 989 pp. 180-186

65. Ma, J., and Zhang, G.-Y. (2003) Lithium reduced N-methyl-d-aspartate receptor subunit 2A tyrosine phosphorylation and its interactions with Src and Fyn mediated by PSD-95 in rat hippocampus following cerebral ischemia. In *Neurosci Lett* Vol. 348 pp. 185-189

66. Hou, X.-Y., Zhang, G.-Y., Yan, J.-Z., and Liu, Y. (2003) Increased tyrosine phosphorylation of α1C subunits of L-type voltage-gated calcium channels and interactions among Src/Fyn, PSD-95 and α1C in rat hippocampus after transient brain ischemia. In *Brain Res* Vol. 979 pp. 43-50

67. Pei, L., Teves, R. L., Wallace, M. C., and Gurd, J. W. (2001) Transient cerebral ischemia increases tyrosine phosphorylation of the synaptic RAS-GTPase activating protein, SynGAP. In *J Cereb Blood Flow Metab* Vol. 21 pp. 955-963

68. Ferriero, D. (2004) Neonatal brain injury. *N Engl J Med* 351, 1985-1995

69. Rice, J. E., Vannucci, R. C., and Brierley, J. B. (1981) The influence of immaturity on hypoxic-ischemic brain damage in the rat. *Ann Neurol.* 9, 131-141

70. Ditelberg, J. S., Sheldon, R. A., Epstein, C. J., and Ferriero, D. M. (1996) Brain injury after perinatal hypoxia-ischemia is exacerbated in copper/zinc superoxide dismutase transgenic mice. *Pediatr Res* 39, 204-208

71. Sheldon, R. A., Sedik, C., and Ferriero, D. M. (1998) Strain-related brain injury in neonatal mice subjected to hypoxia-ischemia. *Brain Res* 810, 114-122

72. Jiang, X., Mu, D., Biran, V., Faustino, J., Chang, S., Rincón, C., Sheldon, R., and Ferriero, D. (2008) Activated Src kinases interact with the N-methyl-D-aspartate receptor after neonatal brain ischemia. *Ann Neurol.* 63, 632-641

73. Lim, S.-H., Kwon, S.-K., Lee, M. K., Moon, J., Jeong, D. G., Park, E., Kim, S. J., Park, B. C., Lee, S. C., Ryu, S. E., Yu, D.-Y., Chung, B. H., Kim, E., Myung, P.-K., and Lee, J.-R. (2009) Synapse formation regulated by protein tyrosine phosphatase

receptor T through interaction with cell adhesion molecules and Fyn. In *EMBO J* Vol. 28 pp. 3564-3578, Nature Publishing Group

74. Rajagopal, R., and Chao, M. V. (2006) A role for Fyn in Trk receptor transactivation by G-protein-coupled receptor signaling. In *Molecular and Cellular Neuroscience* Vol. 33 pp. 36-46

75. Ahn, M., Beacham, D., Westenbroek, R. E., Scheuer, T., and Catterall, W. A. (2007) Regulation of Na(v)1.2 channels by brain-derived neurotrophic factor, TrkB, and associated Fyn kinase. In *Journal of Neuroscience* Vol. 27 pp. 11533-11542

76. Suzuki, T., and Okumura-Noji, K. (1995) NMDA receptor subunits epsilon 1 (NR2A) and epsilon 2 (NR2B) are substrates for Fyn in the postsynaptic density fraction isolated from the rat brain. In *Biochem Biophys Res Commun* Vol. 216 pp. 582-588

77. Liu, H., Nakazawa, T., Tezuka, T., and Yamamoto, T. (2006) Physical and functional interaction of Fyn tyrosine kinase with a brain-enriched Rho GTPase-activating protein TCGAP. In *J Biol Chem* Vol. 281 pp. 23611-23619

78. Taniguchi, S., Liu, H., Nakazawa, T., Yokoyama, K., Tezuka, T., and Yamamoto, T. (2003) p250GAP, a neural RhoGAP protein, is associated with and phosphorylated by Fyn. In *Biochem Biophys Res Commun* Vol. 306 pp. 151-155

79. Brouns, M. R., Matheson, S. F., and Settleman, J. (2001) p190 RhoGAP is the principal Src substrate in brain and regulates axon outgrowth, guidance and fasciculation. In *Nat Cell Biol* Vol. 3 pp. 361-367

80. Sasaki, Y., Cheng, C., Uchida, Y., Nakajima, O., Ohshima, T., Yagi, T., Taniguchi, M., Nakayama, T., Kishida, R., Kudo, Y., Ohno, S., Nakamura, F., and Goshima, Y. (2002) Fyn and Cdk5 mediate semaphorin-3A signaling, which is involved in regulation of dendrite orientation in cerebral cortex. In *Neuron* Vol. 35 pp. 907-920

81. Lee, G., Thangavel, R., Sharma, V. M., Litersky, J. M., Bhaskar, K., Fang, S. M., Do, L. H., Andreadis, A., Van Hoesen, G., and Ksiezak-Reding, H. (2004) Phosphorylation of tau by fyn: implications for Alzheimer's disease. In *Journal of Neuroscience* Vol. 24 pp. 2304-2312

82. Kanaan, N. M., Morfini, G., Pigino, G., LaPointe, N. E., Andreadis, A., Song, Y., Leitman, E., Binder, L. I., and Brady, S. T. (2012) Phosphorylation in the amino terminus of tau prevents inhibition of anterograde axonal transport. In *Neurobiol. Aging* Vol. 33 pp. 826.e815-830

83. Zamora-Leon, S. P., Lee, G., Davies, P., and Shafit-Zagardo, B. (2001) Binding of Fyn to MAP-2c through an SH3 binding domain. Regulation of the interaction by ERK2. In *J Biol Chem* Vol. 276 pp. 39950-39958

84. Zamora-Leon, S. P., Bresnick, A., Backer, J. M., and Shafit-Zagardo, B. (2005) Fyn phosphorylates human MAP-2c on tyrosine 67. In *J Biol Chem* Vol. 280 pp. 1962-1970

85. Nada, S. (2003) Identification of PSD-93 as a Substrate for the Src Family Tyrosine Kinase Fyn. In *Journal of Biological Chemistry* Vol. 278 pp. 47610-47621

86. Du, C.-P., Gao, J., Tai, J.-M., Liu, Y., Qi, J., Wang, W., and Hou, X.-Y. (2009) Increased tyrosine phosphorylation of PSD-95 by Src family kinases after brain ischaemia. In *Biochem J* Vol. 417 pp. 277-285

87. Stoss, O., Novoyatleva, T., Gencheva, M., Olbrich, M., Benderska, N., and Stamm, S. (2004) p59(fyn)-mediated phosphorylation regulates the activity of the tissue-specific splicing factor rSLM-1. In *Mol Cell Neurosci* Vol. 27 pp. 8-21

88. Nakamura, T., Yamashita, H., Takahashi, T., and Nakamura, S. (2001) Activated Fyn Phosphorylates α-Synuclein at Tyrosine Residue 125. In *Biochem Biophys Res Commun* Vol. 280 pp. 1085-1092

89. Nishio, H., Otsuka, M., Kinoshita, S., Tokuoka, T., Nakajima, M., Noda, Y., Fukuyama, Y., and Suzuki, K. (2002) Phosphorylation of c-Cbl protooncogene product following ethanol administration in rat cerebellum: possible involvement of Fyn kinase. In *Brain Res* Vol. 950 pp. 203-209

90. Suetsugu, S., Hattori, M., Miki, H., Tezuka, T., Yamamoto, T., Mikoshiba, K., and Takenawa, T. (2002) Sustained activation of N-WASP through phosphorylation is essential for neurite extension. In *Dev Cell* Vol. 3 pp. 645-658

91. Feng, L., and Cooper, J. A. (2009) Dual functions of Dab1 during brain development. In *Mol Cell Biol* Vol. 29 pp. 324-332

Chapter 2: Developmental localization of NMDA receptors, Src and MAP kinases in the mouse brain

Xiangning Jiang, Renatta Knox, Praneeti Pathipati and Donna Ferriero

Modified from: (1)

Introduction

There are striking differences between the neonatal and adult brain in response to hypoxic-ischemic (HI) brain injury. Due to higher levels of glutamate receptor expression that promote activity-dependent neuronal plasticity, the neonatal brain is more excitable and prone to oxidative stress than the adult brain (2, 3). Recent studies show that the *N*-methyl-D-aspartate receptors (NMDAR), which have long been considered as a critical mediator for excitotoxic cell death, are also able to initiate neuronal survival depending on whether they are synaptically or extrasynaptically located (4-6). Synaptic NMDAR stimulation boosts intrinsic antioxidant defenses (7), activates the Ras-extracellular signal regulated kinase (ERK)-cAMP response element binding protein (CREB) pathway and translation of prosurvival proteins (8), whereas stimulation of extrasynaptic NMDAR induces pro-apoptotic proteins through an ERK-CREB shut-off pathway (9, 10) and activation of p38 (11). Interestingly, coupling of NMDAR to intracellular signaling pathways is developmentally regulated as well (12-14). This raises the question whether the NMDAR and its associated proteins are localized differentially in synaptic membrane components in neonatal and adult brain, which allows for specificity of signaling cascades.

NMDARs are heteromeric complexes of the NR1, NR2 (2A-2D) and NR3 subunits. The NR1 subunit is essential for functional NMDAR channels, whereas the NR2 subunits modulate channel activity and functional properties of the receptors. We have previously shown that, following neonatal HI, the Src family kinases (SFKs) are activated in the postsynaptic densities (PSDs) and interact with the NR2A and

NR2B subunits (15). Protection by inhibiting specific SFKs implicates SFKs in the injury seen in neonatal HI. SFKs, especially Fyn, mediate tyrosine phosphorylation of NR2B at three major sites: tyrosine (Y) 1472, Y1252 and Y1336 (16). By contrast, the striatal-enriched tyrosine phosphatase (STEP) dephosphorylates NR2B at Y1472 and reduces activity of its substrates ERK and p38 (17-19). A recent study demonstrates in mature hippocampal slices that phosphorylation of Y1472 and Y1336 is associated with synaptic and extrasynaptic enrichment of NR2B, respectively (20). This points to the possibility that SFKs and STEP may regulate NMDAR trafficking on the cell surface by phosphorylation or dephosphorylation of different residues. It is important to determine whether SFK modulation of the NMDAR and downstream MAP kinases are uniquely affected by their subcellular localization in the developing brain.

In the present study, we characterized the distribution of the NMDAR, Src and MAP kinases in synaptic and extrasynaptic membranes of neonatal and adult mouse brain to begin to investigate the mechanisms underlying differences between synaptic versus extrasynaptic NMDAR signaling.

Material and Methods

Animals

All animal experiments were approved by the institutional animal care and use committee at the University of California San Francisco and every effort was made to minimize animal suffering and reduce the number of animals used.

Subcellular Fractionation

Cortical tissue was dissected from the brains of postnatal day 7 (P7) and adult (around P48) C57BL/6 mice. Purification of synaptic and extrasynaptic membrane proteins was performed according to Goebel-Goody and colleagues' procedure (20) using a subcellular fractionation approach followed by extraction with Triton X-100. In brief, cortical tissue was homogenized in ice-cold sucrose buffer containing 0.32M sucrose, 10mM Tris-HCl (pH 7.4), 1mM EDTA, 1mM EGTA and protease and phosphatase inhibitors (Complete mini and Phospho-Stop cocktail tablets, Roche, Indianapolis, IN). A low-speed (1,000x*g*) centrifugation was performed to remove the nuclear fraction and tissue debris. The resulting supernatant (S1) was spun at 10,000x*g* for 15 minutes to yield a crude membrane fraction (P2). The supernatant (S2) was then centrifuged at 100,000xg for 60 min to separate cytoplasmic protein (S3) and intracellular light membrane fraction (P3). The P2 was subsequently resuspended in 120 μl sucrose buffer, and mixed with 8 volumes of 0.5% Triton X-100 buffer containing 10mM Tris-HCl (pH 7.4), 1mM EDTA, 1mM EGTA and protease and phosphatase inhibitors. The mixture was homogenized again with 30 pulses of a glass pestle and rotated at 4°C for 30 min followed by centrifugation at 32,000xg for 30 min in a TL-100 tabletop ultracentrifuge (Beckman). The resultant pellet (TxP) containing Triton X-insoluble PSD proteins was considered as the synaptic membrane compartment. The supernatant (TxS) containing proteins soluble in Triton X-100 and not tightly bound to the PSD was defined as the extrasynaptic membrane compartment. The S3 and

TxS fractions were further concentrated by adding 8 volumes of 100% acetone and incubated at -20 °C overnight. The precipitated protein was spun at 3000xg at 4°C for 15 min and dried at room temperature for 15min. All the pellets were dissolved in TE buffer (100 mM Tris-HCl, 10mM EDTA) with 1% SDS. The samples were sonicated, boiled for 5 min and stored at -80 °C until use. Protein concentration was determined by the bicinchoninic acid method (Pierce).

Western Blotting

For Western blot analysis, an equal amount of cytoplasmic (S3), extrasynaptic (TxS) and synaptic (TxP) protein (7μg) from P7 and adult mice was applied to 4-12% Bis-Tris SDS polyacrylamide gel electrophoresis (Invitrogen, Carlsbad, CA) and transferred to polyvinyl difluoride membrane as described elsewhere [10]. The blots were probed with the following primary antibodies overnight at 4°C: NR1 (1:1,000; BD Pharmingen, San Diego, CA), NR2A (1:500; Upstate Cell Signaling Solutions, Lake Placid, NY), NR2B (1:2,000; BD), Fyn (1:800; Santa Cruz Biotechnology, Santa Cruz, CA), Src (1:500; Upstate), the phospho-site specific antibodies against NR2B Tyr1252, Tyr1336, and Tyr1472 (1:800; PhosphoSolutions, Inc. Aurora, CO), ERK (1: 2000; Cell signaling Technology, Danvers, MA), p38 (1:200; Cell signaling), and STEP (1:500; Upstate). The following antibodies were used to verify synaptic and extrasynaptic membrane purity: PSD-95 (1:2,000; Upstate), P97 ATPase (1:1,000; Fitzgerald Industries International, Concord, MA), EEA1 (1:200; Cell signaling) and Rab11 (1:500; Cell signaling). Appropriate secondary horseradish peroxidase-conjugated antibodies (1:2,000,

Santa Cruz) were used, and signal was visualized with enhanced chemiluminescence (Amersham). Image J software was used to measure the mean optical densities (OD) and areas of protein signal on radiographic film after scanning.

To quantify the protein expression from Western blot analysis, the OD values from each blot were normalized to P7 synaptic values. For STEP and p38, the blots were normalized to P7 extrasynaptic values.

Statistical Analysis

Two-tailed Student's t-tests were used to compare protein expression between P7 and adult animals in cytoplasmic, synaptic and extrasynaptic membrane fractions. Statistical significance was determined as $p<0.05$. Data are presented as mean ± SD from three independent experiments.

Results

Purity of the synaptic and extrasynaptic membranes

The purity of the subcellular compartments was assessed by Western blotting (Fig. 1). Synaptic markers used were proteins representative of the PSD (PSD-95, NR1 and NR2A). For identification of extrasynaptic membrane proteins, we used antibodies against EEA1 and Rab11, which are involved in early endosomal transport and receptor endocytic recycling that take place at extrasynaptic sites (21, 22). The p97 ATPase (also called valosin-containing protein) is bound to Golgi and endoplasmic reticulum membrane and was used as a marker for intracellular light

membrane (P3). Consistent with previous studies using the same approach [2], PSD95 was exclusively in synaptic membrane (TxP); NR1 and NR2A were most enriched in synaptic membranes. EEA1 and Rab11 were not expressed in TxP, but most concentrated in extrasynaptic fractions (TxS). p97 ATPase was predominantly present in the intracellular light membrane fraction (P3). These results confirmed that synaptic and extrasynaptic membranes were enriched without contamination with other subcellular components.

Membrane Localization of NMDARs in P7 and adult mouse cortex

NR1, NR2A and NR2B were all concentrated in synaptic membranes in both P7 and adult brains (Fig. 2a). In the synaptic fraction, the expression of NR2B decreased ($p=0.0155$, P7 vs. adult), while NR2A increased ($p=0.0487$, P7 vs. adult), with development (Fig. 2a-c). NR1 remained constant at both ages. Extrasynaptically, there was significantly higher expression of NR1 ($p=0.0348$) and NR2B ($p=0.0276$) at P7 than that in adult brain, suggesting that NR1/NR2B is the primary NMDAR subtype at extrasynaptic sites at P7. NR2B is also the primary subunit to be tyrosine phosphorylated by Fyn in the PSDs, so we chose to examine the localization and expression of NR2B that is phosphorylated at three major tyrosine residues by Fyn. pY1472NR2B and pY1252NR2B were located predominantly in synapses at both ages and increased significantly with development (Fig. 2a, 2d, $p=0.0432$ for NR2BY1472, $p=0.0188$ for NR2BY1252, P7 vs. adult). Although pY1336NR2B was more enriched synaptically Fig. 2a, 2c), it was the major phosphorylated NR2B form located extrasynaptically at P7 (12.56% of

total pY1336NR2B) with no extrasynaptic expression in the adult.

Membrane localization of SFKs and STEP in P7 and adult mouse cortex

Next, we examined the subcellular localization of Src, Fyn and STEP, which are the best-characterized tyrosine kinases and phosphatase involved in phospho-regulation of NMDAR and both are changed following neonatal HI. Fyn was more concentrated at synapses and decreased with age in both synaptic and extrasynaptic membranes (Fig. 3a-b, p=0.0006 for synaptic Fyn; p=0.0048 for extrasynaptic Fyn, P7 vs. adult). Src was equally distributed between synaptic and extrasynaptic membranes with lower levels in the adult brain than at P7 (Fig. 3a-b, p=0.035 for synaptic Src; p=0.0346 for extrasynaptic Src, P7 vs. adult). We used a STEP antibody that detects the three major alternatively spliced variants (61, 46 and 38kD). Membrane-associated STEP61 was located extrasynaptically and was 1.7-fold higher in adult animals compared to P7 mice (Fig. 3a, 3d, p=0.0233). Other STEP isoforms with lower molecular weights were detected in the cytoplasmic fractions and expressed at higher levels in adult animals as well.

Membrane localization of ERK and p38 in P7 and adult mouse cortex

The concentration of ERK and p38 was highest in the cytoplasmic fraction compared with extrasynaptic and synaptic fractions (Fig. 3a). There was no change with age in cytoplasmic ERK or p38 expression. In membranes, ERK was more enriched extrasynaptically with a small fraction in synaptic membranes. ERK1, but

not ERK2, decreased with development at synaptic membranes (p=0.0017, P7 vs. adult). p38 was enriched extrasynaptically and not detectable in the synaptic fraction (Fig. 3a, 3d). Expression of extrasynaptic p38 was higher at P7 than that in adult (p=0.0013).

Discussion

We examined the distribution of the NMDAR, Src and MAP kinases in synaptic and extrasynaptic membranes in the developing brain to investigate their age-related expression on the cell surface. Our major findings are: 1) At all ages, membrane-associated NMDAR and Src kinases are predominantly at synapses, whereas STEP and its substrates ERK and p38 are much more concentrated extrasynaptically. 2) There is a developmental switch from NR2B to NR2A expression in synaptic membranes with more NR1/NR2B expression in extrasynaptic membranes in the developing brain. 3) While Fyn and Src protein levels decrease with age, phosphorylation of NR2BY1472 and NR2BY1252 that is mediated by these kinases is significantly higher in the adult animals. At P7, phosphorylation of NR2B at Y1336 is associated with extrasynaptic NMDARs. 4) The developmental increase in STEP is accompanied by the decrease in p38 extrasynaptically.

NR2B and Fyn are expressed at much higher levels at P7 in both synaptic and extrasynaptic membranes, suggesting the importance of Fyn in regulating NR2B in the developing brain. Fyn modulates NMDAR internalization by phosphorylation at NR2B Y1472. Although NR2B Y1472 has been well characterized, much less is

known about the physiological function of NR2B Y1252 and NR2BY1336. From our study, although NR2B Y1472, Y1252 and Y1336 are all enriched in the synapses, NR1/NR2B is the main subunit occupying extrasynaptic sites with concomitant phosphorylation at Y1336 in the immature brain. This is in agreement with a recent study in adult hippocampal slices showing that phosphorylation of Y1336 is associated with extrasynaptic enrichment of NR2B (20). Other studies suggested that Y1336 phosphorylation enhances calpain-mediated extrasynaptic NR2B cleavage at C terminus, which may affect the ability of NR2B binding to associated proteins and thus change downstream signaling complexes (23). This site also mediates activation of phosphatidylinositol 3-kinase (PI3K) and p38 dephosphorylation in mature hippocampal cultures following extrasynaptic NR2B stimulation, suggesting a possible protective role against NMDA toxicity (24). This phenomenon was not observed in immature cultures since NR2B Y1336 was not increased under the same condition (24). We found elevated NR2B Y1472, Y1252 and Y1336 expression early after neonatal HI at P7 (unpublished data), but how these modifications link to their surface locations after HI and the subsequent downstream NMDAR signaling is unknown.

STEP61, the membrane-associated isoform, was found primarily at extrasynaptic sites in both P7 and the adult brain. STEP substrates ERK and p38 are also associated with extrasynaptic membranes. The extrasynaptic localization of STEP and p38 is consistent with a recent study from adult mouse cortical tissue (11), that supports the preference of p38 activation and STEP cleavage following extrasynaptic NMDAR stimulation or *in vitro* ischemia (11). STEP61 cleavage was

also found in a neonatal P7 rat HI model (25). Compared to the adult brain, P7 animals have lower STEP and higher p38 available at extrasynaptic sites; this may be related to the greater susceptibility of neonates to HI or other brain injury involving excitotoxicity.

ERK, another STEP substrate, while more concentrated extrasynaptically, has been reported to be activated by synaptic NMDAR stimulation and shut-off by extrasynaptic NMDAR. Complex mechanisms are involved in ERK regulation, therefore ERK activity is determined by whether activation or inhibition dominates. The functional significance of extrasynaptic ERK and p38 is not clear. It is possible that in the cytosol ERK and p38 are translocated to different cellular compartments to interact with specific signal proteins in response to different stimuli.

In conclusion, our study demonstrates a developmental regulation in localization and expression of NMDAR, Src and MAP kinases in synaptic and extrasynaptic membranes in mouse cortical tissue. Protein localization could contribute to, but is unlikely to fully account for the differences between synaptic versus extrasynaptic NMDAR signaling. Determining whether pro-death or pro-survival signaling following NMDAR activation predominates will allow for identification of more specific therapeutic targets for neonatal HI.

Figure legends

Figure 1. Characterization of synaptic and extrasynaptic membranes.

Representative Western blots with each subcellular fractions (S3: cytoplasmic fraction; P1: nuclear fraction; P3: intracellular membrane fraction; TxS: extrasynaptic membrane fraction; TxP: synaptic membrane fraction) probed with the PSD markers PSD95, NR1 and NR2A; the early endosomal markers EEA1 and Rab11 and the ER marker p97ATPase.

Figure 2. Localization of the NMDAR and phospho-NR2B at different subcellular fractions in P7 and adult mouse cortex.

Equal amount of protein from cytoplasmic (cyto-), extrasynaptic (extra-) and synaptic (synap-) fractions was used for Western blotting. Primary antibodies are indicated on the left of the blots (2a). For each protein, the OD values were normalized to P7 synaptic values. Data are presented on the right (2b-2d) as mean ± SD from 3 independent experiments. *: $p < 0.05$ versus adult values from the same fraction.

Figure 3. Localization of the Src and MAP kinases, STEP at different subcellular fractions in P7 and adult mouse cortex.

Equal amount of protein from cytoplasmic (cyto-), extrasynaptic (extra-) and synaptic (synap-) fractions was used for Western blotting. Primary antibodies are indicated on the left of the blots (3a). For Fyn, Src and ERK (3b-3c), the OD values were normalized to P7 synaptic values. For STEP and p38 (3d), the OD values were

normalized to P7 extrasynaptic values. Data are presented on the right (3b-3d) as mean ± SD from 3 independent experiments. *: $p < 0.05$ versus adult values from the same fraction.

Fig 1

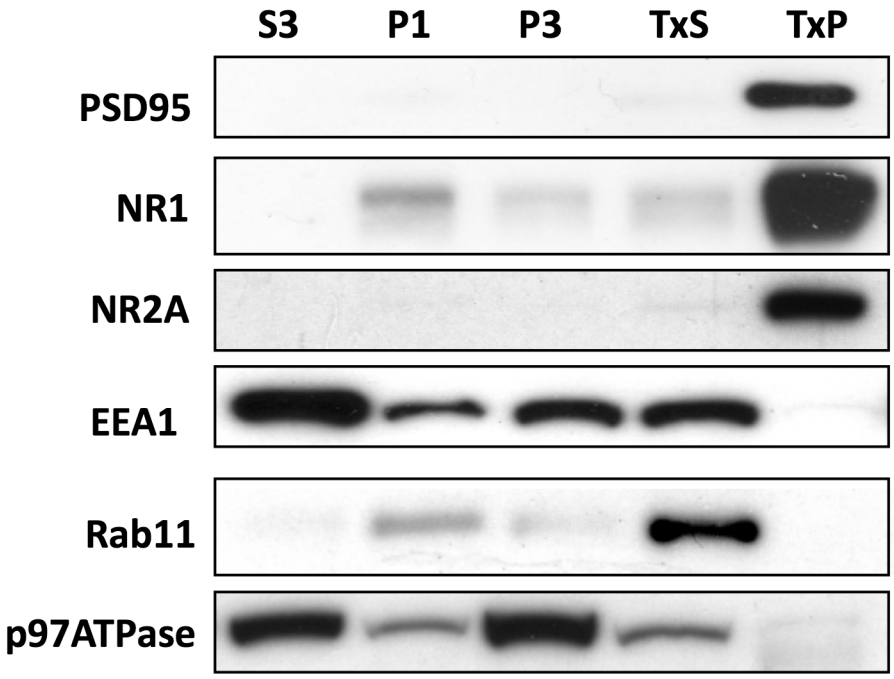

Figure 1. Characterization of synaptic and extrasynaptic membranes. Representative Western blots with each subcellular fractions (S3: cytoplasmic fraction; P1: nuclear fraction; P3: intracellular membrane fraction; TxS: extrasynaptic membrane fraction; TxP: synaptic membrane fraction) probed with the PSD markers PSD95, NR1 and NR2A; the early endosomal markers EEA1 and Rab11 and the ER marker p97ATPase.

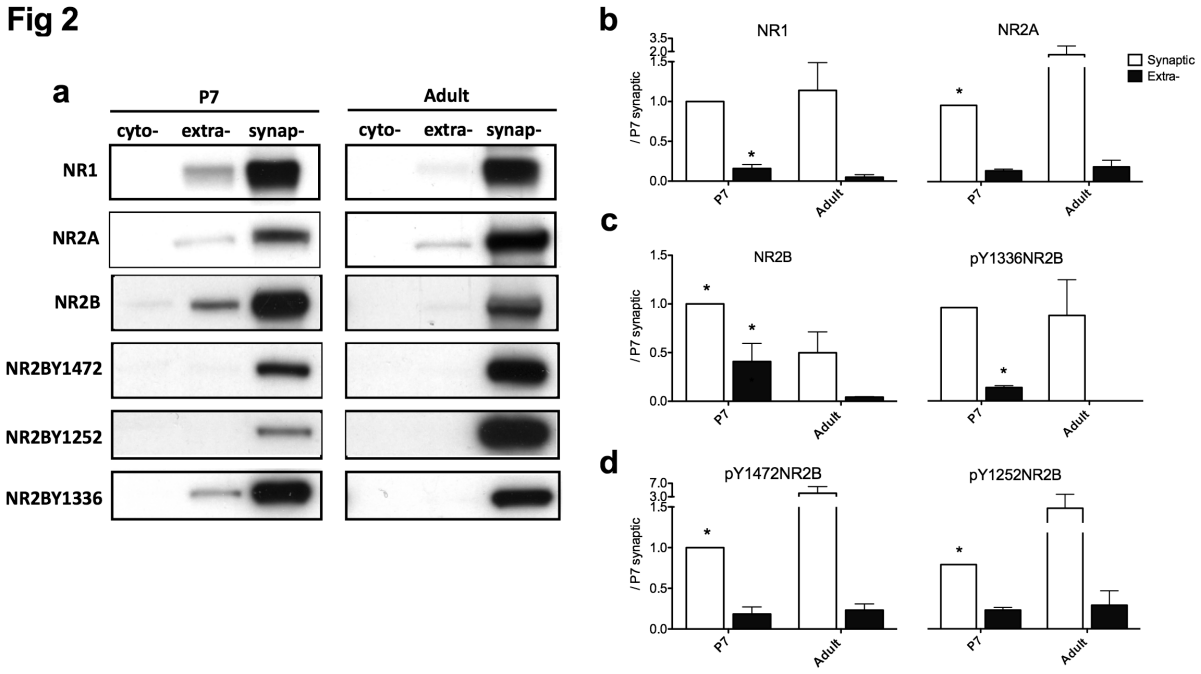

Figure 2. Localization of the NMDAR and phospho-NR2B at different subcellular fractions in P7 and adult mouse cortex.
Equal amount of protein from cytoplasmic (cyto-), extrasynaptic (extra-) and synaptic (synap-) fractions was used for Western blotting. Primary antibodies are indicated on the left of the blots (2a). For each protein, the OD values were normalized to P7 synaptic values. Data are presented on the right (2b-2d) as mean ± SD from 3 independent experiments. *: $p < 0.05$ versus adult values from the same fraction.

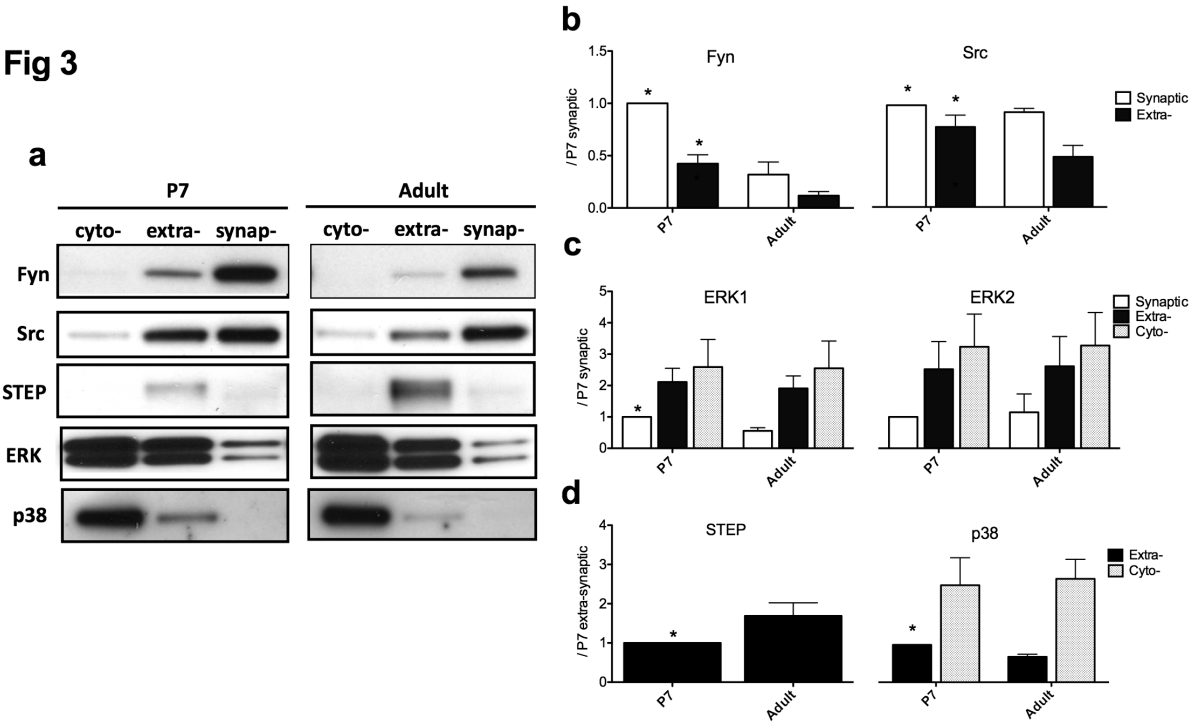

Figure 3. Localization of the Src and MAP kinases, STEP at different subcellular fractions in P7 and adult mouse cortex.
Equal amount of protein from cytoplasmic (cyto-), extrasynaptic (extra-) and synaptic (synap-) fractions was used for Western blotting. Primary antibodies are indicated on the left of the blots (3a). For Fyn, Src and ERK (3b-3c), the OD values were normalized to P7 synaptic values. For STEP and p38 (3d), the OD values were normalized to P7 extrasynaptic values. Data are presented on the right (3b-3d) as mean ± SD from 3 independent experiments. *: $p < 0.05$ versus adult values from the same fraction.

References

1. Jiang, X., Knox, R., Pathipati, P., and Ferriero, D. (2011) Developmental localization of NMDA receptors, Src and MAP kinases in mouse brain. In *Neurosci Lett* Vol. 503 pp. 215-219
2. Johnston, M. V. (2005) Excitotoxicity in perinatal brain injury. In *Brain Pathol* Vol. 15 pp. 234-240
3. Jensen, F. E. (2002) The role of glutamate receptor maturation in perinatal seizures and brain injury. In *Int J Dev Neurosci* Vol. 20 pp. 339-347
4. Hardingham, G. E. (2009) Coupling of the NMDA receptor to neuroprotective and neurodestructive events. In *Biochem Soc Trans* Vol. 37 pp. 1147-1160
5. Hardingham, G. E., and Bading, H. (2010) Synaptic versus extrasynaptic NMDA receptor signalling: implications for neurodegenerative disorders. In *Nat Rev Neurosci* Vol. 11 pp. 682-696
6. Soriano, F. X., and Hardingham, G. E. (2007) Compartmentalized NMDA receptor signalling to survival and death. *J Physiol* 584, 381-387
7. Papadia, S., Soriano, F. X., Léveillé, F., Martel, M.-A., Dakin, K. A., Hansen, H. H., Kaindl, A., Sifringer, M., Fowler, J., Stefovska, V., McKenzie, G., Craigon, M., Corriveau, R., Ghazal, P., Horsburgh, K., Yankner, B. A., Wyllie, D. J. A., Ikonomidou, C., and Hardingham, G. E. (2008) Synaptic NMDA receptor activity boosts intrinsic antioxidant defenses. In *Nat Neurosci* Vol. 11 pp. 476-487

8. Zhang, S.-J., Steijaert, M. N., Lau, D., Schütz, G., Delucinge-Vivier, C., Descombes, P., and Bading, H. (2007) Decoding NMDA receptor signaling: identification of genomic programs specifying neuronal survival and death. In *Neuron* Vol. 53 pp. 549-562

9. Hardingham, G. E., Fukunaga, Y., and Bading, H. (2002) Extrasynaptic NMDARs oppose synaptic NMDARs by triggering CREB shut-off and cell death pathways. *Nat Neurosci* 5, 405-414

10. Ivanov, A., Pellegrino, C., Rama, S., Dumalska, I., Salyha, Y., Ben-Ari, Y., and Medina, I. (2006) Opposing role of synaptic and extrasynaptic NMDA receptors in regulation of the extracellular signal-regulated kinases (ERK) activity in cultured rat hippocampal neurons. *J Physiol (Lond)* 572, 789-798

11. Xu, J., Kurup, P., Zhang, Y., Goebel-Goody, S. M., Wu, P. H., Hawasli, A. H., Baum, M. L., Bibb, J. A., and Lombroso, P. J. (2009) Extrasynaptic NMDA receptors couple preferentially to excitotoxicity via calpain-mediated cleavage of STEP. *J Neurosci* 29, 9330-9343

12. Hardingham, G. E., and Bading, H. (2002) Coupling of extrasynaptic NMDA receptors to a CREB shut-off pathway is developmentally regulated. In *Biochim Biophys Acta* Vol. 1600 pp. 148-153

13. Sala, C., Rudolph-Correia, S., and Sheng, M. (2000) Developmentally regulated NMDA receptor-dependent dephosphorylation of cAMP response element-binding protein (CREB) in hippocampal neurons. In *Journal of Neuroscience* Vol. 20 pp. 3529-3536

14. Zhou, X., Moon, C., Zheng, F., Luo, Y., Soellner, D., Nuñez, J. L., and Wang, H. (2009) N-methyl-D-aspartate-stimulated ERK1/2 signaling and the transcriptional up-regulation of plasticity-related genes are developmentally regulated following in vitro neuronal maturation. In *J Neurosci Res* Vol. 87 pp. 2632-2644

15. Jiang, X., Mu, D., Biran, V., Faustino, J., Chang, S., Rincón, C., Sheldon, R., and Ferriero, D. (2008) Activated Src kinases interact with the N-methyl-D-aspartate receptor after neonatal brain ischemia. *Ann Neurol.* 63, 632-641

16. Nakazawa, T., Komai, S., Tezuka, T., Hisatsune, C., Umemori, H., Semba, K., Mishina, M., Manabe, T., and Yamamoto, T. (2001) Characterization of Fyn-mediated tyrosine phosphorylation sites on GluR epsilon 2 (NR2B) subunit of the N-methyl-D-aspartate receptor. *J Biol Chem* 276, 693-699

17. Nguyen, T.-H., Liu, J., and Lombroso, P. J. (2002) Striatal enriched phosphatase 61 dephosphorylates Fyn at phosphotyrosine 420. *J Biol Chem* 277, 24274-24279

18. Muñoz, J. J., Tárrega, C., Blanco-Aparicio, C., and Pulido, R. (2003) Differential interaction of the tyrosine phosphatases PTP-SL, STEP and HePTP with the mitogen-activated protein kinases ERK1/2 and p38alpha is determined by a kinase specificity sequence and influenced by reducing agents. In *Biochem J* Vol. 372 pp. 193-201

19. Braithwaite, S. P., Adkisson, M., Leung, J., Nava, A., Masterson, B., Urfer, R., Oksenberg, D., and Nikolich, K. (2006) Regulation of NMDA receptor

trafficking and function by striatal-enriched tyrosine phosphatase (STEP). In *Eur J Neurosci* Vol. 23 pp. 2847-2856

20. Goebel-Goody, S. M., Davies, K. D., Alvestad Linger, R. M., Freund, R. K., and Browning, M. D. (2009) Phospho-regulation of synaptic and extrasynaptic N-methyl-d-aspartate receptors in adult hippocampal slices. *Neuroscience* 158, 1446-1459

21. Mu, F. T., Callaghan, J. M., Steele-Mortimer, O., Stenmark, H., Parton, R. G., Campbell, P. L., McCluskey, J., Yeo, J. P., Tock, E. P., and Toh, B. H. (1995) EEA1, an early endosome-associated protein. EEA1 is a conserved alpha-helical peripheral membrane protein flanked by cysteine "fingers" and contains a calmodulin-binding IQ motif. In *J Biol Chem* Vol. 270 pp. 13503-13511

22. Park, M., Penick, E. C., Edwards, J. G., Kauer, J. A., and Ehlers, M. D. (2004) Recycling endosomes supply AMPA receptors for LTP. In *Science* Vol. 305 pp. 1972-1975

23. Wu, H., Hsu, F., Gleichman, A., Baconguis, I., Coulter, D., and Lynch, D. (2007) Fyn-mediated Phosphorylation of NR2B Tyr-1336 Controls Calpain-mediated NR2B Cleavage in Neurons and Heterologous Systems. *Journal of Biological Chemistry* 282, 20075-20087

24. Waxman, E. A., and Lynch, D. R. (2005) N-methyl-D-aspartate receptor subtype mediated bidirectional control of p38 mitogen-activated protein kinase. In *J Biol Chem* Vol. 280 pp. 29322-29333

25. Gurd, J. W., Bissoon, N., Nguyen, T. H., Lombroso, P. J., Rider, C. C., Beesley, P. W., and Vannucci, S. J. (1999) Hypoxia-ischemia in perinatal rat brain induces the formation of a low molecular weight isoform of striatal enriched tyrosine phosphatase (STEP). *J Neurochem* 73, 1990-1994

Chapter 3: Elevated NMDA receptor tyrosine phosphorylation and increased brain injury following neonatal hypoxia-ischemia in mice with neuronal Fyn overexpression

Renatta Knox, Chong Zhao, Dario Miguel-Perez, Steven Wang, Jinwei Yuan, Donna Ferriero and Xiangning Jiang

Introduction

Neonatal hypoxic-ischemic brain injury is an important cause of morbidity and mortality (1). Src family kinases (SFKs) have recently been implicated in a rodent model of neonatal hypoxia-ischemia (HI). SFKs Src and Fyn are expressed in the developing brain and are activated in the postsynaptic density in response to neonatal HI. Specific inhibition of SFKs is protective against neonatal HI (2) suggesting that SFKs are involved in HI brain injury.

The *N*-Methyl-$_D$-aspartate receptor (NMDAR) is an important determinant of survival and cell death in the developing brain (3, 4). The NMDAR is a heteromeric glutamate receptor composed of an obligatory NR1 subunit and modulatory subunits NR2A-D. Excessive glutamate release in the setting of ischemia and subsequent overactivation of the NMDAR cause an influx of calcium ions that damages neurons leading to excitotoxicity (5-7). Increased levels of intracellular calcium (8) and recruitment of signaling molecules to the NMDAR (2, 9, 10) are critical for the evolution of brain injury in the neonate.

Tyrosine phosphorylation of NR2A and NR2B by Src or Fyn enhances NMDAR channel conductance (11), prevents NMDAR internalization via phosphorylation at tyrosine (Y) 1472 (12-15) and controls calpain-mediated cleavage via phosphorylation at Y1336 (16). One of the mechanisms by which SFKs are thought to contribute to excitotoxicity, is through ischemia-induced tyrosine phosphorylation and enhanced activation of the NMDAR (2, 17). In the present study we determined the specific contribution of Fyn to neonatal HI brain injury by using mice with neuronal Fyn overexpression (OE).

Materials and Methods

Animals

C57BL/6 WT and Fyn OE mice (generously provided by Dr. Nobuhiko Kojima, Gunma University School of Medicine, Japan, as described in (18)) were bred at the Laboratory Animal Resource Center (LARC) at the University of California, San Francisco. Both sexes were used for these studies at postnatal day 7 (P7). Fyn OE mice express Fyn under the control of the CaMKIIα promoter, overexpressing Fyn postnatally in excitatory neurons in the forebrain (18).

Hypoxic-Ischemic Brain Injury

HI was induced with an adaptation of the Vannucci procedure (19). At P7, pups were anesthetized with isoflurane (2-3% isoflurane/balance oxygen) and the right common carotid artery was ligated. Animals were allowed to recover for 1.5 hours with their dam and then exposed to 40 minutes of hypoxia in a humidified chamber at 37°C with 8% oxygen/balance nitrogen. Sham-operated control animals received isoflurane anesthesia and exposure of the right common carotid artery without ligation or hypoxia. HI and sham animals were returned to their dams until they were euthanized.

Evaluation of Brain Injury

Five days after the HI procedure, brains were examined histologically with cresyl violet and Perl's stain to assess the degree of damage as previously described (20).

Briefly, animals were anesthetized with pentobarbital (50mg/kg) and perfused with 4% paraformaldehyde (PFA) in 0.1M phosphate buffer (pH 7.4). Brains were postfixed in the same solution for 4 hours, then transferred to 30% sucrose in 0.1M phosphate buffer. Coronal sections were cut through the forebrain at 50μM intervals with a vibratome. Alternate sections were stained with cresyl violet for morphology or with Perl's stain enhanced with diaminobenzidine to localize iron deposition. Brain sections were scored as described (2).

Western Blotting from Whole Cell Lysates

Cortical tissue from sham-operated and the ipsilateral side of HI-injured animals was homogenized in modified radioimmunoprecipitation assay buffer (RIPA buffer, 1X sodium phosphate buffer with 1% NP-40, 0.5% sodium deoxycholate, 0.1% SDS, protease and phosphatase inhibitors). 30μg of protein from sham or ipsilateral cortex was applied to 4-12% Bis-Tris SDS polyacrylamide gel electrophoresis (Invitrogen, Carlsbad, CA) and transferred to polyvinyl difluoride membrane (Bio-Rad, Hercules, CA) as described elsewhere (2). The membranes were probed with the following primary antibodies overnight at 4°C: Fyn (1:1000; Santa Cruz Biotechnology, Santa Cruz, CA), Src (1:1000; Millipore, Billerica, MA), phospho-Src (phospho-Tyr416; 1:500; Cell Signaling Technology, Boston, MA), NR2B (1:1000; BD Transduction Laboratories, San Jose, CA), phospho-Y1252 NR2B (1:500; PhosphoSolutions, Aurora, CO), phospho-Y1336 NR2B (1:600; PhosphoSolutions), phospho-Y1472 NR2B (1:500; AbD Serotec, Oxford, UK), and β-actin (1:3000; Santa Cruz Biotechnology). Appropriate secondary horseradish peroxidase-conjugated

antibodies (1:2000, Santa Cruz Biotechnology) were used and signal was visualized with enhanced chemiluminescence (Amersham, Buckinghamshire, UK). Image J software was used to measure the optical densities (OD) and areas of protein signal on radiographic film after scanning.

Subcellular Fractionation

Purification of synaptic and extrasynaptic membrane proteins was performed according to Goebel-Goody and colleagues' procedure (15) using a subcellular fractionation approach followed by extraction with Triton X-100. In brief, cortical tissue was homogenized in ice-cold sucrose buffer containing 0.32M sucrose, 10mM Tris-HCl (pH 7.4), 1mM EDTA, 1mM EGTA and protease and phosphatase inhibitors (Complete mini and Phospho-Stop cocktail tablets, Roche, Indianapolis, IN). A low-speed (1,000x*g*) centrifugation was performed to remove the nuclear fraction and tissue debris. The resulting supernatant (S1) was spun at 10,000x*g* for 15 minutes to yield a crude membrane fraction (P2). The supernatant (S2) was then centrifuged at 100,000xg for 60 min to separate cytoplasmic protein (S3) and intracellular light membrane fraction (P3). The P2 was subsequently resuspended in 120 μl sucrose buffer, and mixed with 8 volumes of 0.5% Triton X-100 buffer containing 10mM Tris-HCl (pH 7.4), 1mM EDTA, 1mM EGTA and protease and phosphatase inhibitors. The mixture was homogenized again with 30 pulses of a glass pestle and rotated at 4°C for 30 min followed by centrifugation at 32,000xg for 30 min in a TL-100 tabletop ultracentrifuge (Beckman). The resultant pellet (TxP) containing Triton X-insoluble postsynaptic density (PSD) proteins was considered as the synaptic

membrane compartment. The supernatant (TxS) containing proteins soluble in Triton X-100 and not tightly bound to the PSD was defined as the extrasynaptic membrane compartment. The S3 and TxS fractions were further concentrated by adding 8 volumes of 100% acetone and incubated at -20 °C overnight. The precipitated protein was spun at 3000xg at 4°C for 15 min and dried at room temperature for 15min. All the pellets were dissolved in TE buffer (100 mM Tris-HCl, 10mM EDTA) with 1% SDS. The samples were sonicated, boiled for 5 min and stored at -80 °C until use. Protein concentration was determined by the bicinchoninic acid method (Pierce).

Western blotting from Membrane Preparations

For Western blot analysis, an equal amount of cytoplasmic (S3), extrasynaptic (TxS) and synaptic (TxP) protein (5μg) from P7 cortex was applied to 4-12% Bis-Tris SDS polyacrylamide gel electrophoresis and transferred to polyvinyl difluoride membrane as described elsewhere (2). The blots were probed with the following primary antibodies overnight at 4°C: phospho-Y416 (1:500; Cell Signaling), phospho-Y1472 NR2B (1:500; Cell Signaling), phospho-Y1252 NR2B (1:800; Cell Signaling) , and NR2B (1:1000; Cell signaling). Appropriate secondary horseradish peroxidase-conjugated antibodies (1:2,000, Santa Cruz) were used, and signal was visualized with enhanced chemiluminescence (Amersham). Image J software was used to measure the mean optical densities (OD) and areas of protein signal on radiographic film after scanning.

Immunoprecipitation (IP)

IP experiments were performed to measure tyrosine phosphorylation of NR2A and NR2B, the specific Fyn activity and the association of NR2A or NR2B with Fyn or Src. Cortical tissue from sham-operated and the ipsilateral side of HI-injured animals was homogenized in RIPA buffer. An equal amount of protein (250μg) was diluted with RIPA buffer and pre-cleared by incubation with Protein G-agarose (Invitrogen) for 30 minutes at 4°C. For NMDAR IPs, cell lysates were incubated with 4μg of appropriate antibodies (goat polyclonal NR2A or NR2B antibody; Santa Cruz Biotechnology) or 4μg of normal goat IgG (Santa Cruz Biotechnology) as a negative control and Protein G-PLUS (Santa Cruz Biotechnology) overnight at 4°C. For Fyn IP, cell lysates were incubated with 15μg of Fyn-conjugated agarose (Santa Cruz Biotechnology) or 15μg of mouse IgG-conjugated agarose (Santa Cruz Biotechnology) as a negative control at 4°C overnight. After centrifugation, IPs were washed 3X with RIPA buffer, then boiled with 30μL of LDS sample buffer (Invitrogen). Eluted immune complexes were loaded onto a 4-12% Bis-Tris SDS polyacrylamide gel electrophoresis and transferred to polyvinylidene fluoride membrane. Membranes from NR2A and NR2B IPs were incubated with mouse 4G10 anti-phosphotyrosine (anti-pY) antibody (1:800; Millipore), then stripped and reprobed with Src (1:800; Millipore) or Fyn (1:1000; Santa Cruz Biotechnology) and NR2A (1:1000; Cell Signaling) or NR2B (1:1000; BD Transduction Laboratories) antibodies. NR2A or NR2B tyrosine phosphorylation was expressed as the OD ratio of phosphotyrosine (pY) to NR2A or NR2B. Membranes of Fyn IPs were incubated with phospho-Src (pY416; 1:500; Cell Signaling) antibody, which is the active form

of SFKs. The membranes were then stripped and reprobed with Fyn (1:1000; Santa Cruz) antibody. Specific Fyn activity was expressed as the OD ratio of pY416 to Fyn.

Statistical Analysis

Data are presented as median and interquartile range for brain injury score using Prism 4 nonparametric tests for analysis of variance (Kruskal-Wallis test). Contingency tables were used to determine mortality differences. Data of optical densities of immunoblots are presented as mean ± SD and were evaluated statistically using SAS Wilcoxon-Mann-Whitney test. Differences were considered significant at $p<0.05$.

Results

Fyn is overexpressed in the developing cortex in Fyn OE mice

We first assessed whether Fyn overexpression leads to changes in protein levels. We made cortical lysates from wild type and Fyn-transgenic mice at different postnatal ages (P3, P7, P14, P21, P48). We examined the expression of Src, Fyn and NMDAR subunits NR2A and NR2B. As previously reported, the Fyn transgene continues to increase in expression into adulthood (21). There were no changes in Src, NR2A or NR2B protein levels in Fyn-transgenic mice (Fig. 1A). Importantly, Fyn is overexpressed approximately 2-fold relative to wild-type animals at P7, the age at which we performed hypoxia-ischemia (Fig. 1B).

Neuronal Fyn overexpression worsens brain injury and increases mortality after neonatal HI

We examined the effect of neuronal Fyn overexpression on the degree of brain injury and mortality after HI. Fyn OE mice had more severe brain injury than WT controls [median = 10, range 7.5-13.5 in OE (n=34); median = 8, range 6.5-10 in WT (n=37), WT vs. OE p=0.0141, Fig. 2A, B and Table 1]. The cortex and striatum showed a statistically significant increase in brain injury in Fyn OE mice compared to WT mice (cortex p=0.0139, striatum p=0.0077, Fig. 2C,E). Additionally, we found that Fyn OE mice had a 4-fold higher mortality than WT mice (Fyn OE 23.26% vs. WT 5.26%, p=0.0229, Table 1). The distribution of injury scores indicated that more Fyn OE mice had relatively severe injury (scores ≥12) than the WT animals (Fig. 2G, Table 1). There were no gender differences in mortality or brain injury in WT or Fyn OE mice after HI (Fig. 2F).

Fyn OE mice have elevated Fyn expression and activity after HI

Next, we examined the expression and activity of SFKs after neonatal HI. In WT mice, Fyn protein expression did not change in response to HI (Fig. 3A,C). Fyn OE mice had significantly higher Fyn protein expression compared to WT mice in sham-operated animals and 15min after HI (sham WT vs. OE p=0.003, 15min WT vs. OE p=0.004, Fig. 3A,C). Fyn activity was higher in OE mice than WT mice 1hr after injury (1hr WT vs. OE p=0.037, Fig. 3D,E), which correlated with elevated SFK activity as measured by phospho-Y416 (1hr WT vs. OE p=0.025, Fig. 3B).

Fyn OE mice have sustained phosphorylation of NR2A and NR2B after HI

To determine if Fyn overexpression affects tyrosine phosphorylation of NR2A and NR2B, we immunoprecipitated NMDAR subunits and performed western blots for phosphorylated tyrosine. In sham animals, Fyn OE mice had higher NR2A and NR2B tyrosine phosphorylation than WT mice (Fig. 4A,B and 5A,B). NR2A tyrosine phosphorylation peaked 15min after HI in WT animals (Fig. 4A,B). Interestingly, we found that Src but not Fyn was recruited to NR2A in response to HI in WT and Fyn OE animals 15min and 1hr after injury (Fig. 4A,C). NR2B tyrosine phosphorylation was elevated in Fyn OE animals relative to WT at all time points (Fig. 5A,B). Neither Src nor Fyn co-immunoprecipitated with NR2B after HI (data not shown).

Fyn-mediated tyrosine phosphorylation of NR2B

Next, we examined three NR2B tyrosine phosphorylation sites regulated by Fyn (13, 16, 22). We measured the protein expression of NR2B phosphorylated at tyrosine 1472, 1336 and 1252. Compared to WT sham animals, Fyn OE sham mice had increased NR2B phosphorylation at tyrosine 1472 (pY1472) and pY1252 with decreased pY1336 (Fig. 5C-F). pY1472 and pY1336 peaked 15min after injury while pY1252 NR2B peaked at 1hr in both WT and Fyn OE mice (Fig. 5C-G). Relative to WT mice, Fyn OE mice had less pY1336 15min after HI and more pY1252 1hr after injury (Fig. 5E-G). We did not observe the 115 kDa calpain cleavage fragment generated by pY1336 NR2B (data not shown) (16).

In synaptic membranes, we found significant increases in SFK activity, pY1472, and pY1252 up to 6hrs after injury in WT mice (Fig. 6A-D). Fyn OE mice had significantly more pY1472 in synaptic fractions in sham-operated animals, 15min and 1hr after injury (Fig. 6A,C). pY1252 was higher in Fyn OE mice compared to WT at 1hr and 24hrs (Fig. 6A,D).

Fyn OE mice have elevated calpain activity after HI

We assessed the activity of calcium-activated proteases calpain and caspase implicated in necrotic and apoptotic cell death (23). Calpain cleavage of α-spectrin produces a 150 and 145 kDa fragment, also known as spectrin breakdown pattern (SBDP) 150 and SBDP145 that is evident in cells undergoing necrosis and apoptosis (23, 24). Caspase cleavage of α-spectrin produces a 120 kDa fragment (SBDP120) which is present in apoptotic cells (23, 25). WT mice had elevated SBDP150/145 6hr and 24hr after injury (Fig. 7A,B). Fyn OE mice had elevated SBDP150/145 1hr, 6hr, and 24hrs after injury, with significantly higher SBDP150/145 at 24hr compared to WT mice (Fig. 7A,B). There were no significant differences in SBDP120 at the time points investigated (data not shown).

Discussion

This study demonstrates that neuronal Fyn overexpression leads to increased mortality and brain injury in response to neonatal HI. Fyn overexpression is associated with sustained NR2A and NR2B tyrosine phosphorylation. There is

also elevated pY1252 and pY1472 NR2B in synaptic membranes in Fyn OE mice. These early changes in NMDAR tyrosine phosphorylation correlate with elevated calpain activity. Taken together, our results implicate Fyn and NMDAR tyrosine phosphorylation in neuronal cell death after neonatal HI (Fig. 8).

Our results may underestimate the effect of neuronal Fyn overexpression due to the high mortality in Fyn OE mice during hypoxia. The elevated mortality in Fyn OE mice may be due to more seizures that occur during hypoxia. One study found that overexpression of constitutively active Fyn resulted in premature death due to seizures (18). Therefore it is possible that mice with high levels of Fyn kinase activity may be more susceptible to seizures and mortality during HI.

While there is some evidence of gender differences in response to cell death pathways initiated by neonatal HI and to genetic mutations or treatments (26-28), we find that male and female Fyn OE mice have more injury compared to WT mice of the same gender. While Fyn overexpression could differentially regulate cell death pathways on a molecular level, we find that the outcome is the same in male and female mice.

We found that NR2A tyrosine phosphorylation peaked at 15min in WT animals, consistent with our previous report (2). Fyn OE mice had prolonged phosphorylation of NR2A, with a peak at 1hr, coinciding with elevated Fyn activity. Contrary to our previous study, we found that Src was specifically recruited to NR2A after neonatal HI, while Fyn did not co-immunoprecipitate with NR2A or NR2B. The duration of Src association with NR2A was shorter than previously reported (1hr vs. 6hrs). However, Src interaction with NR2A coincided with the peak of NR2A

tyrosine phosphorylation. This discrepancy may be due to mouse strain or the duration of hypoxia as the previous study was done in CD1 mice with a shorter duration of hypoxia (15min) and this study utilized C57BL/6 mice which are more resistant to neonatal HI injury (20). Husi et al found that in C57BL/6 mice, Src but not Fyn is a component of the NMDAR complex (29). Alternatively, Fyn could be transiently associating with the NMDAR or could be mediating its affects through Src or an adaptor protein (30).

At baseline, NR2A and NR2B tyrosine phosphorylation was higher in Fyn OE mice compared to WT, as reported in adult mice (18). In response to injury, tyrosine phosphorylation of NR2B and NR2A remained elevated in the Fyn OE mice. These results suggest that Fyn leads to phosphorylation of NR2A and NR2B during HI. One study found that phosphorylation of the NR2B CTD by SFKs leads to a more open conformation of the CTD *in vitro* (31). Fyn could transiently associate with the NMDAR and cause prolonged phosphorylation by increasing the accessibility of the CTD to other kinases. Additionally, SFK activity is elevated in synaptic membranes and could lead to elevated NMDAR phosphorylation by activating another tyrosine kinase in the PSD.

In this study, we provide the first description of three NR2B phosphorylation sites regulated by Fyn in response to neonatal HI. In WT mice, we found early phosphorylation of tyrosine (pY) 1336 and 1472 NR2B, followed by pY1252 NR2B. Consistent with a previous report, pY1472 is increased up to 1hr after neonatal HI (32). Y1472 is associated with surface expression of NR1/NR2B and synaptic

enrichment of the receptor (13-15). In neonatal HI, pY1472 may contribute to excitotoxic cell death by maintaining synaptic expression of the NMDAR.

Wu *et al.* found that phosphorylation of Y1336 by Fyn promotes calpain cleavage of NR2B in an *in vitro* glutamate toxicity model (16). We did not observe the calpain cleavage fragment generated by pY1336, however we did observe less pY1336 NR2B in sham-operated mice and 15min after HI in Fyn OE animals compared to WT mice. The function of NR2B phosphorylation at Y1336 and Y1252 in the developing brain is unknown. Our results suggest that at baseline, Fyn preferentially phosphorylates Y1472 and Y1252 in the neonatal cortex, since Fyn OE mice had elevated pY1472 and pY1252 and decreased pY1336 relative to WT sham animals. pY1472 NR2B and pY1252 NR2B were absent in Fyn KO mice (data not shown). Additionally, pY1472 and pY1252 were up-regulated in synaptic membranes in Fyn OE mice where SFK activity was also increased. Further biochemical studies are required to determine the functional consequences of Fyn-mediated NR2B phosphorylation at specific sites following neonatal HI.

Although Fyn has been implicated in the apoptosis pathway (33-35), there was no increase in caspase-3 cleavage or caspase activity as assessed by α-spectrin cleavage in Fyn OE mice relative to WT mice. Our data suggests that Fyn increases calpain activity which functions in necrotic and apoptotic cell death. Calpain activity may be elevated in Fyn OE mice due to increased calcium signaling via NMDAR-dependent and independent pathways (24). Calpain is activated downstream of NR2B in the hippocampus during traumatic mechanical injury (36). Fyn may lead to increased calpain activity by upregulating NR2B receptor activity via tyrosine

phosphorylation. Changes in calpain activity are indicative of calcium dysregulation and can also occur independent of calcium flux from the NMDAR (37).

In the next chapter, we will determine the mechanism by which Fyn phosphorylation of the NR2B contributes to cell death after neonatal HI.

Figure Legends

Table 1. Fyn OE mice have increased mortality and more severe brain injury due to HI.

Mortality occurred during hypoxia. Brain sections were scored for injury with Cresyl violet (morphology) and Perl's Stain (iron deposition). Injury scores were considered mild (≤5), moderate (6-12) and severe (≥12). Contingency tables were used for mortality differences. Brain injury score was analyzed using nonparametric tests for analysis of variance (Kruskal-Wallis test), where $p<0.05$ was considered significant.

Figure 1. Fyn overexpression does not lead to compensatory changes in Src or NMDAR protein expression.

A) Westerns blots were performed on cortical lysates for Fyn, c-Src, NR2B, NR2A, and β-actin at P3, P7, P14, P21, and P48. B) Fyn developmental expression was normalized to β-actin. Representative data for n=2 experiments.

Figure 2. Fyn overexpression enhances brain injury in the cortex and striatum following neonatal HI.

A modified Vannucci procedure was performed on WT (n=37) and Fyn OE mice (n=34) at postnatal day 7 (P7). A) Animals were perfused at P12, brains were sectioned and stained with Cresyl violet (morphology) and Perl's Stain (iron deposition). Arrows indicate patches of cell loss in Cresyl violet stained sections.

Arrowheads show iron accumulation in similar injured areas in Perl-stained adjacent sections. B) Composite injury score. Regional injury scores in the C) cortex, D) hippocampus, and E) striatum. Data are represented by box and whisker plots: the median is represented by the central horizontal line, 25^{th} and 75^{th} percentiles by the space within the box, and the range by the vertical lines extending from the box. Brain injury score was analyzed using nonparametric tests for analysis of variance (Kruskal-Wallis test). *$p<0.05$, ** $p<0.01$.

Figure 3. Fyn activity is elevated 1 hour after neonatal HI in Fyn OE compared to WT animals.

A) Western blots using anti-Fyn, Src, pY416 (activated SFKs), and β-actin antibodies were carried out on cortical lysates from sham and HI animals at the time points shown. B) pY416 and C) Fyn protein levels were normalized to β-actin. D) Fyn was immunoprecipitated from cortical lysates and blotted for anti-pY416 antibody, then stripped and reprobed with anti-Fyn antibody. E) Fyn activity is expressed as an OD ratio of pY416 to Fyn. Data was normalized to WT sham values. Representative data for n=6 experiments. Graphs indicate mean ± SD. Data were analyzed using SAS Wilcoxon-Mann-Whitney test. *$p<0.05$, ** $p<0.01$.

Figure 4. Src is recruited to NR2A during the peak of NR2A tyrosine phosphorylation.

A) NR2A was immunoprecipitated from sham and HI cortical samples and blotted with antibodies for phosphotyrosine (pY), Src, and NR2A. B) NR2A tyrosine

phosphorylation was measured as an OD ratio of phosphotyrosine to NR2A. C) Src association with NR2A was expressed as a ratio of coimmunoprecipitated Src to immunoprecipitated NR2A. Data was normalized to WT sham values. Representative data for n=6 experiments. Graphs indicate mean ± SD. Data were analyzed using SAS Wilcoxon-Mann-Whitney test. *$p<0.05$, ** $p<0.01$.

Figure 5. Fyn-mediated tyrosine phosphorylation of NR2B following neonatal HI. A) NR2B was immunoprecipitated from sham and HI cortical lysates and blotted with antibodies for phosphotyrosine (pY) and NR2B. B) NR2B tyrosine phosphorylation was measured as an OD ratio of phosphotyrosine to NR2B. Data was normalized to WT sham values. C) Tyrosine phosphorylation of specific residues on NR2B was ascertained by western blotting in sham and HI cortical lysates using anti-pY1472, pY1336, and pY1252 NR2B antibodies. Expression of D) pY1472 NR2B, E) pY1336 NR2B, and F) pY1252 NR2B was normalized to total NR2B and then to WT sham. Representative data for n=4 experiments. Graphs indicate mean ± SD. Data were analyzed using SAS Wilcoxon-Mann-Whitney test. *$p<0.05$.

Figure 6. pY1472 NR2B and pY1252 NR2B are elevated in synaptic membranes in Fyn OE mice in response to HI.
Western blots using anti-pY416, pY1472, pY1252, and NR2B were carried out on synaptic and extrasynaptic membrane fractions from sham and HI animals at the time points shown. B) pY416 was normalized to WT sham in synaptic membranes.

C,D) pY1472 and pY1252 were normalized to synaptic NR2B and then to WT sham. Representative data for n=3 experiments. Graphs indicate mean ± SD. Data were analyzed using SAS Wilcoxon-Mann-Whitney test. *p<0.05, ** p<0.01.

Figure 7. Fyn OE mice have elevated calpain activity in response to neonatal HI.
A) Western blots were carried out for α-spectrin and β-actin in sham animals and after HI. B) Expression of α-spectrin 150/145 kDa cleavage product was normalized to β-actin and then to WT sham. Representative data for n=6 experiments. Graph indicates mean ± SD. Data were analyzed using SAS Wilcoxon-Mann-Whitney test. *p<0.05, ** p<0.01.

Figure 8. Model.
In response to neonatal HI, Src interacts with NR2A and Fyn phosphorylates NR2A and NR2B subunits. These changes are associated with increased calpain activity and brain injury.

Table 1: Mortality and degree of brain injury in WT and Fyn OE mice following neonatal HI

genotype	animal number	mortality (%)	injury score		distribution of injury scores		
			median	range	≤5	6-12	≥12
WT	37	5.26	8	6.5-10	8	25	4
OE	34	23.26	10	7.5-13.5	4	18	12

WT vs. OE: p=0.0229 (mortality), p=0.014 (injury score)

Table 1. Fyn OE mice have increased mortality and more severe brain injury due to HI.
Mortality occurred during hypoxia. Brain sections were scored for injury with Cresyl violet (morphology) and Perl's Stain (iron deposition). Injury scores were considered mild (≤5), moderate (6-12) and severe (≥12). Contingency tables were used for mortality differences. Brain injury score was analyzed using nonparametric tests for analysis of variance (Kruskal-Wallis test). $p<0.05$ was considered significant.

Fig. 1

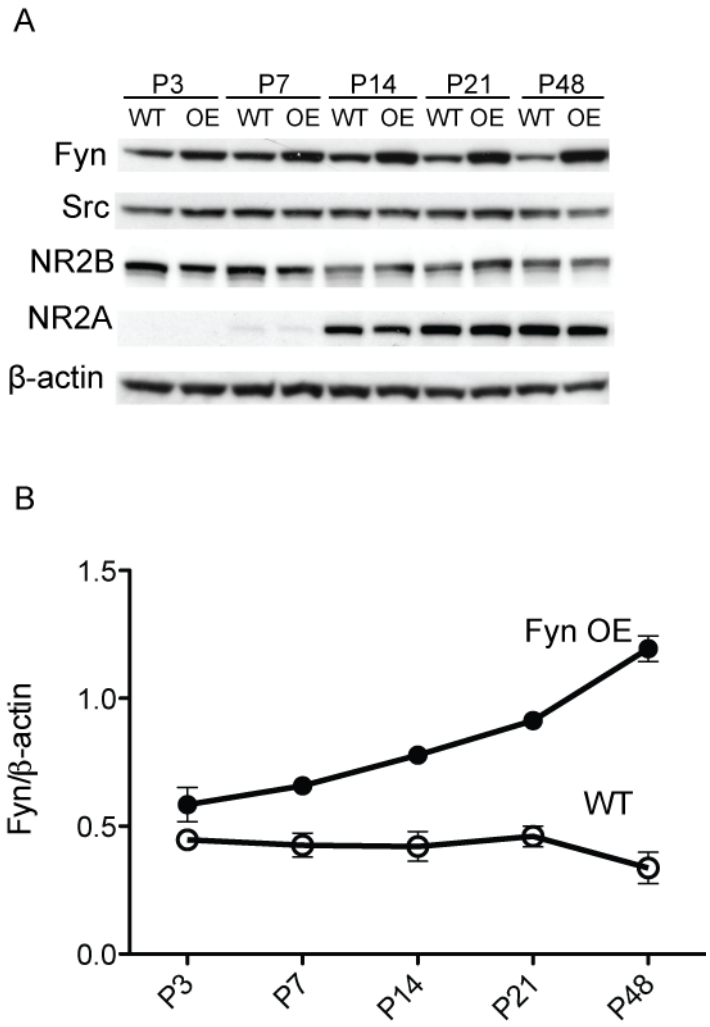

Figure 1. Fyn overexpression does not lead to compensatory changes in Src or NMDAR protein expression.
A) Westerns blots were performed on cortical lysates for Fyn, c-Src, NR2B, NR2A, and β-actin at P3, P7, P14, P21, and P48. B) Fyn developmental expression was normalized to β-actin. Representative data for n=2 experiments.

Fig. 2

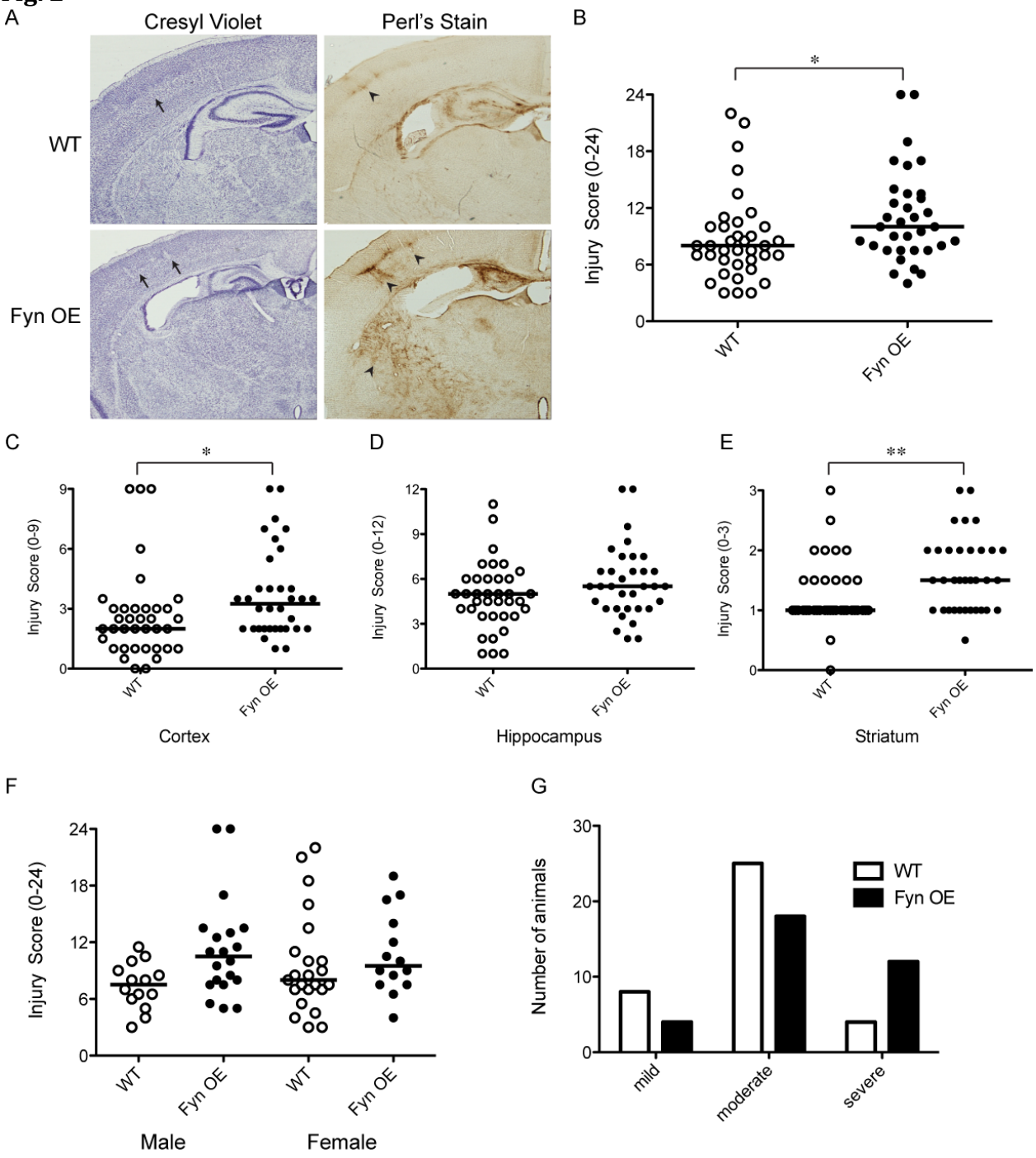

Figure 2. Fyn overexpression enhances brain injury in the cortex and striatum following neonatal HI.
A modified Vannucci procedure was performed on WT (n=37) and Fyn OE mice (n=34) at postnatal day 7 (P7). A) Animals were perfused at P12, brains were sectioned and stained with Cresyl violet (morphology) and Perl's Stain (iron

deposition). Arrows indicate patches of cell loss in Cresyl violet stained sections. Arrowheads show iron accumulation in similar injured areas in Perl-stained adjacent sections. B) Composite injury score. Regional injury scores in the C) cortex, D) hippocampus, and E) striatum. Data are represented by box and whisker plots: the median is represented by the central horizontal line, 25^{th} and 75^{th} percentiles by the space within the box, and the range by the vertical lines extending from the box. Brain injury score was analyzed using nonparametric tests for analysis of variance (Kruskal-Wallis test). *$p<0.05$, ** $p<0.01$.

Fig. 3

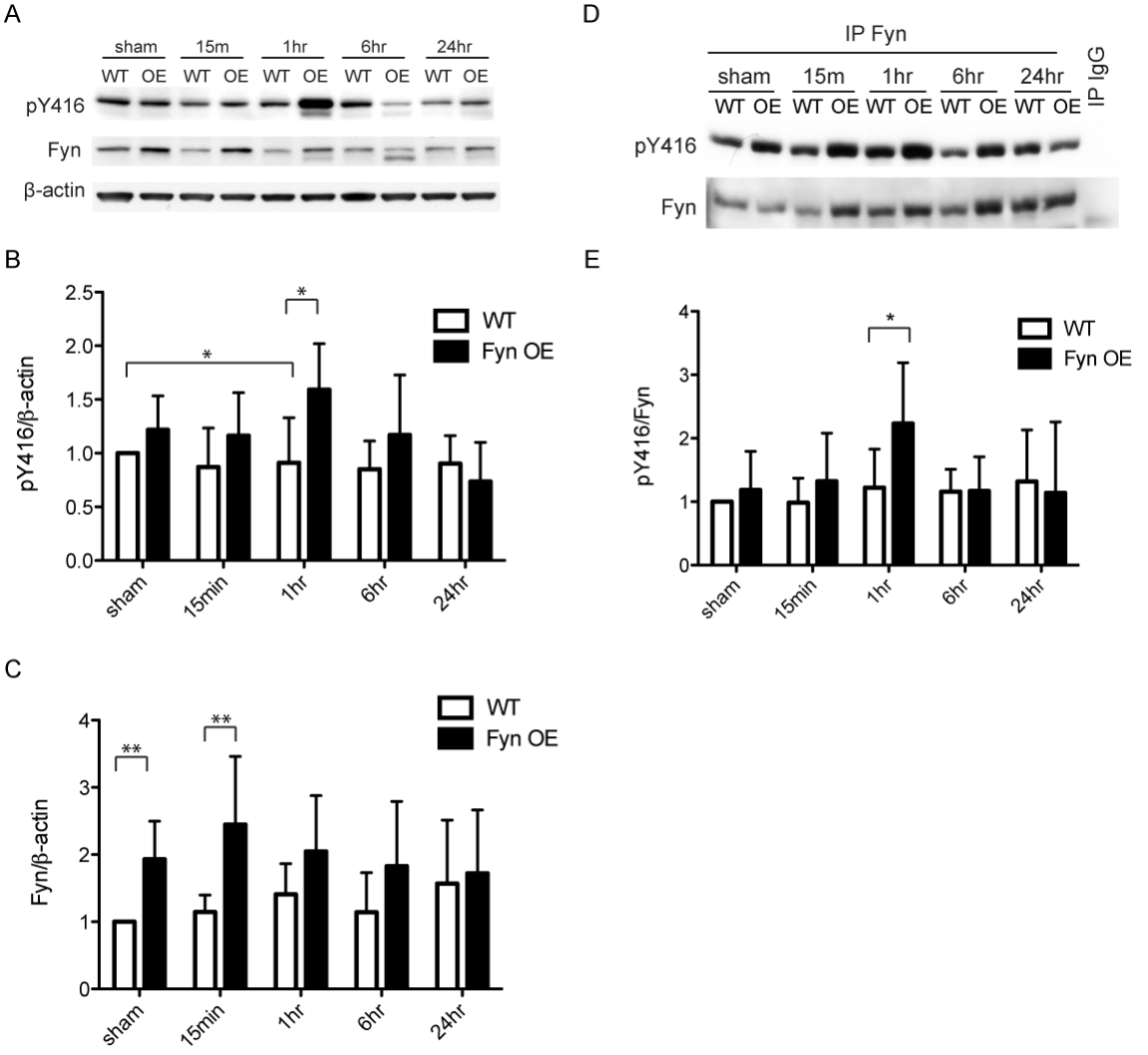

Figure 3. Fyn activity is elevated 1 hour after neonatal HI in Fyn OE compared to WT animals.

A) Western blots using anti-Fyn, Src, pY416 (activated SFKs), and β-actin antibodies were carried out on cortical lysates from sham and HI animals at the time points shown. B) pY416 and C) Fyn protein levels were normalized to β-actin. D) Fyn was immunoprecipitated from cortical lysates and blotted for anti-pY416 antibody, then stripped and reprobed with anti-Fyn antibody. E) Fyn activity is expressed as an OD ratio of pY416 to Fyn. Data was normalized to WT sham values. Representative data for n=6 experiments. Graphs indicate mean ± SD. Data were analyzed using SAS Wilcoxon-Mann-Whitney test. *p<0.05, ** p<0.01.

Fig. 4

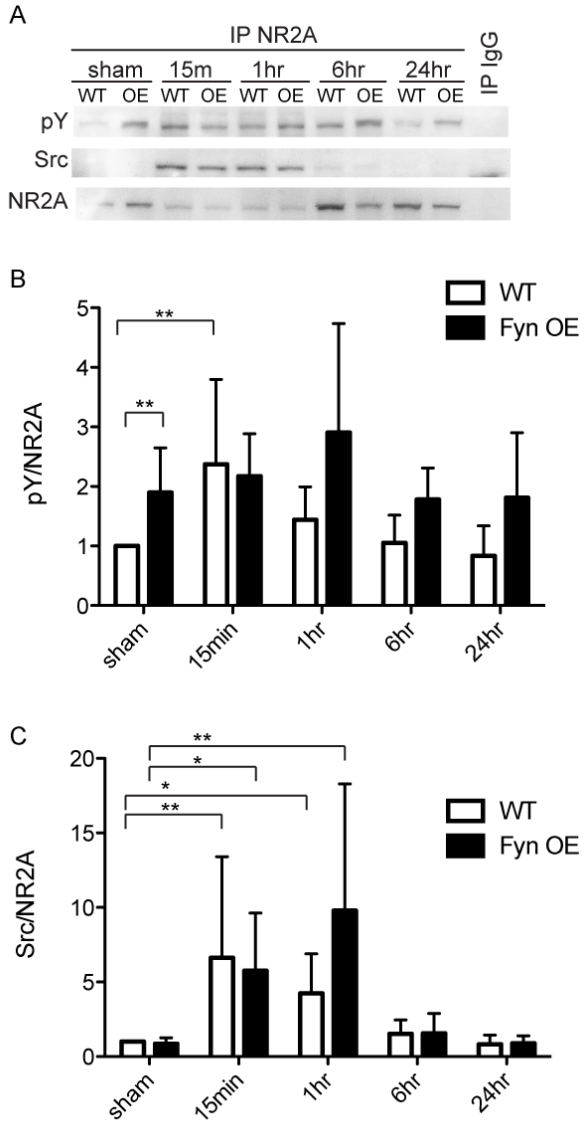

Figure 4. Src is recruited to NR2A during the peak of NR2A tyrosine phosphorylation.
A) NR2A was immunoprecipitated from sham and HI cortical samples and blotted with antibodies for phosphotyrosine (pY), Src, and NR2A. B) NR2A tyrosine phosphorylation was measured as an OD ratio of phosphotyrosine to NR2A. C) Src association with NR2A was expressed as a ratio of coimmunoprecipitated Src to immunoprecipitated NR2A. Data was normalized to WT sham values. Representative data for n=6 experiments. Graphs indicate mean ± SD. Data were analyzed using SAS Wilcoxon-Mann-Whitney test. *$p<0.05$, ** $p<0.01$.

Fig. 5

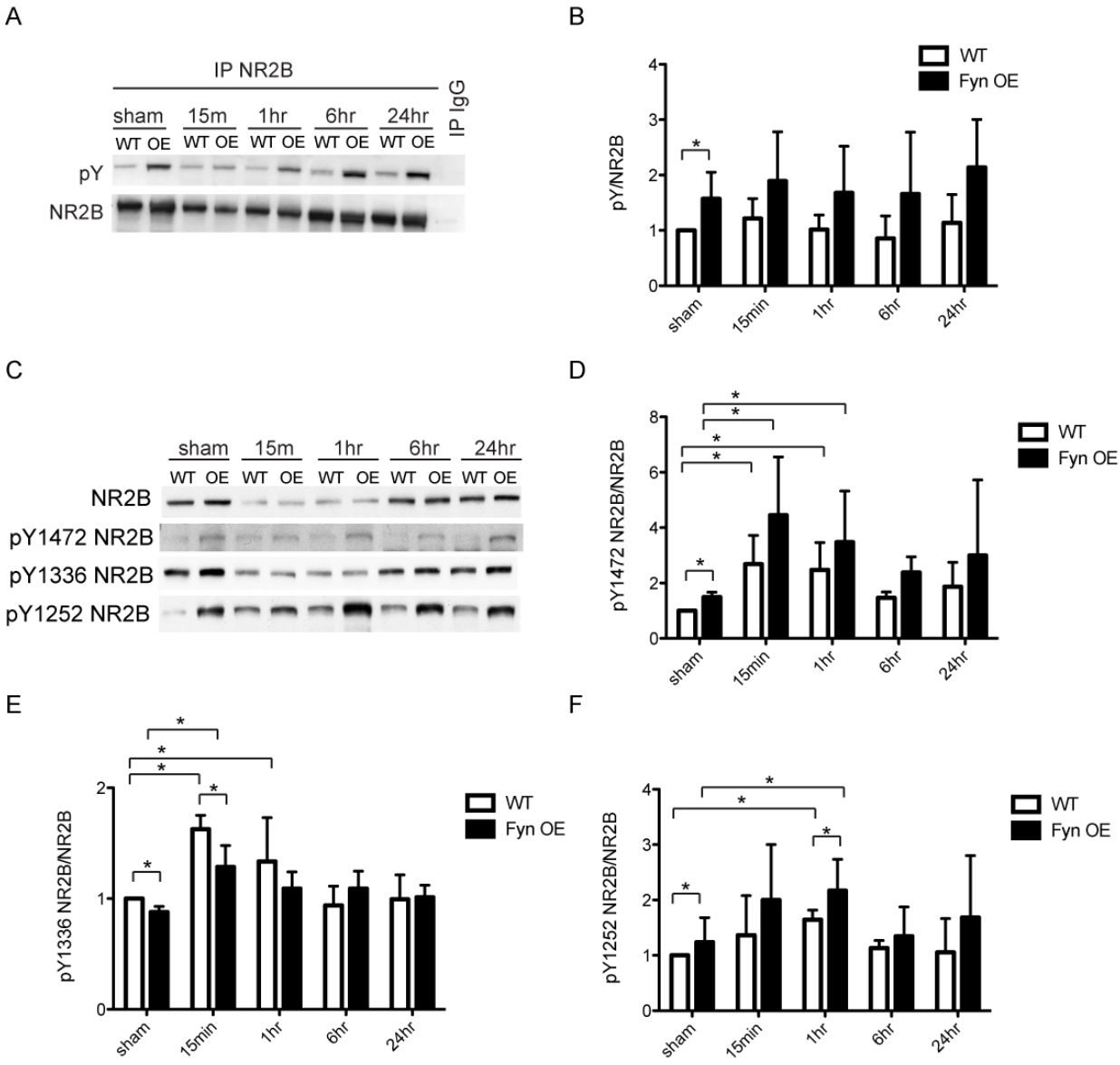

Figure 5. Fyn-mediated tyrosine phosphorylation of NR2B following neonatal HI. A) NR2B was immunoprecipitated from sham and HI cortical lysates and blotted with antibodies for phosphotyrosine (pY) and NR2B. B) NR2B tyrosine phosphorylation was measured as an OD ratio of phosphotyrosine to NR2B. Data was normalized to WT sham values. C) Tyrosine phosphorylation of specific residues on NR2B was ascertained by western blotting in sham and HI cortical lysates using anti-pY1472, pY1336, and pY1252 NR2B antibodies. Expression of D) pY1472 NR2B, E) pY1336 NR2B, and F) pY1252 NR2B was normalized to total NR2B and then to WT sham. Representative data for n=4 experiments. Graphs indicate mean ± SD. Data were analyzed using SAS Wilcoxon-Mann-Whitney test. *$p<0.05$.

Fig. 6

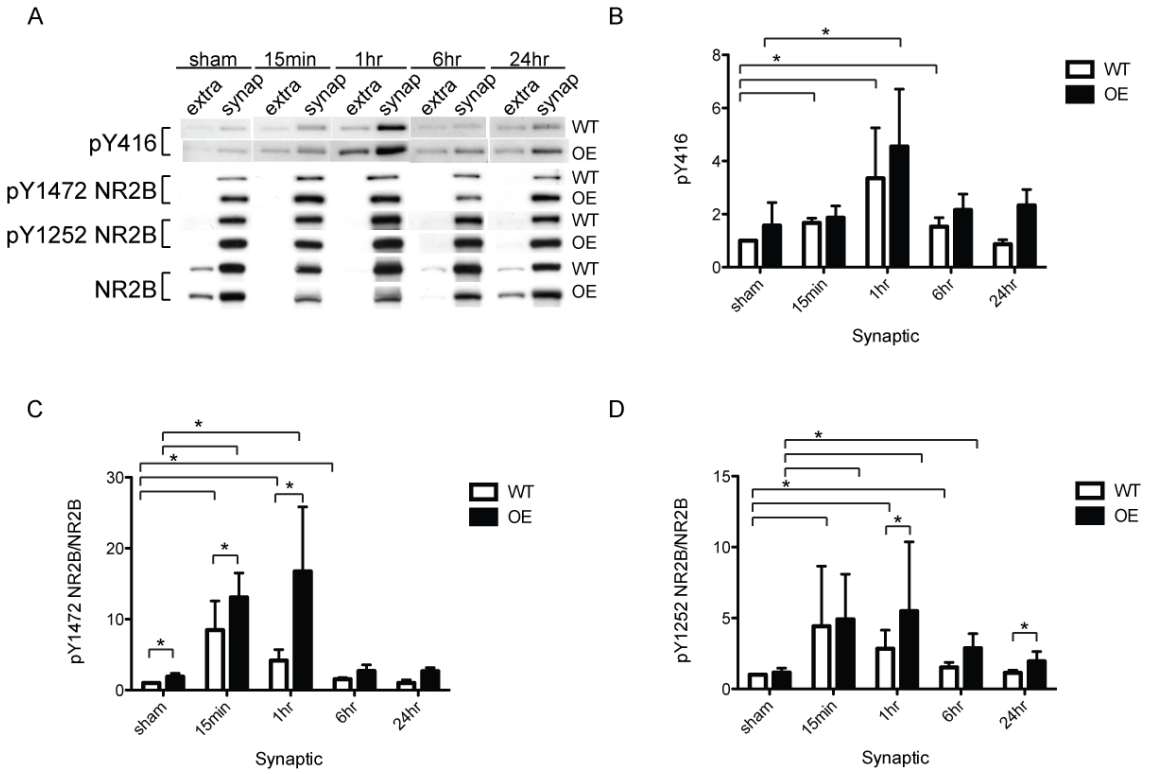

Figure 6. pY1472 and pY1252 are elevated in synaptic membranes in Fyn OE mice in response to HI.
Western blots using anti-pY416, pY1472, pY1252, and NR2B were carried out on synaptic and extrasynaptic membrane fractions from sham and HI animals at the time points shown. B) pY416 was normalized to WT sham in synaptic membranes. C,D) pY1472 and pY1252 were normalized to synaptic NR2B and then to WT sham. Representative data for n=3 experiments. Graphs indicate mean ± SD. Data were analyzed using SAS Wilcoxon-Mann-Whitney test. *p<0.05, ** p<0.01.

Fig. 7

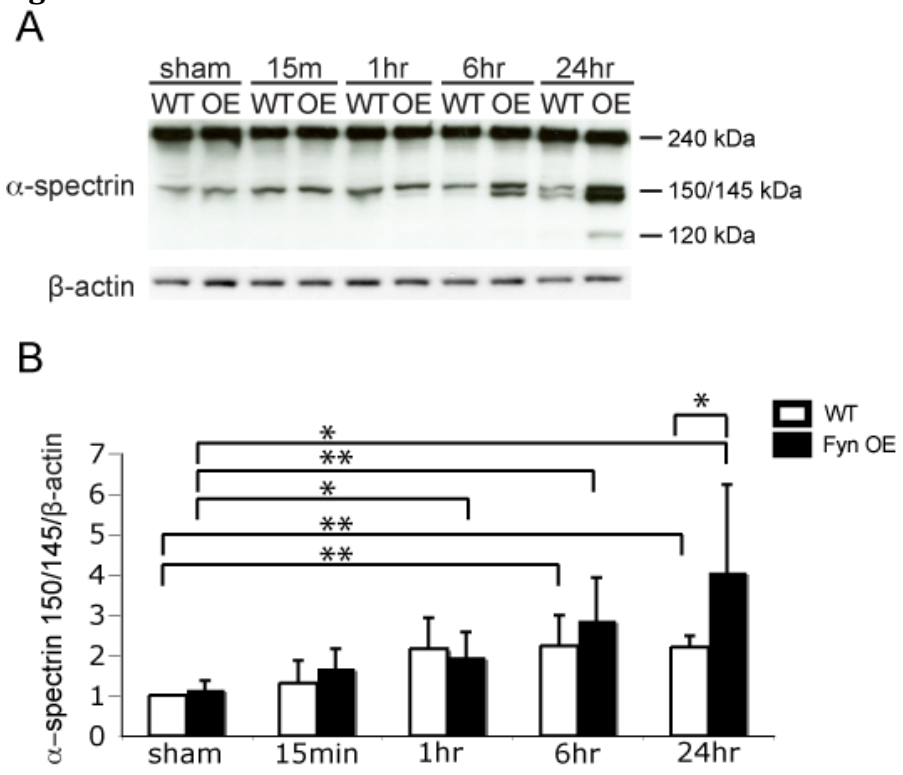

Figure 7. Fyn OE mice have elevated calpain activity in response to neonatal HI. A) Western blots were carried out for α-spectrin and β-actin in sham animals and after HI. B) Expression of α-spectrin 150/145 kDa cleavage product was normalized to β-actin and then to WT sham. Representative data for n=6 experiments. Graph indicates mean ± SD. Data were analyzed using SAS Wilcoxon-Mann-Whitney test. *p<0.05, ** p<0.01.

Fig. 8

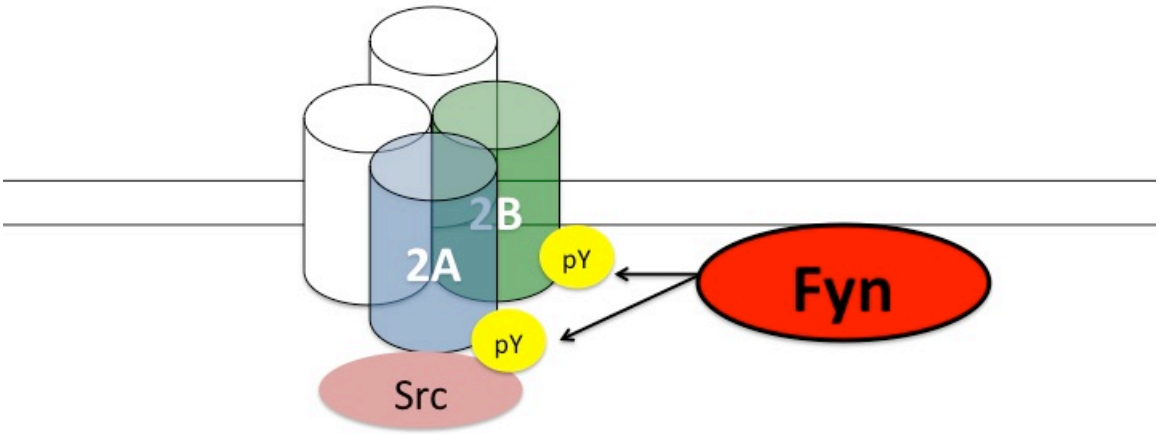

Figure 8. Model.
In response to neonatal HI, Src interacts with NR2A and Fyn phosphorylates NR2A and NR2B subunits. These changes are associated with increased calpain activity and brain injury.

References

1. Ferriero, D. (2004) Neonatal brain injury. *N Engl J Med* 351, 1985-1995
2. Jiang, X., Mu, D., Biran, V., Faustino, J., Chang, S., Rincón, C., Sheldon, R., and Ferriero, D. (2008) Activated Src kinases interact with the N-methyl-D-aspartate receptor after neonatal brain ischemia. *Ann Neurol.* 63, 632-641
3. McDonald, J. W., Silverstein, F. S., and Johnston, M. V. (1987) MK-801 protects the neonatal brain from hypoxic-ischemic damage. *Eur J Pharmacol* 140, 359-361
4. Ikonomidou, C., Bosch, F., Miksa, M., Bittigau, P., Vöckler, J., Dikranian, K., Tenkova, T. I., Stefovska, V., Turski, L., and Olney, J. W. (1999) Blockade of NMDA receptors and apoptotic neurodegeneration in the developing brain. *Science* 283, 70-74
5. Olney, J. W. (1969) Brain lesions, obesity, and other disturbances in mice treated with monosodium glutamate. *Science* 164, 719-721
6. Olney, J. W., Ho, O. L., and Rhee, V. (1971) Cytotoxic effects of acidic and sulphur containing amino acids on the infant mouse central nervous system. *Exp Brain Res* 14, 61-76
7. Choi, D. W. (1987) Ionic dependence of glutamate neurotoxicity. *J Neurosci* 7, 369-379
8. Vexler, Z. S., and Ferriero, D. M. (2001) Molecular and biochemical mechanisms of perinatal brain injury. *Seminars in neonatology* 6, 99-108

9. Ferriero, D. M., Sheldon, R. A., Black, S. M., and Chuai, J. (1995) Selective destruction of nitric oxide synthase neurons with quisqualate reduces damage after hypoxia-ischemia in the neonatal rat. *Pediatr Res* 38, 912-918

10. Jiang, X., Mu, D., Sheldon, R. A., Glidden, D. V., and Ferriero, D. (2003) Neonatal hypoxia-ischemia differentially upregulates MAGUKs and associated proteins in PSD-93-deficient mouse brain. *Stroke* 34, 2958-2963

11. Köhr, G., and Seeburg, P. H. (1996) Subtype-specific regulation of recombinant NMDA receptor-channels by protein tyrosine kinases of the src family. *J Physiol (Lond)* 492, 445-452

12. Roche, K. W., Standley, S., McCallum, J., Dune Ly, C., Ehlers, M. D., and Wenthold, R. J. (2001) Molecular determinants of NMDA receptor internalization. *Nat Neurosci* 4, 794-802

13. Prybylowski, K., Chang, K., Sans, N., Kan, L., Vicini, S., and Wenthold, R. J. (2005) The synaptic localization of NR2B-containing NMDA receptors is controlled by interactions with PDZ proteins and AP-2. *Neuron* 47, 845-857

14. Nakazawa, T., Komai, S., Watabe, A. M., Kiyama, Y., Fukaya, M., Arima-Yoshida, F., Horai, R., Sudo, K., Ebine, K., Delawary, M., Goto, J., Umemori, H., Tezuka, T., Iwakura, Y., Watanabe, M., Yamamoto, T., and Manabe, T. (2006) NR2B tyrosine phosphorylation modulates fear learning as well as amygdaloid synaptic plasticity. *EMBO J* 25, 2867-2877

15. Goebel-Goody, S. M., Davies, K. D., Alvestad Linger, R. M., Freund, R. K., and Browning, M. D. (2009) Phospho-regulation of synaptic and extrasynaptic N-

methyl-d-aspartate receptors in adult hippocampal slices. *Neuroscience* 158, 1446-1459

16. Wu, H., Hsu, F., Gleichman, A., Baconguis, I., Coulter, D., and Lynch, D. (2007) Fyn-mediated Phosphorylation of NR2B Tyr-1336 Controls Calpain-mediated NR2B Cleavage in Neurons and Heterologous Systems. *Journal of Biological Chemistry* 282, 20075-20087
17. Takagi, N., Cheung, H. H., Bissoon, N., Teves, L., Wallace, M. C., and Gurd, J. W. (1999) The effect of transient global ischemia on the interaction of Src and Fyn with the N-methyl-D-aspartate receptor and postsynaptic densities: possible involvement of Src homology 2 domains. *J Cereb Blood Flow Metab* 19, 880-888
18. Kojima, N., Ishibashi, H., Obata, K., and Kandel, E. R. (1998) Higher seizure susceptibility and enhanced tyrosine phosphorylation of N-methyl-D-aspartate receptor subunit 2B in fyn transgenic mice. *Learn Mem* 5, 429-445
19. Rice, J. E., Vannucci, R. C., and Brierley, J. B. (1981) The influence of immaturity on hypoxic-ischemic brain damage in the rat. *Ann Neurol.* 9, 131-141
20. Sheldon, R. A., Sedik, C., and Ferriero, D. M. (1998) Strain-related brain injury in neonatal mice subjected to hypoxia-ischemia. *Brain Res* 810, 114-122
21. Kojima, N., Wang, J., Mansuy, I. M., Grant, S. G., Mayford, M., and Kandel, E. R. (1997) Rescuing impairment of long-term potentiation in fyn-deficient mice by introducing Fyn transgene. In *Proc Natl Acad Sci USA* Vol. 94 pp. 4761-4765

22. Nakazawa, T., Komai, S., Tezuka, T., Hisatsune, C., Umemori, H., Semba, K., Mishina, M., Manabe, T., and Yamamoto, T. (2001) Characterization of Fyn-mediated tyrosine phosphorylation sites on GluR epsilon 2 (NR2B) subunit of the N-methyl-D-aspartate receptor. *J Biol Chem* 276, 693-699

23. Nath, R., Raser, K. J., Stafford, D., Hajimohammadreza, I., Posner, A., Allen, H., Talanian, R. V., Yuen, P., Gilbertsen, R. B., and Wang, K. K. (1996) Non-erythroid alpha-spectrin breakdown by calpain and interleukin 1 beta-converting-enzyme-like protease(s) in apoptotic cells: contributory roles of both protease families in neuronal apoptosis. *Biochem J* 319, 683-690

24. Wang, K. (2000) Calpain and caspase: can you tell the difference?, by kevin K.W. WangVol. 23, pp. 20-26. *Trends in Neurosciences* 23, 59

25. Nath, R., Probert, A., McGinnis, K. M., and Wang, K. K. (1998) Evidence for activation of caspase-3-like protease in excitotoxin- and hypoxia/hypoglycemia-injured neurons. *J Neurochem* 71, 186-195

26. Johnston, M. V., Fatemi, A., Wilson, M. A., and Northington, F. (2011) Treatment advances in neonatal neuroprotection and neurointensive care. In *Lancet Neurol* Vol. 10 pp. 372-382

27. Hurn, P. D., Vannucci, S. J., and Hagberg, H. (2005) Adult or perinatal brain injury: does sex matter? In *Stroke* Vol. 36 pp. 193-195

28. Renolleau, S., Fau, S., and Charriaut-Marlangue, C. (2008) Gender-related differences in apoptotic pathways after neonatal cerebral ischemia. In *The Neuroscientist* Vol. 14 pp. 46-52

29. Husi, H., Ward, M. A., Choudhary, J. S., Blackstock, W. P., and Grant, S. G. (2000) Proteomic analysis of NMDA receptor-adhesion protein signaling complexes. *Nat Neurosci* 3, 661-669

30. Ubersax, J., and Ferrell Jr, J. (2007) Mechanisms of specificity in protein phosphorylation. *Nat Rev Mol Cell Biol* 8, 530-541

31. Choi, U. B., Xiao, S., Wollmuth, L. P., and Bowen, M. E. Effect of Src kinase phosphorylation on disordered C-terminal domain of N-methyl-D-aspartic acid (NMDA) receptor subunit GluN2B protein. *J Biol Chem* 286, 29904-29912

32. Gurd, J. W., Bissoon, N., Nguyen, T. H., Lombroso, P. J., Rider, C. C., Beesley, P. W., and Vannucci, S. J. (1999) Hypoxia-ischemia in perinatal rat brain induces the formation of a low molecular weight isoform of striatal enriched tyrosine phosphatase (STEP). *J Neurochem* 73, 1990-1994

33. Du, C.-P., Tan, R., and Hou, X.-Y. (2012) Fyn Kinases Play a Critical Role in Neuronal Apoptosis Induced by Oxygen and Glucose Deprivation or Amyloid-β Peptide Treatment. In *CNS Neurosci Ther* pp. n/a-n/a

34. Xia, Z., Dickens, M., Raingeaud, J., Davis, R. J., and Greenberg, M. E. (1995) Opposing effects of ERK and JNK-p38 MAP kinases on apoptosis. *Science* 270, 1326-1331

35. Atkinson, E. A., Ostergaard, H., Kane, K., Pinkoski, M. J., Caputo, A., Olszowy, M. W., and Bleackley, R. C. (1996) A physical interaction between the cell death protein Fas and the tyrosine kinase p59fynT. *J Biol Chem* 271, 5968-5971

36. DeRidder, M. N., Simon, M. J., Siman, R., Auberson, Y. P., Raghupathi, R., and Meaney, D. F. (2006) Traumatic mechanical injury to the hippocampus in vitro causes regional caspase-3 and calpain activation that is influenced by NMDA receptor subunit composition. *Neurobiol Dis* 22, 165-176

37. Vanderklish, P. W., and Bahr, B. A. (2000) The pathogenic activation of calpain: a marker and mediator of cellular toxicity and disease states. *Int J Exp Pathol* 81, 323-339

Chapter 4: NR2B phosphorylation at Tyr 1472 contributes to brain injury in a mouse model of neonatal hypoxia-ischemia

Renatta Knox, Angela Brennan, Diana Yang, Ashley Bach, Matthew Lam, Stefan Lowenstein, Jinwei Yuan, Takanobu Nakazawa, Tadashi Yamamoto, Raymond Swanson, Donna Ferriero, Xiangning Jiang

Introduction

Previous studies have implicated NR2B tyrosine phosphorylation in neonatal hypoxic-ischemic (HI) brain injury. In postnatal day 7 (P7) rats exposed to HI, NR2B tyrosine phosphorylation increases at 1hr after injury as does pY1472 NR2B (1). Previously, we found that in P7 mice, NR2B tyrosine phosphorylation increases in the cortex immediately after HI (2). We also observed early increases in pY1472, pY1336 and pY1252 after HI (See Chp 2). However, it is unknown whether elevated tyrosine phosphorylation of NR2B contributes to brain injury. In this study, we determined the function of pY1472 NR2B *in vivo* and *in vitro* using mice with a knock-in mutation of the Y1472 to phenylalanine (YF-KI).

Methods

Animals

C57BL/6 YF-KI mice (generously provided by Dr. Tadashi Yamamoto, Department of Cancer Biology, University of Tokyo, as described in (3)) were bred with WT mice from Charles River to generate heterozygous animals at the Laboratory Animal Resource Center (LARC) of the University of California, San Francisco. Heterozygous mice were crossed to generate WT and homozygous YF-KI littermates for experiments. Both sexes were used for these studies at postnatal day 7 (P7).

Hypoxic-Ischemic Brain Injury

HI was induced with an adaptation of the Vannucci procedure (4). At P7, pups were anesthetized with isoflurane (2-3% isoflurane/balance oxygen) and the right common carotid artery was ligated. Animals were allowed to recover for 1.5 hours with their dam and then exposed to 40 minutes of hypoxia in a humidified chamber at 37°C with 8% oxygen/balance nitrogen. Hypoxia was staggered, so that each animal recovered for 1.5 hours. Sham-operated control animals received isoflurane anesthesia and exposure of the right common carotid artery without ligation or hypoxia. HI and sham animals were returned to their dams until they were euthanized.

Evaluation of Brain Injury

Five days after the HI procedure, brains were examined histologically with cresyl violet and Perl's stain to assess the degree of damage as previously described (2). Briefly, animals were anesthetized with pentobarbital (50mg/kg) and transcardially perfused with 4% paraformaldehyde (PFA) in 0.1M phosphate buffer (pH 7.4). Brains were post-fixed in the same solution for 4 hours, and then transferred to 30% sucrose in 0.1M phosphate buffer. Coronal sections were cut through the forebrain at 50μM intervals with a vibratome. Alternate sections were stained with cresyl violet for morphology or with Perl's stain enhanced with diaminobenzidine to localize iron deposition. Brain sections were scored as described (5).

Western Blotting

Cortical tissue from sham-operated and the ipsilateral side of HI-injured animals was homogenized in modified radioimmunoprecipitation assay buffer (RIPA buffer, 1X sodium phosphate buffer with 1% NP-40, 0.5% sodium deoxycholate, 0.1% SDS, protease and phosphatase inhibitors). 25μg of protein from sham or ipsilateral cortex was applied to 4-12% Bis-Tris SDS polyacrylamide gel electrophoresis (Invitrogen, Carlsbad, CA) and transferred to polyvinyl difluoride membrane (Bio-Rad, Hercules, CA) as described elsewhere (2). The membranes were probed with the following primary antibodies overnight at 4°C: Fyn (1:1000; Santa Cruz Biotechnology, Santa Cruz, CA), Src (1:1000; Millipore, Billerica, MA), phospho-Src (phospho-Tyr416; 1:500; Cell Signaling Technology, Boston, MA), NR2B (1:1000; BD Transduction Laboratories, San Jose, CA), phospho-Y1252 NR2B (1:800; PhosphoSolutions, Aurora, CO), phospho-Y1336 NR2B (1:800; PhosphoSolutions), phospho-Y1472 NR2B (1:500; Cell Signaling Technology, Boston, MA), phospho-Y1070 NR2B (1:500; Cell Signaling Technology, Boston, MA), phospho-p38 (1:500; Cell Signaling Technology, Boston, MA), p38 (1:500; Cell Signaling Technology, Boston, MA), phospho-T286CaMKII (1:1000; Cell Signaling Technology, Boston, MA), CaMKIIα (1:1000; Millipore, Billerica, MA), phospho-S831GluR1 (1:1000; Millipore, Billerica, MA), GluR1 (1:1000; Millipore, Billerica, MA), α-spectrin (1:1000; Millipore, Billerica, MA), cleaved caspase 3 (1:500; Cell Signaling Technology, Boston, MA) and β-actin (1:2000; Santa Cruz Biotechnology). Appropriate secondary horseradish peroxidase-conjugated antibodies (1:2000, Santa Cruz Biotechnology) were used and signal was visualized with enhanced

chemiluminescence (Amersham, Buckinghamshire, UK). Image J software was used to measure the optical densities (OD) and areas of protein signal on radiographic film after scanning.

Primary Neuronal Cultures

Cultures were prepared from the cortices of embryonic day 14 mice and plated in 24-well culture plates or poly-D-lysine coated glass coverslips at a density of 1.65 x 10^6 cells/mL. After 1 day in culture, 10 μM cytosine arabinoside was added for 24 hours to prevent glial proliferation. The neurons were subsequently maintained with serum-free NeuroBasal medium (Gibco) containing 5 mM glucose, and used at day 10 in vitro. These cultures contain > 95% neurons and no detectable microglia. Experiments were initiated by exchanging the culture medium with a balanced salt solution (BSS) containing 1.2 mM $CaCl_2$, 0.8 mM $MgSO_4$, 5.3 mM KCl, 0.4 mM KH_2PO_4,137 mM $NaCl_2$, 0.3 mM $NaHPO_4$, 5 mM glucose, and 10 mM 1,4-piperazinediethanesulfonate (PIPES) buffer, pH 7.2. Drugs were added from concentrated stocks in BSS 10 minutes prior to the addition of NMDA.

Intracellular calcium and mitochondrial membrane potential imaging

On day *in vitro* 10 (DIV10) neurons were loaded for 30 minutes with 4 μM Fura-2 AM (Molecular Probes) and washed once with BSS prior to imaging. If simultaneous detection of superoxide production was conducted, Fura-2 was removed and exchanged for BSS containing 5uM dihydroethidium (Invitrogen) 10 - 20 minutes

prior to the addition of NMDA, and maintained throughout the duration of the experiment. Images were acquired at 30 second intervals, using excitation which alternated between 340 nm and 380 nm (emission > 510 nm) for Fura-2, and 510-550 nm excitation (> 580 nm emission) for Eth. For both Fura-2 and Eth, raw fluorescence was normalized to baseline levels prior to stimulus. Calcium transients were then determined by calculating the ratio of 340 nm / 380 nm fluorescence from these normalized values.

Cell death

Dead neurons were identified by using fluorescence markers, propidium iodide and calcein-AM which were added to the culture wells 24 hours after NMDA exposures. Live and dead neurons were counted in 3 randomly chosen fields in a minimum of 4 wells per plate, and results of each experiment were expressed as the percent of neurons that were dead.

Statistical Analysis

Data are presented as median and interquartile range for brain injury score using Prism 4 nonparametric tests for analysis of variance (Kruskal-Wallis test). Contingency tables were used to determine mortality differences. Data of optical densities of immunoblots are presented as mean ± SD and were evaluated statistically using SAS Wilcoxon-Mann-Whitney test. For cell culture experiments, one way analysis of variance (Tukeys post hoc test) was used and data are

presented as mean ± SEM. For *in vivo* and *in vitro* studies, differences were considered significant at $p<0.05$.

Results

YF-KI mice have decreased brain injury following neonatal HI

We examined the effect of pY1472 NR2B on the degree of brain injury after neonatal HI using mice in which Y1472 is mutated to phenylalanine (YF-KI) (3). YF-KI mice had decreased overall brain injury compared to WT animals [median = 16.25, range 11.5-19 in WT (n=18); median = 11, range 7.5-15 in YF-KI (n=23), WT vs. YF-KI p=0.03434, Fig. 1A, B]. The cortex showed a statistically significant decrease in brain injury in YF-KI mice compared to WT and the striatum showed a trend toward a significant decrease in brain injury (cortex p=0.013, striatum p=0.067, Fig. 1C-E). There were no differences in degree of brain injury in the hippocampus (Fig.1D). There were no gender differences in brain injury in WT or YF-KI mice after HI (Figure 1F).

pY1472 affects NR2B tyrosine phosphorylation at specific sites and Src family kinase activity

Next we determined the phosphorylation status of the NR2B subunit, as YF-KI mice are hypo-tyrosine phosphorylated in the amygdala (3). We performed western blots on cortical lysates from sham and HI operated WT and YF-KI mice and examined the expression of pY1472, pY1336, pY1252, pY1070 and NR2B at

different time points following injury. Consistent with our previous study, we found that pY1472, pY1336 and pY1252 increase in response to HI in WT mice (Fig. 2A-E). We also examined the expression of another Fyn-mediated NR2B phosphorylation site, Y1070, which has not been characterized in the literature (6). We found a small increase in pY1070 after HI at 15min in WT animals (Fig. 2A, E).

Interestingly, YF-KI mice had a significant decrease in the expression of pY1070, pY1252 and pY1336 in sham-operated animals. There was a 20% reduction in pY1336, a 50% reduction in pY1252 and a 70% reduction in pY1070 ($p<0.05$ WT vs. YF-KI). After HI, YF-KI mice had significantly less pY1252 at 15min, and less pY1070 for up to 6hrs after injury compared to WT mice. pY1336 had a trend toward decreased expression at 15min after HI in YF-KI mice compared to WT (pY1336 WT vs. YF-KI, $p=0.08326$) (Fig. 2A-E).

To elucidate the molecular basis of decreased NR2B tyrosine phosphorylation in YF-KI mice, we did western blots on cortical lysates from WT and YF-KI mice for Fyn, Src, and activated SFKs (pY416). In sham-operated animals, there was a 30% reduction in pY416 in YF-KI mice compared to WT (WT vs. YF-KI, $p=0.01387$), but there were no differences in Fyn or Src expression (Fig. 3A, B).

YF-KI mice have less cell death in vivo in response to neonatal HI

We assessed cell death *in vivo* by examining the activity of calcium-activated protease calpain and caspase 3 for their substrate α-spectrin. Calpain cleavage of α-spectrin produces a 150 and 145 kDa fragment while caspase cleavage of α-spectrin produces a 120 kDa fragment (7). In WT mice, we found increased calpain and

caspase activity, as measured by α-spectrin cleavage, at 1hr, 6hr and 24hr after injury. However, YF-KI mice did not differ from sham animals in calpain and caspase activity (Fig 4A-C). Consistent with these findings, cleaved-caspase 3 (activated caspase 3) protein levels were elevated in WT mice at 6hr and 24hr after injury, but not in YF-KI mice (Fig. 4A, D).

To ascertain how decreased NR2B tyrosine phosphorylation could lead to less cell death, we examined the activity of the p38 MAP kinase (MAPK) that is implicated in neonatal HI brain injury and NMDAR activity (8, 9). While there was elevated p38 MAPK activity in response to neonatal HI, there was no difference in p38 phosphorylation between WT and YF-KI mice (Fig. 5A, B). Previous studies have shown that YF-KI mice have decreased CaMKII activity and decreased phosphorylation of CaMKII substrate GluR1 AMPA receptor in the spinal cord (10). We found decreased CaMKII activity in response to neonatal HI in cortical lysates from WT animals and no difference in pS831 GluR1 between WT and YF-KI mice in response to injury (Fig. 5A,C,D).

YF-KI neurons have decreased superoxide production in response to NMDA

Next, we performed *in vitro* experiments to determine the effect of pY1472 on calcium flux and superoxide generation, which have both been implicated in neuronal cell death. There was no significant difference in the total increase in intracellular calcium between WT and YF-KI neurons (Fig. 6A) (mean peak fluorescence; wt neurons 3.27 ± 0.24 vs Y1472 neurons 3.19 ± 0.28). NMDA treatment of WT neurons caused a significant increase in superoxide production

which was diminished substantially in YF-KI neurons (Fig. 6B). Exposure of cortical neurons to NMDA resulted in a 1.6 fold increase in cell death relative to control. However, YF-KI neurons had a significant decrease in cell death relative to WT neurons when treated with NMDA or glutamate (Fig. 7A,B).

Discussion

In summary, we find that Y1472 mutation to phenylalanine results in neuroprotection from cell death *in vivo* and *in vitro*. YF-KI mice exposed to neonatal HI have less brain injury, NR2B tyrosine phosphorylation, SFK activity, and decreased activity of proteases implicated in necrotic and apoptotic cell death. *In vitro*, YF-KI neurons have less superoxide generation in response to NMDA and are protected from NMDA and glutamate induced cell death.

We report for the first time, that in the neonatal cortex, pY1472 affects tyrosine phosphorylation of at least 3 other tyrosine residues on NR2B - Y1336, Y1252, and Y1070. Two previous studies did not find changes in phosphorylation of Y1336 or Y1252 in YF-KI mice in the amygdala or spinal cord (3, 11). These discrepancies may be due to different brain regions or brain maturity. While the function of Y1070 and Y1252 is unknown, pY1336 mediates the interaction of NR2B with the p85 subunit of PI-3 kinase (12). Additionally, YF-KI mice have decreased CaMKII and α-actinin associated with NR2B (3). Therefore, it is likely that changes in multiple tyrosine phosphorylation sites affects the recruitment of proteins to the NR2B complex in naive animals and in the setting of injury.

Decreased NR2B tyrosine phosphorylation correlated with lower SFK activity. SFKs can be activated directly via kinases, phosphatases, and in response to many stimuli in the brain (13). Y1472 may be involved in SFK regulation by recruiting SFKs to the NMDAR complex in the PSD where they can be activated.

One study found that in response to neuropathic pain in the spinal cord, there was decreased intracellular calcium in YF-KI mice but there was no effect on intracellular calcium at baseline. Changes in intracellular calcium correlated with decreased activity of CaMKII which is known to be activated by calcium flux from the NMDAR (11). We found no difference in calcium load *in vitro* and *in vivo* we did not observe differences in CaMKII activity following neonatal HI brain injury. This suggests that *in vivo*, there is no difference in NMDAR-mediated calcium flux in response to neonatal HI in WT and YF-KI mice. However, the calcium activated protease calpain did have decreased activity in YF-KI mice suggesting that calcium signaling may be dysregulated. We also found that in synaptic fractions, CaMKII activity is increased but not in whole cell lysates (Knox and Jiang, unpublished observations). The additional cellular stress of HI could lead to changes in calcium flux in synaptic membranes downstream of the NMDAR or other calcium channels.

Although we did not find differences in the p38 MAPK pathway that is involved in neonatal HI brain injury, we did find a dramatic reduction of superoxide production *in vitro* in YF-KI neurons, implicating Y1472 phosphorylation in superoxide production independent of calcium flux for the first time. Since neonatal mice are more vulnerable to free radical injury (14), this finding may explain the neuroprotection we observed in YF-KI mice following neonatal HI. pY1472 could

affect reactive oxygen species through the PSD95-nNOS pathway. PSD95 interacts with the NR2B subunit in the extreme C-terminus and has an increased association with the NMDAR in response to ischemia (15). Although the PSD95-NR2B interaction is preserved in naive YF-KI mice (Knox and Jiang, unpublished observations), the association may be diminished in YF-KI mice following neonatal HI.

pY1472 NR2B is enriched in synaptic membranes in the neonatal cortex (16) and increases in this compartment in response to neonatal HI (See Chp 3). While there has been some debate over the function of synaptic and extrasynaptic NMDARs in survival and cell death (17), a recent study found that synaptic NMDARs contribute to hypoxic cell death (18). Another report found that the C-terminal domain (CTD) of NR2B is linked to excitotoxic cell death *in vitro* and *in vivo* (19). Therefore pY1472 is situated to affect cell death processes synaptically through its ability to modify proteins associated with the CTD of NR2B. It may also participate in diverse cell death pathways which occur during neonatal HI brain injury as we found less activity in calpain and caspase which function in apoptotic and necrotic cell death (20).

Here, we provide a mechanistic basis for the increased Fyn-mediated NR2B tyrosine phosphorylation that occurs during neonatal HI brain injury. Future studies will determine how pY1472 alters the NR2B complex in the immature brain and elucidate the function of additional Fyn-mediated tyrosine phosphorylation sites in neonatal HI.

Figure Legends

Figure 1. YF-KI mice have decreased brain injury following neonatal HI.
A modified Vannucci procedure was performed on WT (n=18) and YF-KI mice (n=23) at postnatal day 7 (P7). A) Animals were perfused at P12, brains were sectioned and stained with Cresyl violet (morphology) and Perl's Stain (iron deposition). Arrows indicate patches of cell loss in Cresyl violet stained sections. Arrowheads show iron accumulation in similar injured areas in Perl-stained adjacent sections. B) Composite injury score and F) composite injury score by gender. Regional injury scores in the C) cortex, D) hippocampus, and E) striatum. The median is represented by the central horizontal line. Brain injury score was analyzed using nonparametric tests for analysis of variance (Kruskal-Wallis test). *$p<0.05$.

Figure 2. Y1472 affects NR2B tyrosine phosphorylation at specific residues.
A) Western blots using anti-pY1472, pY1336, pY1252, pY1070, and NR2B were carried out on cortical lysates from sham and HI animals at the time points shown. B-E) Expression of NR2B tyrosine phosphorylation sites was normalized to NR2B. Data was normalized to an internal control and WT sham values. Representative data for n=4 experiments. Graphs indicate mean ± SD. Data were analyzed using SAS Wilcoxon-Mann-Whitney test. *$p<0.05$, ** $p<0.01$.

Figure 3. YF-KI mice have decreased Src Family Kinase Activity.

A) Western blots using anti-pY416, Fyn, c-Src and β-actin were carried out on cortical lysates from sham and HI animals at the time points shown. B) Expression of p416 was were normalized to β-actin. Data was normalized to an internal control and WT sham values. Representative data for n=4 experiments. Graphs indicate mean ± SD. Data were analyzed using SAS Wilcoxon-Mann-Whitney test. *p<0.05.

Figure 4. YF-KI mice have less activity of calpain and caspase after HI.
A) Western blots using anti-α-spectrin, cleaved caspase 3 and β-actin were carried out on cortical lysates from sham and HI animals at the time points shown. B) Expression of spectrin and cleaved-caspase 3 was normalized to β-actin. Data was normalized to an internal control and WT sham values. Representative data for n=4 experiments. Graphs indicate mean ± SD. Data were analyzed using SAS Wilcoxon-Mann-Whitney test. *p<0.05.

Figure 5. p38 MAPK and CaMKII pathways are not differentially activated in WT and YF-KI mice after neonatal HI.
A) Western blots using anti-p-p38, p38, pT286 CaMKII, CaMKIIα, pS831 GluR1, GluR1 and β-actin were carried out on cortical lysates from sham and HI animals at the time points shown. B) p-p38 was normalized to p38, C) pCaMKII was normalized to β-actin , and D) pS831 GluR1 was normalized to GluR1. Data was normalized to WT sham values. Representative data for n=3 experiments. Graphs indicate mean ± SD. Data were analyzed using SAS Wilcoxon-Mann-Whitney test. *p<0.05.

Figure 6. YF-KI neurons have decreased superoxide production in response to NMDA.

A) Representative Fura-2 transients (from n = 5) show robust calcium increases after NMDA application (arrow) in both WT (black circles) and YF-KI neurons (open circles). B) Panels illustrate Eth fluorescence before NMDA application (0 minutes), at the time of NMDA addition (5 minutes) and then at 5 minute intervals in both wild-type or in YF-KI neurons. Representative Eth fluorescence transients show only wild-type neurons (black circles) have a significant increase in superoxide production following NMDA application (arrow) compared to Y1472 neurons (open circles). Mean peak Eth fluorescence; WT neurons 2.75 ± 0.09 vs. YF-KI neurons 1.34 ± 0.04.

Figure 7. Protection from NMDA and Glutamate induced cell death in YF-KI neurons.

A) Panels illustrate propidium iodide labeled dead neurons 24 hours after NMDA or glutamate treatment in either wild-type neurons or in YF-KI neurons. B) Quantification shows that NMDA or glutamate-induced neuronal death occurred only in wild-type cultures but not in Y1472 neurons. $p < 0.01$, $n = 3$. Data were analyzed using Tukeys test. ** $p<0.01$, ***$p<0.001$.

Figure 8. Model.

pY1472 contributes to cell death during neonatal HI through the regulation of NR2B tyrosine phosphorylation, generation of superoxide, and activation of proteases calpain and caspase 3.

Fig. 1

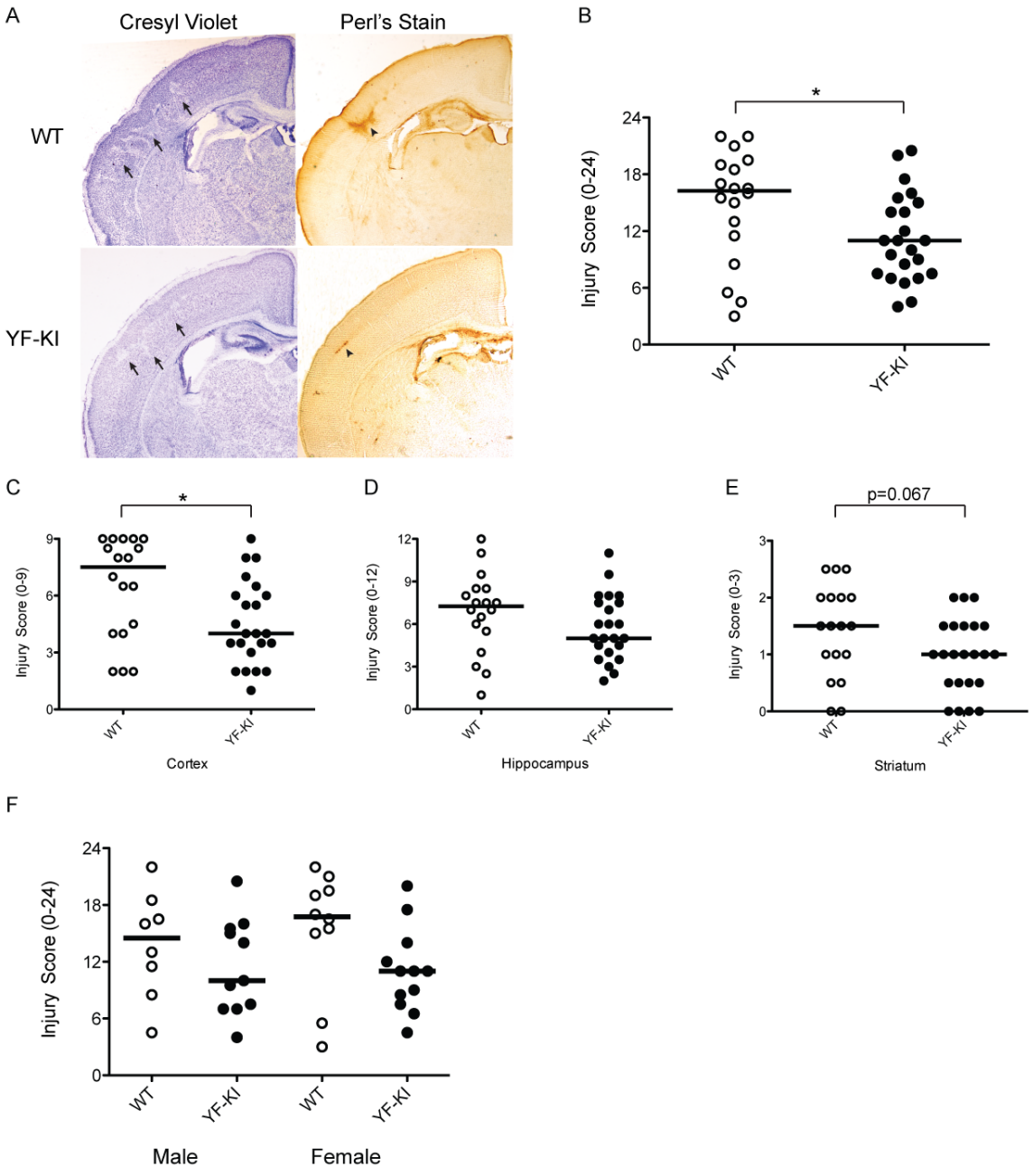

Figure 1. YF-KI mice have decreased brain injury following neonatal HI.
A modified Vannucci procedure was performed on WT (n=18) and YF-KI mice (n=23) at postnatal day 7 (P7). A) Animals were perfused at P12, brains were sectioned and stained with Cresyl violet (morphology) and Perl's Stain (iron deposition). Arrows indicate patches of cell loss in Cresyl violet stained sections. Arrowheads show iron accumulation in similar injured areas in Perl-stained

adjacent sections. B) Composite injury score and F) composite injury score by gender. Regional injury scores in the C) cortex, D) hippocampus, and E) striatum. The median is represented by the central horizontal line. Brain injury score was analyzed using nonparametric tests for analysis of variance (Kruskal-Wallis test). *$p<0.05$.

Fig. 2

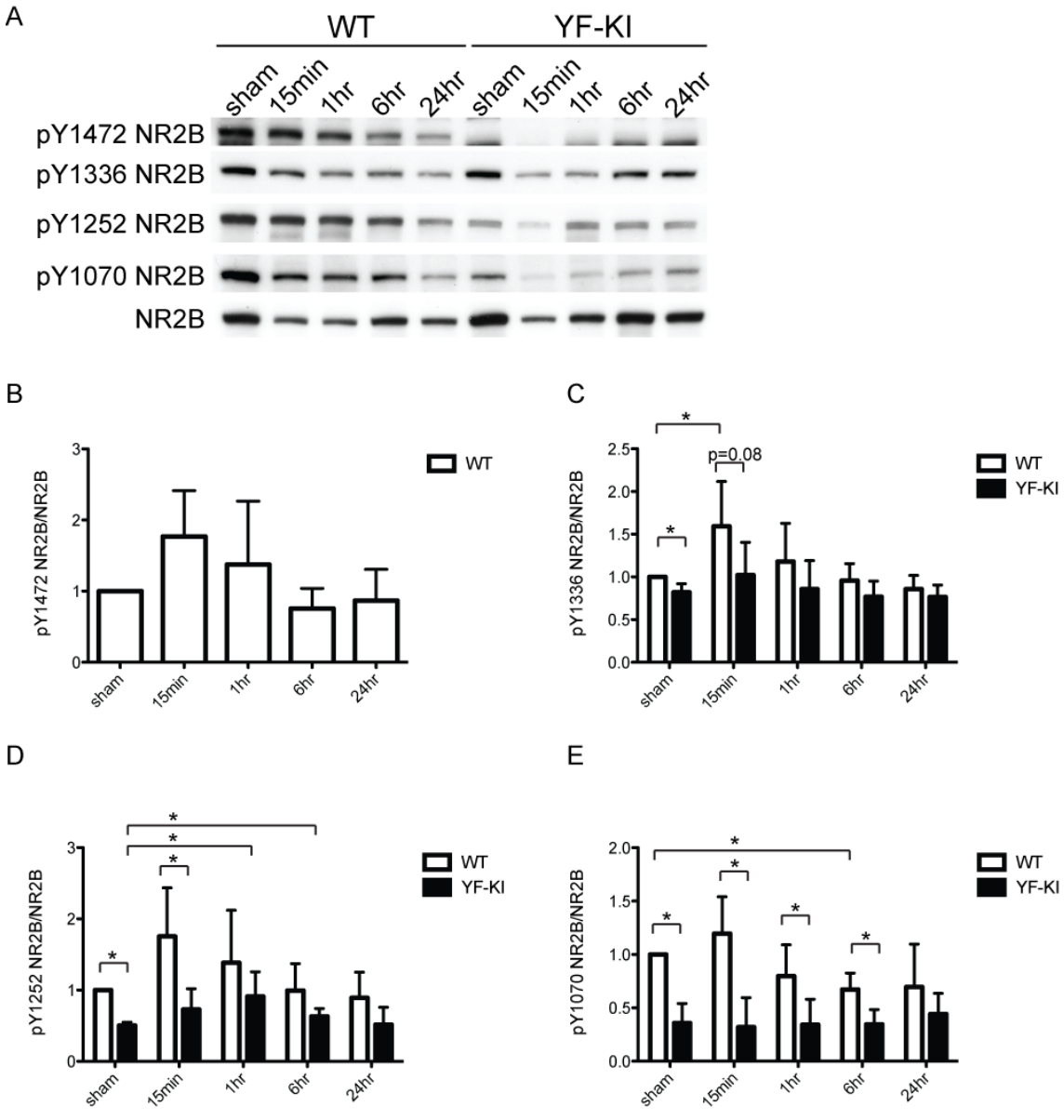

Figure 2. Y1472 affects NR2B tyrosine phosphorylation at specific residues.
A) Western blots using anti-pY1472, pY1336, pY1252, pY1070, and NR2B were carried out on cortical lysates from sham and HI animals at the time points shown. B-E) Expression of NR2B tyrosine phosphorylation sites was normalized to NR2B. Data was normalized to an internal control and WT sham values. Representative data for n=4 experiments. Graphs indicate mean ± SD. Data were analyzed using SAS Wilcoxon-Mann-Whitney test. *p<0.05, ** p<0.01.

Fig. 3

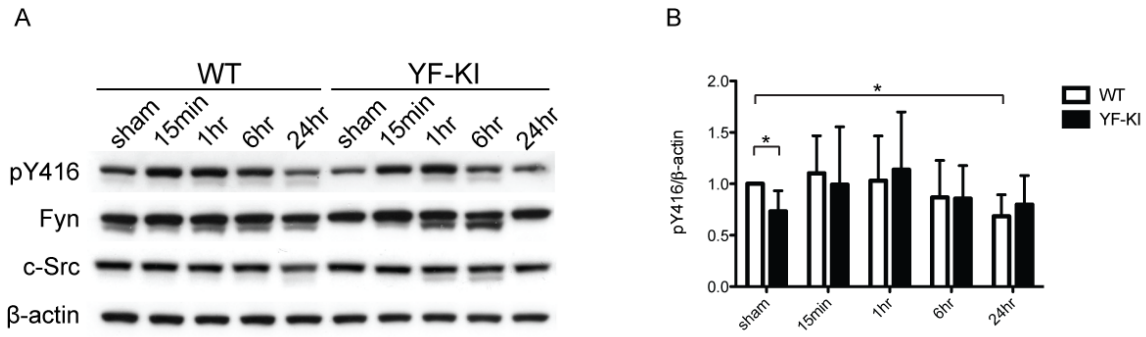

Figure 3. YF-KI mice have decreased Src Family Kinase Activity.
A) Western blots using anti-pY416, Fyn, c-Src and β-actin were carried out on cortical lysates from sham and HI animals at the time points shown. B) Expression of p416 was were normalized to β-actin. Data was normalized to an internal control and WT sham values. Representative data for n=4 experiments. Graphs indicate mean ± SD. Data were analyzed using SAS Wilcoxon-Mann-Whitney test. *$p<0.05$.

Fig. 4

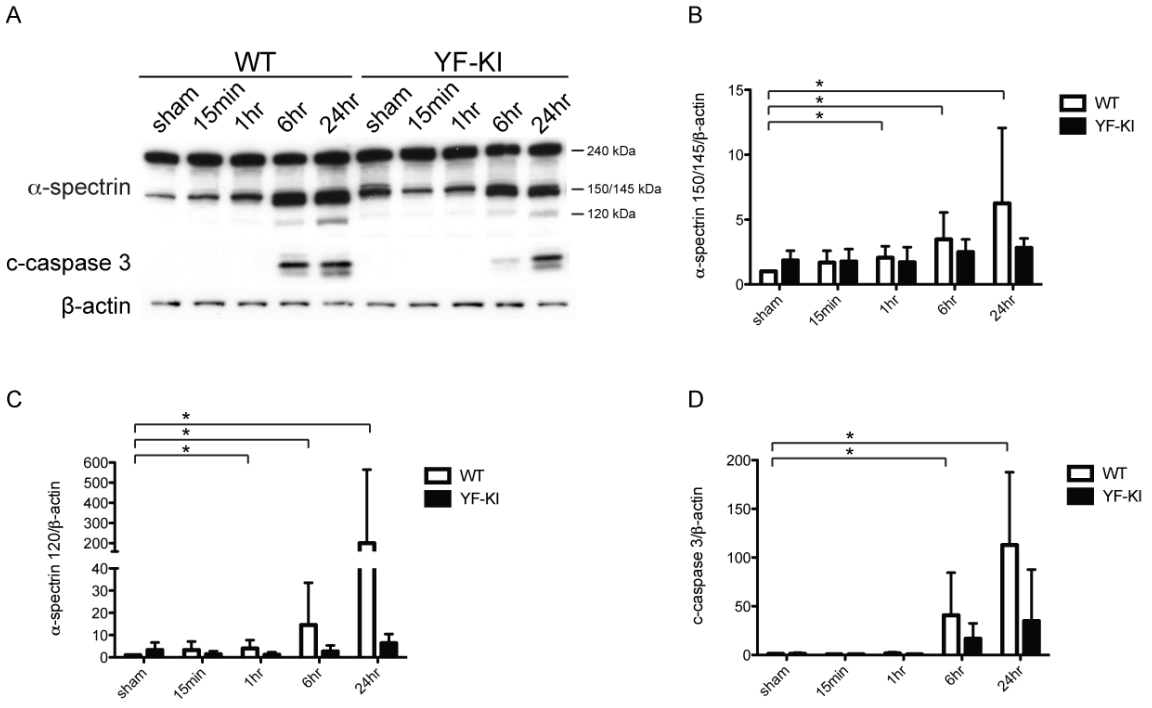

Figure 4. YF-KI mice have less activity of calpain and caspase after HI.
A) Western blots using anti-α-spectrin, cleaved caspase 3 and β-actin were carried out on cortical lysates from sham and HI animals at the time points shown. B) Expression of spectrin and cleaved-caspase 3 was normalized to β-actin. Data was normalized to an internal control and WT sham values. Representative data for n=4 experiments. Graphs indicate mean ± SD. Data were analyzed using SAS Wilcoxon-Mann-Whitney test. *$p<0.05$.

Fig. 5

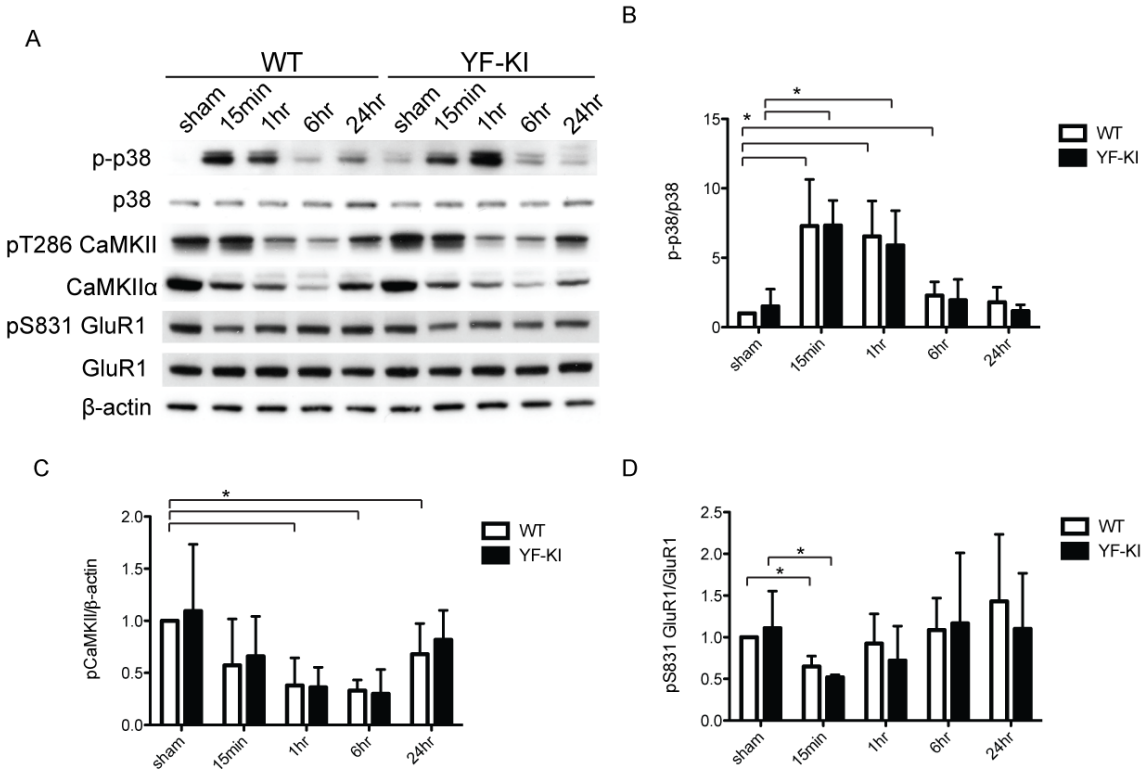

Figure 5. p38 MAPK and CaMKII pathways are not differentially activated in WT and YF-KI mice after neonatal HI.
A) Western blots using anti-p-p38, p38, pT286 CaMKII, CaMKIIα, pS831 GluR1, GluR1 and β-actin were carried out on cortical lysates from sham and HI animals at the time points shown. B) p-p38 was normalized to p38, C) pCaMKII was normalized to β-actin , and D) pS831 GluR1 was normalized to GluR1. Data was normalized to WT sham values. Representative data for n=3 experiments. Graphs indicate mean ± SD. Data were analyzed using SAS Wilcoxon-Mann-Whitney test. *p<0.05.

Fig. 6

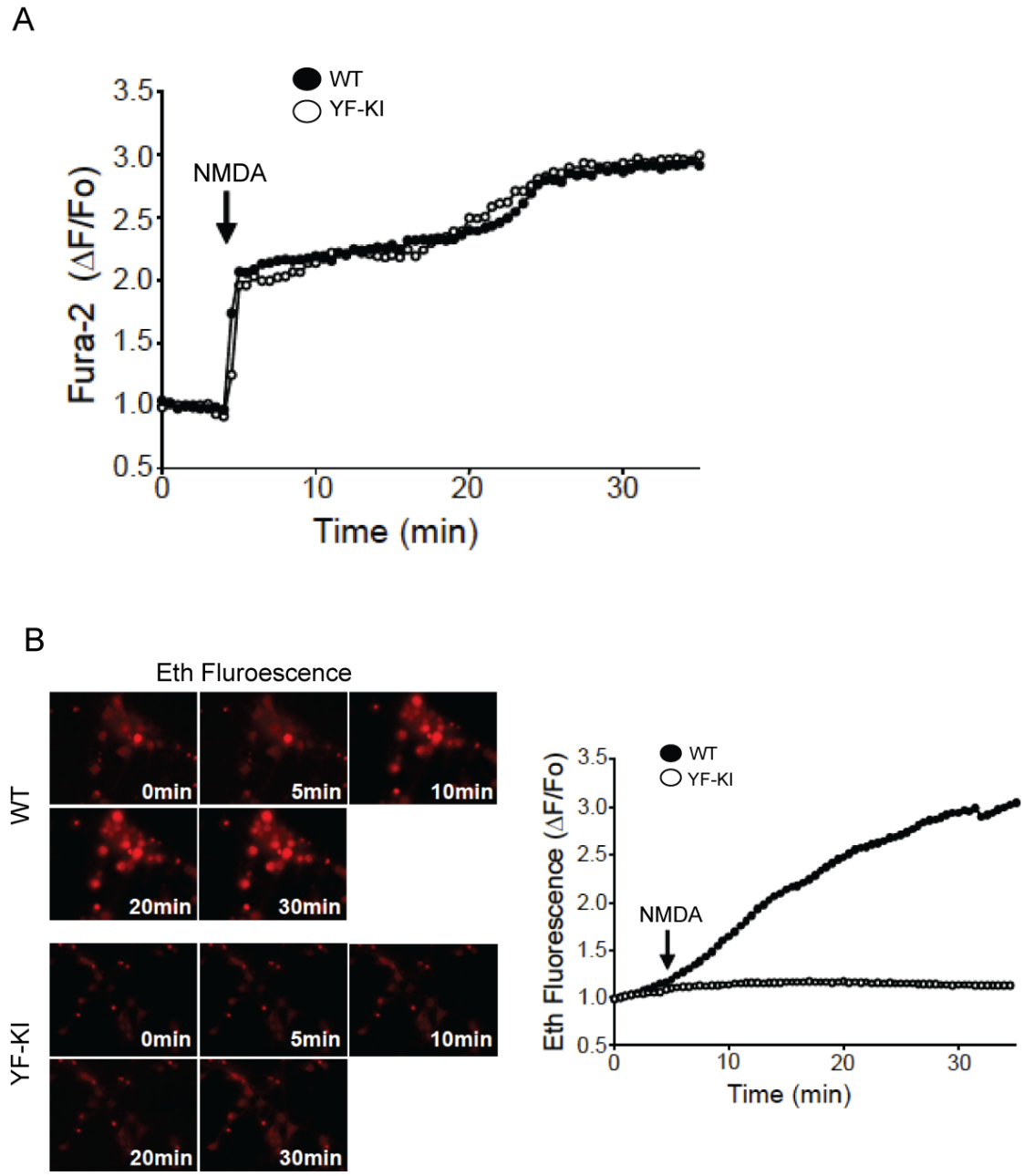

Figure 6. YF-KI neurons have decreased superoxide production in response to NMDA.
A) Representative Fura-2 transients (from n = 5) show robust calcium increases after NMDA application (arrow) in both WT (black circles) and YF-KI neurons (open circles). B) Panels illustrate Eth fluorescence before NMDA application (0 minutes), at the time of NMDA addition (5 minutes) and then at 5 minute intervals in both wild-type or in YF-KI neurons. Representative Eth fluorescence transients show only wild-type neurons (black circles) have a significant increase in superoxide

production following NMDA application (arrow) compared to Y1472 neurons (open circles). Mean peak Eth fluorescence; WT neurons 2.75 ± 0.09 vs. YF-KI neurons 1.34 ± 0.04.

Fig. 7

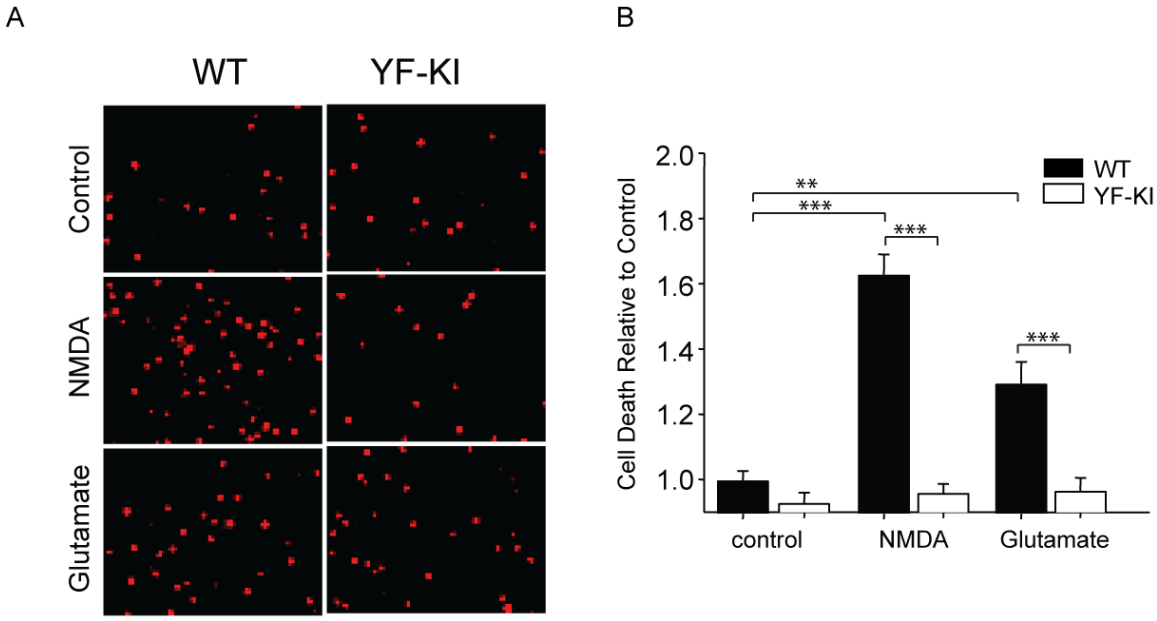

Figure 7. Protection from NMDA and Glutamate induced cell death in YF-KI neurons. A) Panels illustrate propidium iodide labeled dead neurons 24 hours after NMDA or glutamate treatment in either wild-type neurons or in YF-KI neurons. B) Quantification shows that NMDA or glutamate-induced neuronal death occurred only in wild-type cultures but not in Y1472 neurons. $p < 0.01$, $n = 3$. Data were analyzed using Tukeys test. ** $p<0.01$, ***$p<0.001$.

Fig. 8

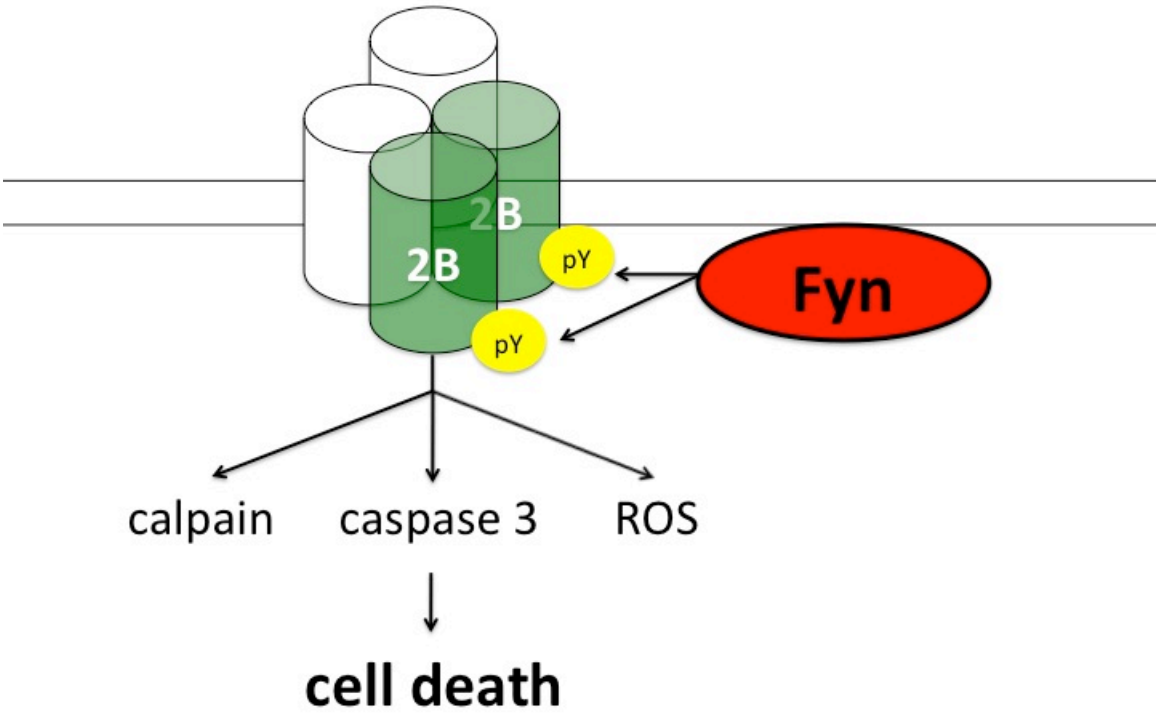

Figure 8. Model.
pY1472 contributes to cell death during neonatal HI through the regulation of NR2B tyrosine phosphorylation, generation of superoxide, and activation of proteases calpain and caspase 3.

References

1. Gurd, J. W., Bissoon, N., Beesley, P. W., Nakazawa, T., Yamamoto, T., and Vannucci, S. J. (2002) Differential effects of hypoxia-ischemia on subunit expression and tyrosine phosphorylation of the NMDA receptor in 7- and 21-day-old rats. In *J Neurochem* Vol. 82 pp. 848-856
2. Jiang, X., Mu, D., Biran, V., Faustino, J., Chang, S., Rincón, C., Sheldon, R., and Ferriero, D. (2008) Activated Src kinases interact with the N-methyl-D-aspartate receptor after neonatal brain ischemia. *Ann Neurol.* 63, 632-641
3. Nakazawa, T., Komai, S., Watabe, A. M., Kiyama, Y., Fukaya, M., Arima-Yoshida, F., Horai, R., Sudo, K., Ebine, K., Delawary, M., Goto, J., Umemori, H., Tezuka, T., Iwakura, Y., Watanabe, M., Yamamoto, T., and Manabe, T. (2006) NR2B tyrosine phosphorylation modulates fear learning as well as amygdaloid synaptic plasticity. *EMBO J* 25, 2867-2877
4. Ditelberg, J. S., Sheldon, R. A., Epstein, C. J., and Ferriero, D. M. (1996) Brain injury after perinatal hypoxia-ischemia is exacerbated in copper/zinc superoxide dismutase transgenic mice. *Pediatr Res* 39, 204-208
5. Sheldon, R. A., Sedik, C., and Ferriero, D. M. (1998) Strain-related brain injury in neonatal mice subjected to hypoxia-ischemia. *Brain Res* 810, 114-122
6. Nakazawa, T. (2000) Characterization of Fyn-mediated Tyrosine Phosphorylation Sites on GluRepsilon 2 (NR2B) Subunit of the N-Methyl-D-aspartate Receptor. In *Journal of Biological Chemistry* Vol. 276 pp. 693-699
7. Wang, K. (2000) Calpain and caspase: can you tell the difference?, by kevin K.W. WangVol. 23, pp. 20-26. *Trends in Neurosciences* 23, 59

8. Xu, J., Kurup, P., Zhang, Y., Goebel-Goody, S. M., Wu, P. H., Hawasli, A. H., Baum, M. L., Bibb, J. A., and Lombroso, P. J. (2009) Extrasynaptic NMDA receptors couple preferentially to excitotoxicity via calpain-mediated cleavage of STEP. *J Neurosci* 29, 9330-9343

9. Han, B. H., Choi, J., and Holtzman, D. M. (2002) Evidence that p38 mitogen-activated protein kinase contributes to neonatal hypoxic-ischemic brain injury. In *Dev Neurosci* Vol. 24 pp. 405-410

10. Katano, T., Nakazawa, T., Nakatsuka, T., Watanabe, M., Yamamoto, T., and Ito, S. (2011) Involvement of spinal phosphorylation cascade of Tyr1472-NR2B, Thr286-CaMKII, and Ser831-GluR1 in neuropathic pain. In *Neuropharmacology* Vol. 60 pp. 609-616

11. Matsumura, S., Kunori, S., Mabuchi, T., Katano, T., Nakazawa, T., Abe, T., Watanabe, M., Yamamoto, T., Okuda-Ashitaka, E., and Ito, S. (2010) Impairment of CaMKII activation and attenuation of neuropathic pain in mice lacking NR2B phosphorylated at Tyr1472. In *European Journal of Neuroscience* Vol. 32 pp. 798-810

12. Hisatsune, C., Umemori, H., Mishina, M., and Yamamoto, T. (1999) Phosphorylation-dependent interaction of the N-methyl-D-aspartate receptor epsilon 2 subunit with phosphatidylinositol 3-kinase. In *Genes Cells* Vol. 4 pp. 657-666

13. Salter, M., and Kalia, L. (2004) Src kinases: a hub for NMDA receptor regulation. In *Nat Rev Neurosci* Vol. 5 pp. 317-328

14. Vexler, Z. S., and Ferriero, D. M. (2001) Molecular and biochemical mechanisms of perinatal brain injury. *Seminars in neonatology* 6, 99-108

15. Aarts, M. (2002) Treatment of Ischemic Brain Damage by Perturbing NMDA Receptor- PSD-95 Protein Interactions. In *Science* Vol. 298 pp. 846-850

16. Jiang, X., Knox, R., Pathipati, P., and Ferriero, D. (2011) Developmental localization of NMDA receptors, Src and MAP kinases in mouse brain. In *Neurosci Lett* Vol. 503 pp. 215-219

17. Hardingham, G. E., and Bading, H. (2010) Synaptic versus extrasynaptic NMDA receptor signalling: implications for neurodegenerative disorders. In *Nat Rev Neurosci* Vol. 11 pp. 682-696

18. Wroge, C. M., Hogins, J., Eisenman, L., and Mennerick, S. (2012) Synaptic NMDA Receptors Mediate Hypoxic Excitotoxic Death. In *Journal of Neuroscience* Vol. 32 pp. 6732-6742

19. Martel, M.-A., Ryan, T. J., Bell, K. F. S., Fowler, J. H., McMahon, A., Al-Mubarak, B., Komiyama, N. H., Horsburgh, K., Kind, P. C., Grant, S. G. N., Wyllie, D. J. A., and Hardingham, G. E. (2012) The Subtype of GluN2 C-terminal Domain Determines the Response to Excitotoxic Insults. In *Neuron* Vol. 74 pp. 543-556, Elsevier Inc.

20. Northington, F. J., Chavez-Valdez, R., and Martin, L. J. (2011) Neuronal cell death in neonatal hypoxia-ischemia. In *Ann Neurol* Vol. 69 pp. 743-758

Chapter 5: Concluding Remarks

Summary

This dissertation examines the role of Fyn and its regulation of NMDAR tyrosine phosphorylation in neonatal hypoxic-ischemic (HI) brain injury. In chapter 2, we show that Fyn and NR2B are expressed in synaptic and extrasynaptic membranes at P7. Fyn-mediated NR2B phosphorylation at Y1472, Y1336, and Y1252 are enriched at synaptic membranes and pY1336 NR2B is also present at extrasynaptic membranes.

The consequences of neuronal Fyn overexpression on neonatal HI brain injury and NMDAR tyrosine phosphorylation are explored in chapter 3. Fyn OE mice have increased brain injury and mortality following injury. This is associated with increased tyrosine phosphorylation of NR2A and NR2B as well as increased calpain activity. NR2B phosphorylation at Y1252 and Y1472 is higher in Fyn OE mice in synaptic fractions.

In chapter 4 we determine whether phosphorylation of Y1472 of NR2B affects brain injury. Y1472F (YF-KI) mice have less brain injury, decreased NR2B tyrosine phosphorylation of Y1070, Y1252 and Y1336, decreased SFK activity, and less activity of calpain and caspase. YF-KI neurons exposed to NMDA have less superoxide production and significantly less cell death in response to 100 μM NMDA and glutamate.

Taken together our results support the following model for Fyn and the NMDAR in neonatal hypoxic-ischemic brain injury (See Model). At synaptic

membranes, Fyn phosphorylates NR2A and NR2B. Downstream of pY1472, Fyn promotes brain injury through up-regulation of reactive oxygen species and increased activity of calpain and caspase. The function of extrasynaptic Fyn is unknown, however based on our studies, it does not appear to regulate extrasynaptic Y1336 or p38, and may function in other pathways (Knox and Jiang, unpublished observations).

Future Directions

While most of our experiments focused on NR2B, NR2A is also a Fyn substrate and NR2A tyrosine phosphorylation increases after HI (1). It will be interesting to identify which sites Fyn phosphorylates on NR2A and to see if they overlap with the three tyrosine residues that Src phosphorylates on NR2A (Y1292, Y1325, Y1387) (2).

Although Fyn-mediated NR2B tyrosine phosphorylation sites are often studied in isolation, we have chosen to study phosphorylation sites for which there are antibodies (Y1472, Y1336, Y1252, Y1070). In the original publication identifying tyrosine residues on NR2B that Fyn phosphorylates *in vitro*, seven residues were identified (3). They span the entire C-terminal region of NR2B and likely cooperate to affect NMDAR channel properties and the NR2B complex. We identified important differences among these sites. For example, pY1336 is present in synaptic and extrasynaptic membranes and is less affected by Fyn overexpression. pY1070 decreased to a greater extent than the other sites in YF-KI mice after HI. These findings suggest a complex dynamic interplay between the

residues on the C-terminal domain (CTD) of NR2B. To understand this in greater detail, I generated several constructs that will allow us to determine the function of these sites alone and in combination (See Appendix). These reagents will allow us to assign functions to the phosphorylation sites on the CTD of NR2B in the normal brain and in response to injury.

Therapeutic Implications

Our lab has shown that PP2, a SFK inhibitor, is protective, that Fyn overexpression worsens injury, and that a NR2B phosphorylation mutant is protective against neonatal brain hypoxia-ischemia. These results implicate SFKs, Fyn and the NMDAR in the pathogenesis of neonatal HI brain injury and would make attractive therapeutic targets. However, there are two potential caveats. First, although two loss-of-function approaches were neuroprotective (PP2 and YF-KI mice), neither strategy resulted in complete protection. One advantage of the PP2 data obtained from our lab is that it was performed in an outbred mouse strain (CD1) and the drug was delivered after injury intraperitoneally. Although PP2 was not completely protective, it did reduce brain injury from severe to moderate (1). Since brain injury correlates with outcome in neonatal encephalopathy, this could be a significant finding (4). We also do not know how PP2 would affect brain injury if combined with hypothermia, the standard of care for neonatal HIE, or if given in multiple doses.

Although it is possible to disrupt pY1472 using peptides which span this region, such an approach would be difficult to deliver *in vivo*. SFKs likely affect

brain injury through NR2A and other signaling pathways, therefore it would be more advantageous to target the kinase family than one substrate.

The second caveat is that we do not know if SFKs are important for neonatal HI injury in humans. Before considering a therapeutic intervention, it will be important to determine the expression, timing, and regional localization of SFKs and NMDAR phosphorylation in neonatal HI lesions. Genetic studies could also uncover polymorphisms in SFKs and the NMDAR that predispose infants to brain injury, which would provide further rationale for targeting this pathway.

After considering the possible limitations and the progress we have made, targeting Fyn, the NMDAR and other SFKs is a promising therapeutic strategy. As we obtain more information on the link between NMDAR phosphorylation, ROS generation, and cell death and the contribution of other SFKs, we can design therapies that target critical nodes mediating brain injury that do not disrupt normal brain development.

Model

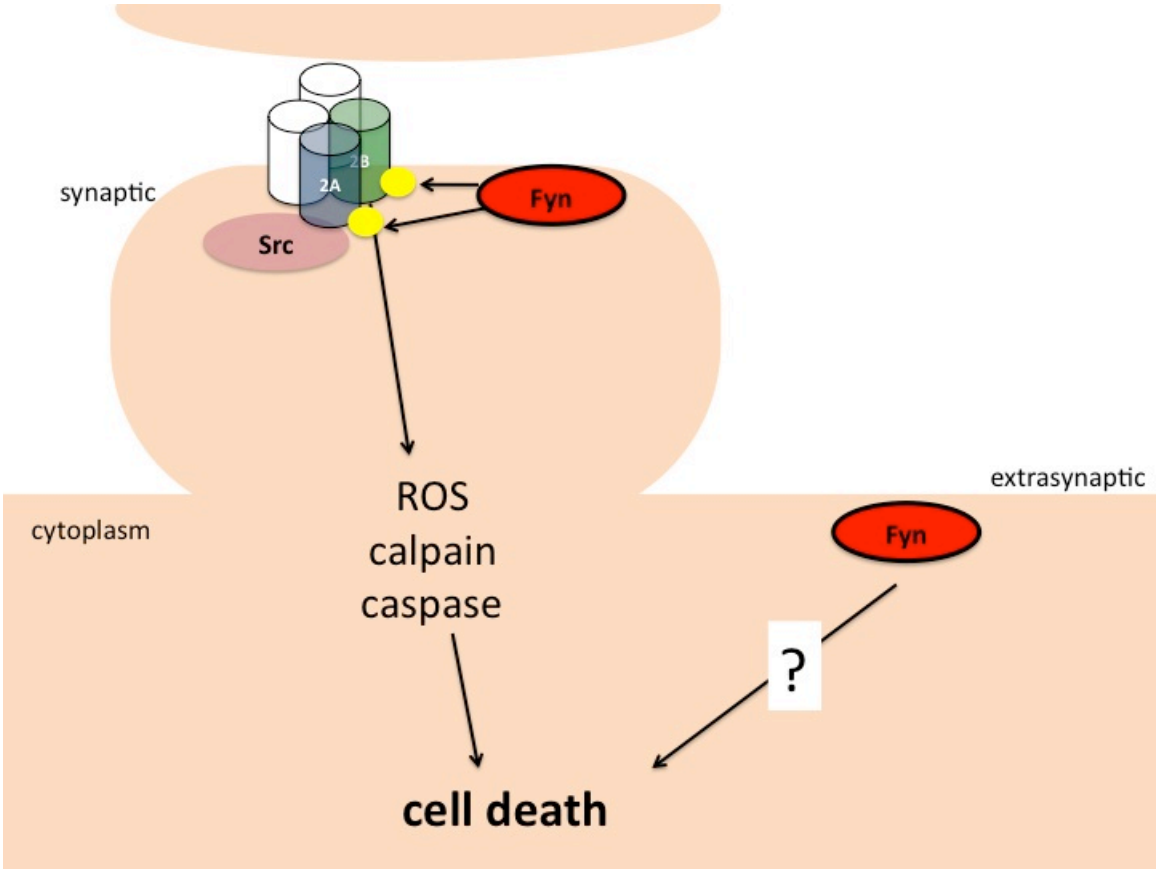
synaptic
2B
2A
Fyn
Src
ROS
calpain
caspase
extrasynaptic
cytoplasm
Fyn
?
cell death

References

1. Jiang, X., Mu, D., Biran, V., Faustino, J., Chang, S., Rincón, C., Sheldon, R., and Ferriero, D. (2008) Activated Src kinases interact with the N-methyl-D-aspartate receptor after neonatal brain ischemia. *Ann Neurol.* 63, 632-641
2. Salter, M., and Kalia, L. (2004) Src kinases: a hub for NMDA receptor regulation. In *Nat Rev Neurosci* Vol. 5 pp. 317-328
3. Nakazawa, T., Komai, S., Tezuka, T., Hisatsune, C., Umemori, H., Semba, K., Mishina, M., Manabe, T., and Yamamoto, T. (2001) Characterization of Fyn-mediated tyrosine phosphorylation sites on GluR epsilon 2 (NR2B) subunit of the N-methyl-D-aspartate receptor. *J Biol Chem* 276, 693-699
4. Miller, S. P., Ramaswamy, V., Michelson, D., Barkovich, A. J., Holshouser, B., Wycliffe, N., Glidden, D. V., Deming, D., Partridge, J. C., Wu, Y. W., Ashwal, S., and Ferriero, D. M. (2005) Patterns of brain injury in term neonatal encephalopathy. In *J Pediatr* Vol. 146 pp. 453-460

Appendix: DNA Constructs

Cloning Strategy

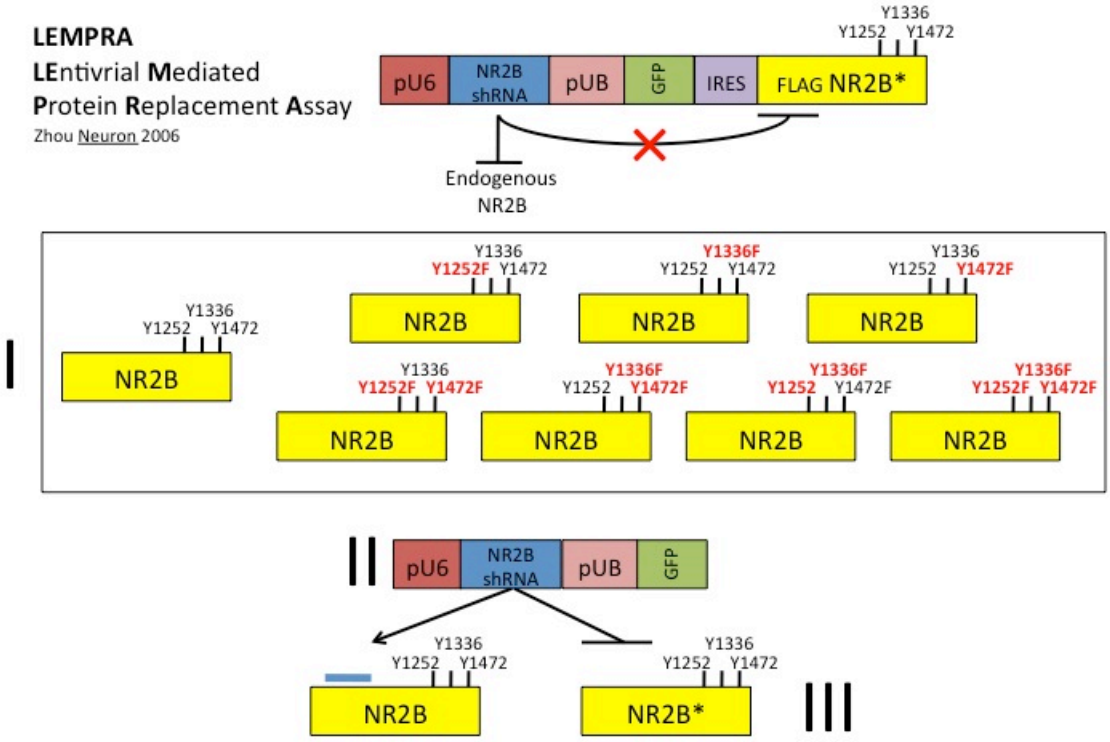

Zhaolan Zhou generously provided us with the pLEMPRA construct, Takanobu Nakazawa provided us with WT and phosphorylation mutant NR2B constructs, and I made additional NR2B phosphorylation mutant constructs. I generated a NR2B shRNA and tested it in primary cortical neurons. I introduced seven silent mutants to make NR2B resistant to the shRNA. This led to the generation of a construct which depletes endogenous NR2B and overexpresses shRNA-resistant NR2B.

pLEMPRA Constructs

The following constructs have been verified by sequencing:

- pLEMPRA NR2B
- pLEMPRA Y1472F NR2B
- pLEMPRA Y1336F NR2B
- pLEMPRA Y1252F NR2B
- pLEMPRA Y1252F/Y1336F NR2B
- pLEMPRA Y1336F/Y1472F NR2B
- pLEMPRA Y1252F/Y1336F/Y1472F NR2B
- pLEMPRA CTD NR2B

Fyn Overexpression Constructs

- pCMV6 FynB
- pCMV6 FynT

Lentiviral shRNA Constructs

- pLLX NR2B
- pLLX Fyn 1
- pLLX Fyn 2

Future Directions

The pLEMPRA NR2B constructs will allow us to determine the function Y1252, Y1336 and Y1472 in response to an array of stimuli such as NMDA, glutamate, and oxygen glucose deprivation. Additionally, we can knock down Fyn using shRNAs and rescue with the FynB construct. We can also generate FynB kinase dead and constitutively active mutants using site directed mutagenesis to determine whether Fyn kinase activity is dispensable in neuronal cell death. These tools will allow us to further dissect the molecular mechanisms by which Fyn and NMDAR tyrosine phosphorylation contribute to neuronal cell death *in vitro*.

Publishing Agreement

It is the policy of the University to encourage the distribution of all theses, dissertations, and manuscripts. Copies of all UCSF theses, dissertations, and manuscripts will be routed to the library via the Graduate Division. The library will make all theses, dissertations, and manuscripts accessible to the public and will preserve these to the best of their abilities, in perpetuity.

Please sign the following statement:

I hereby grant permission to the Graduate Division of the University of California, San Francisco to release copies of my thesis, dissertation, or manuscript to the Campus Library to provide access and preservation, in whole or in part, in perpetuity.

Renatta Kuy
Author Signature

8/13/12
Date